Chemical Communications

FEATURE

# Conformational control of cofactors in nature – The influence of protein-induced macrocycle distortion on the biological function of tetrapyrroles

Received 00th January 20xx,
Accepted 00th January 20xx

DOI: 10.1039/c5cc06254c

www.rsc.org/

Mathias O. Senge,[a,b*] Stuart A. MacGowan[a] and Jessica O'Brien[b]

Tetrapyrrole-containing proteins are one of the most fundamental classes of enzymes in nature and it remains an open question to give a chemical rationale for the multitude of biological reactions that can be catalyzed by these pigment-protein complexes. There are many fundamental processes where the same (*i.e.*, chemically identical) porphyrin cofactor is involved in chemically quite distinct reactions. For example, heme is the active cofactor for oxygen transport and storage (hemoglobin, myoglobin) and for the incorporation of molecular oxygen in organic substrates (cytochrome $P_{450}$). It is involved in the terminal oxidation (cytochrome c oxidase) and the metabolism of $H_2O_2$ (catalases and peroxidases) and catalyzes various electron transfer reactions in cytochromes. Likewise, in photosynthesis the same chlorophyll cofactor may function as a reaction center pigment (charge separation) or as an accessory pigment (exciton transfer) in light harvesting complexes (*e.g.*, chlorophyll a). Whilst differences in the apoprotein sequences alone cannot explain the often drastic differences in physicochemical properties encountered for the same cofactor in diverse protein complexes, a critical factor for all biological functions must be the close structural interplay between bound cofactors and the respective apoprotein *in addition* to factors such as hydrogen bonding or electronic effects. Here, we explore how nature can use the same chemical molecule as a cofactor for chemically distinct reactions using the concept of conformational flexibility of tetrapyrroles. The multifaceted roles of tetrapyrroles are discussed in the context of the current knowledge on distorted porphyrins. Contemporary analytical methods now allow a more quantitative look at cofactors in protein complexes and the development of the field is illustrated by case studies on hemeproteins and photosynthetic complexes. Specific tetrapyrrole conformations are now used to prepare bioengineered designer proteins with specific catalytic or photochemical properties.

## Introduction

Proteins present one of the fundamental building blocks of life. This is due to the potentially limitless scope afforded by their modular and hierarchical structure that proceeds from the primary to quaternary through sequence, conformation, fold (shape) and assembly. Many proteins also incorporate biophysically active or catalytic small-molecules. These cofactors are often situated in – or even constitute – the 'active site(s)' of the protein and affect or assist in whatever function the protein is required to perform. The chemical structure of the cofactor grossly determines what role it may play and thus, for example, redox active metal containing compounds may be found in electron transfer proteins, ligand transport or sensing systems. This additional level of structure extends the scope in which nature may construct proteins even beyond that alluded to above.

In spite of this fact, although complex, the set of known proteins is fathomable and amenable to both structural and functional classification.[1] This may be indicative that the set of biologically useful proteins is a mere fraction of the structures that are possible. Indeed, the notion of biological utility implies the presence of functional driving forces that direct the evolution of proteins and also that the set of useful functions is finite. With this in mind, functional variation in some cases may have been restricted to adaption or fine-tuning since the time that the biochemical paradigms for life on earth had evolved. The structural principles of proteins and cofactors are also relevant in this context in the limit of small perturbations characterized for example by minor biosynthetic modification or a few sequence substitutions. Additionally, in protein-cofactor complexes covalent and non-covalent interactions between the protein and cofactor may be considered as modulators of their chemical and physical properties, providing an additional mechanism beyond purely structural considerations for the fine-tuning of function.[2]

Proteins have attained such a central role in the processes of life as a result of the diversity and complexity that emerges

[a] *School of Chemistry, SFI Tetrapyrrole Laboratory, Trinity Biomedical Sciences Institute, 152-160 Pearse Street, Trinity College Dublin, The University of Dublin, Dublin 2, Ireland.*
[b] *Medicinal Chemistry, Institute of Molecular Medicine, Trinity Centre for Health Sciences, Trinity College Dublin, St. James's Hospital, Dublin 8, Ireland. E-mail: sengem@tcd.ie*
† *In memoriam* John. A. Shelnutt

from the opportunities afforded by the many levels of structure available to affect their construction and impart function. Amongst these possible 'design principles' the fine-tuning of cofactor properties via its interactions with the apoprotein plays a key-role in ensuring efficient performance and proper adaption to a particular environment.

In order to study the modulation of a cofactor by the apoprotein in detail a reliable set of structures depicting the cofactor-protein interactions is mandatory. Ideally, the cofactor should be the same for different biochemical functions and its chemistry well understood. Such a situation is found for tetrapyrroles – notably the porphyrins. Here we use these to illustrate how the interplay between apoproteins and cofactors modulates the macrocycle conformation of the latter and can be interpreted with the concept of conformational control.

## Tetrapyrrole cofactors

Tetrapyrroles, and most prominently porphyrins, are a unique class of natural compounds that are ubiquitous in nature and function in a wide variety of roles ranging from oxygen transport, electron transfer and oxidation reactions to photosynthesis (Fig. 1).[3] They are amongst the most important cofactors found in nature and are crucial regulatory effectors in many biochemical processes. On a chemical basis, these effects are related to their chemical properties, namely their photochemical (energy and exciton transfer),[4] redox (electron transfer, catalysis),[5] coordination properties (metal and axial ligand binding),[6] ***and their conformational flexibility*** (functional control).[7] By virtue of these properties they are also some of the most important fine chemicals in industry and are involved in an ever expanding array of biochemical processes and applications ranging from use as pigments and oxidation catalysts, to emerging areas such as photodynamic cancer therapy, artificial photosynthesis, sensors, optics and nanomaterials.[8,9]

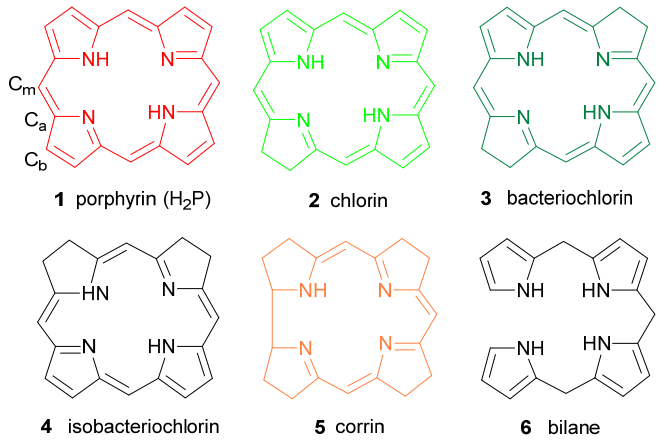


**Fig. 1** The main chemical classes of biologically relevant tetrapyrroles.

The porphyrins as cyclic tetrapyrroles are complemented in nature by linear tetrapyrroles (*i.e.* derivatives of bilane **6**), which are derived from the former *via* ring-opening reactions. Examples are the bile pigments, such as bilirubin and biliverdin, the photosensory pigment phytochromobilin, the phycobilins as accessory photoreceptors, and other porphyrin or chlorophyll breakdown products.

### Functional classes of tetrapyrroles

Tetrapyrrole-containing proteins are a particular class of proteins that contain cofactors related to the porphyrin nucleus. Aside from the ubiquitous hemes and chlorophylls, which have been dubbed "The Pigments of Life",[10] this includes proteins that contain as prosthetic groups the vitamin $B_{12}$-derivatives (cobalamins **11**),[11] cofactor $F_{430}$ (**10**),[12] or siroheme, to name a few others (Fig. 2).[13] Additionally, there are many other proteins whose substrates are one or a group of these cofactors, or else their immediate precursors such as the heme degrading protein IsdI[14] or ferrochelatase,[15] as examples of each, respectively. Similarly, bilins as components of phycobiliproteins,[16,17] act as light-harvesting pigments in cyanobacteria and red algae, and (bacterio)phytochromes contain photoresponsive bilins functioning as the 'visual pigment' of plants in photomorphogenesis and photoperiodism, as well as light-controlled kinases.[18]

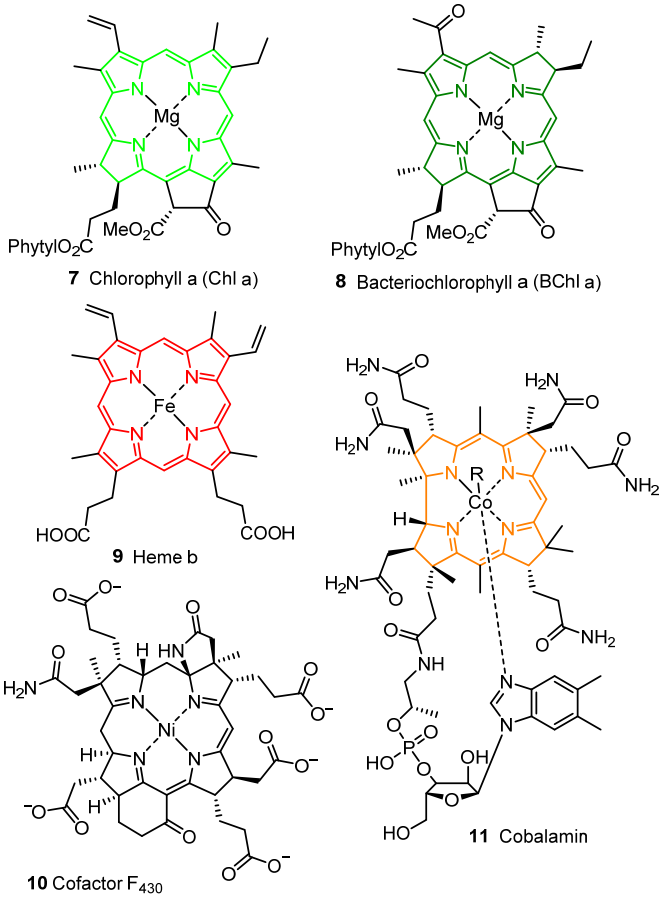


**Fig. 2** Examples of cyclic tetrapyrrole cofactors illustrating structural diversity. Chlorophyll a **7** is an accessory and reaction center pigment in the photosynthesis of higher plants; bacteriochlorophyll a **8** is found in the reaction centers and light-harvesting complexes of purple bacteria; heme b **9** is most well-known for its function in hemeproteins; particular cobalamins (vitamin $B_{12}$ **11**) are cofactors in methionine synthase and methylmalonyl coenzyme A mutase; and cofactor $F_{430}$ **10** is essential for methanogenisis by methyl coenzyme M reductase.

The diversity of these proteins is impressive since they encompass whole swathes of biochemistry including respiration, photosynthesis, ligand-sensing and -transport, metabolism, photomorphogenesis, metal-sequestration and much more. Of significance is the fact that many of these processes rely upon fundamentally different chemistries, and thus properties ranging from ligand-binding constants, redox potentials, absorption maxima, excited-state lifetimes, ion-selectivity and chemical stability may need to be regulated. This begs the question as to how nature has succeeded in managing these properties for its desired ends, especially when it was noted that the chemical identity of the cofactor largely dictates what it is capable of doing as well as what can be done to it.

Across all tetrapyrrole-containing proteins the relevance of the latter point of this question is perhaps moot; nature has provided enough significant variation within the chemical structures of tetrapyrrole cofactors to provide them with properties suitable for their intended task (Fig. 2). However, within a particular class, the variation in structure is often quite subtle and does not usually account for the entirety of their functional diversity. In many cases too, chemically identical species are used to perform disparate functions.

In these situations, differences between protein-cofactor interactions may be invoked to explain the functional variation that minor differences in chemical structure, or the complete lack thereof, does not. Amongst the possible interactions, hydrogen bonding, electrostatic effects, axial ligation and covalent binding are known to affect both the kinetic and mechanistic properties of catalysis and the energetics of biophysical processes such as electron transfer.[19] Higher-order architectural organization is also critical in determining the role of the protein through control of its interactions[20] with others and access to the cofactor, as well as maintaining defined spatial orientations[21] in multi-cofactor proteins (hence the term, 'protein scaffold'). Whilst these features of protein design are relevant to all or at least most prosthetic groups, perhaps there is something else unique to tetrapyrroles that would provide an additional rationale for their apparent ubiquity? Indeed, the suggestion that there is will form the central argument of this article (*vide infra*).

#### Porphyrins have flexible macrocycles

Porphyrinoid-cofactors have found such multifaceted use in nature as a result of the properties conferred to them by the aromatic core, in tandem with their ability to complex with and stabilize biologically useful metals. Focusing on the former, the delocalization of electrons across the relatively large surface area of the macrocycle is also present in the charged species generated following electron transfer events during photosynthesis, allowing the delocalization of charge which minimizes the reorganization energies.[22] The extended conjugation also results in strong absorptions in the visible region[23] that, when combined with the substitution patterns observed in the chlorophylls, are quite befitting for the harvesting of light energy from the sun.

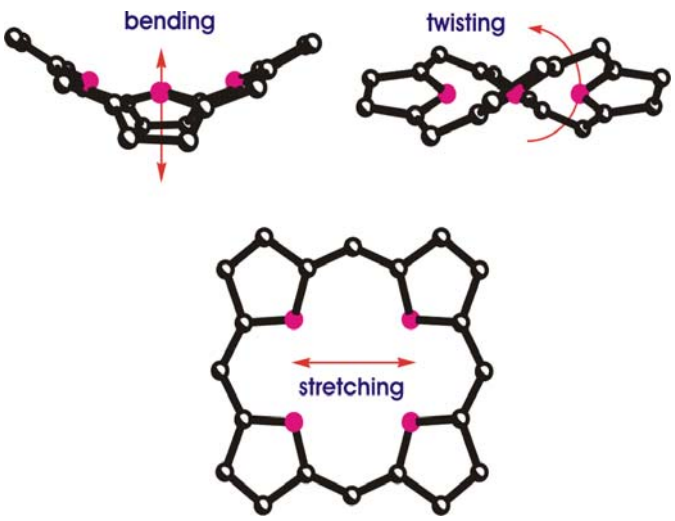


**Fig. 3** Schematic illustrations of some of the characteristic distortions and 'molecular exercises' of the porphyrin macrocycle.

A superficial consideration of the aromatic conjugation of the macrocycle in **1** would perhaps demand the conclusion that it must remain planar. However, this is not necessarily the case, and indeed appears to be the exception rather than the rule in protein complexes (*vide infra*).[7,24,25,26] Likewise, many small molecule X-ray crystallographic analyses have identified different types of macrocycle distortion (Fig. 3).[27] Concurrently, a basic consideration of the effect of macrocycle non-planarity on the p-orbital overlaps that contribute to the aromaticity suggests that they may become disrupted and thus produce some alteration of the detailed electronic structure and properties of the macrocycle, whilst the symmetry of the macrocycle is also perturbed by distortion. Perhaps unsurprisingly then, many empirically observed correlations between the extent of non-planarity and physicochemical properties have been reported.[25,26,28,29,30,31,32,33]

## The concept of conformational flexibility

#### Hypothesis and concept

The observations outlined above allow speculation that protein-induced macrocycle deformation of tetrapyrrole cofactors could serve as a mechanism by which a protein may modulate its biophysical or biochemical function. This concept of the conformational flexibility of porphyrins was first formulated over 25 years ago and is now based on an expanding body of structural data for porphyrins and hydroporphyrins as isolated molecules and in proteins, which has illustrated the considerable flexibility of the molecules and the significant distortions that can be imposed on tetrapyrrole macrocycles by crystal packing, steric effects, or protein constraints.[2,7,24,31,34]

The concept is not as farfetched as it may sound. Indeed, in a sense there is a relationship between the idea of conformational control and the notions of "Induced Fit"[35] (the antecedent of Fischer's[36] "Lock-and-Key" theory) and Pauling's concept of the "Activated Complex".[37] In the former, binding

of substrate to enzyme effects a mutual conformational change that is necessary for catalytic function and specificity,[35] while the latter deals with the stabilization of particular transition states, evident in the tight binding-constants for their analogues, and has been implicated as the origin of enzymatic catalytic acceleration.[37] Similarly, the main goal of this feature is to present new evidence in support of the idea that the protein-induced deformation of cyclic and open-chain tetrapyrroles is a mechanism exploited by proteins to impart desired physicochemical properties (Fig. 4).

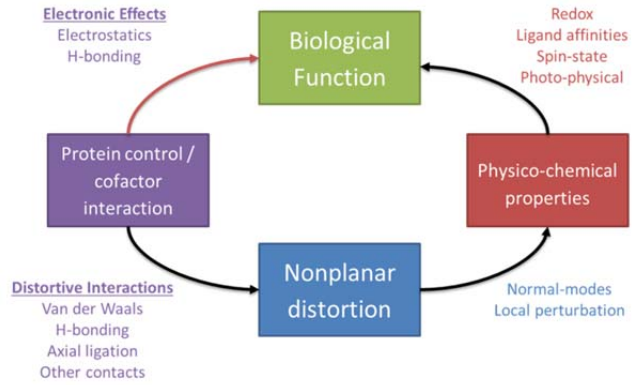


**Fig. 4** Schematic illustration of the proposed mechanism of 'conformational control'. The protein exerts a distortive influence upon the cofactor which induces a specific non-planar conformation; this in turn modifies the cofactor's physicochemical properties, and thus impacts its biological function. Direct electronic influences are also utilized by the protein to influence function (*e.g.*, axial ligands, H-bonding and electrostatic effects) that are not a part of conformational control, and these too are represented in the diagram.

### Methods and approaches

There are several options that present themselves when considering how to go about testing the hypothesis that macrocycle flexibility is in some way related to the diversity of tetrapyrrole functions. One is to design and synthesize model compounds which exhibit different macrocycle conformations and attempt to correlate these conformations with measurements of relevant physicochemical properties. Pioneered by Smith and Fajer,[7] this was also our initial point of entry into the field in 1990. While interested in the chemical basis for the multiple functions of chlorophylls, at that time only a 'biomimetic' appeared feasible.[27] The approach of using 'highly substituted' porphyrins as conformationally designed systems was in fact instrumental in the development of the concept,[24,25,27,31] but is not without its limitations where, on the one hand, conformational effects are confounded with the varying chemical structures and on the other, the compounds often deviate chemically from the cofactors found in nature. Nevertheless, this method is exceedingly useful thanks to the many clever designs that have been utilized to mitigate its drawbacks, and publications from such approaches supported many of the interpretations of conformational effects discussed here.

A second option is the use of quantum chemical techniques, and this method can overcome both of these problems as within the limits of the computing facilities available any conceivable structural model may be implemented. However, this advantage has proved also to be a weakness since the freedom runs the risk of introducing an intractable level of arbitrariness that has no parallel in reality. Another feature that renders such studies imperfect is simply that for many electron wave functions, all contemporary methods yield only approximate solutions to the Schrödinger wave equation, so that the calculated electronic structure is only accurate within the context of the model and method employed.[38] Fortunately, modern methods are often sufficiently accurate for many purposes and more importantly, numerous benchmarks and comprehensive comparisons to experiment are available to assess relevance so that the issue is often pragmatic in nature when deciding how to balance computational complexity against accuracy and available resources.

The last and the most important method to be discussed is the direct measurement of the cofactor conformations within intact protein complexes. To this end X-ray crystallography is often viewed as the definitive experimental technique for the observation of chemical structure and conformation. Although capable of resolutions on the order of a few tenths of an Ångstrom (~0.4 Å) for small-molecules, proteins are typically more complex and so 'atomic detail' is not always achieved.[39,40,41]

Thus, reliance upon good chemical sense in the form of refinement constraints and restraints is necessary.[42] This leads to difficulties in the aggregation of measurements *via* averaging because differences in the implementation of these artificial observations introduces significant bias into the final recorded structure. The ensuing conundrum is how to select the structures that will yield the best representation of the actual cofactor conformations. Fortunately, as X-ray crystallography ultimately provides a numerical description of the structure (*i.e.,* atomic coordinates), the results of many studies are particularly amenable to statistical analysis.

In fact, the main difference between now and our first foray into this 20 years ago is the availability of multiple protein crystal structures for functionally similar biological systems. While only individual protein-cofactor studies were available, allowing at best the accumulation of anecdotal evidence, the number of published porphyrin-protein crystal structures now allows a statistically reliable analysis of data.

A statistical approach provides an unbiased logical rigor for the study, as any stated hypothesis must be objectively supported by the data in order to remain upheld. In more practical terms, multivariate analysis allows one to cope with large numbers of observations of many variables and extract the salient features quickly and efficiently whilst simultaneously drawing attention to the individual cases that do not fit expectations, so that suitable measures may be taken to assess their importance. Another important facet of the statistical approach is that it provides a method of establishing the confidence that can be assumed with respect to the uncertainty of an observation, such as the variability of a particular conformational parameter of a tetrapyrrole in a protein.

Ultimately, these methods are combined with those from molecular biology to alter the cofactor conformation through specifically "designed" interactions with the protein scaffold, *e.g.*, *via* mutations, reconstitution with non-natural pigments and other means of protein engineering to yield proteins with novel functions.

## Analytical methods

### Simple conformational analysis of porphyrins

The structural characterization of non-planar porphyrins can be achieved using a number of the macrocycle's geometric parameters that generally may be considered to fall into one of two groups. Specifically, there are those which utilize the internal angles and interatomic vectors 'as is', such as the $C_a$-$N_{opp}$-$N_{opp}$-$C_{a'}$ dihedral angles to quantify distortion types, or alternatively, parameters derived relative to the 4N- or 24-macrocycle atom mean-plane. Although both of these approaches are valid, it is generally considered that deviations from the mean-plane best capture the non-planar conformations of porphyrins and are most suitable for comparative analyses.

Two useful quantifiers of the degree of non-planar distortion are Δ24 and $D_{oop}$, which are defined as the root mean square deviation of the 24 macrocycle atoms from their least-squares plane and the related root sum-of-squares, respectively. Alternatively, skeletal deviation plots[43] reveal local features of the individual z-displacements from the 24-atom mean-plane ($\Delta z_i$) by means of plotting $\Delta z_i$ against an arbitrary positional parameter, assigned such that the view of each pyrrole unit is along its N-mid ($C_b$-$C_b$) bisector, and reading from left to right one 'walks around' the macrocycle (Fig. 5)[44].

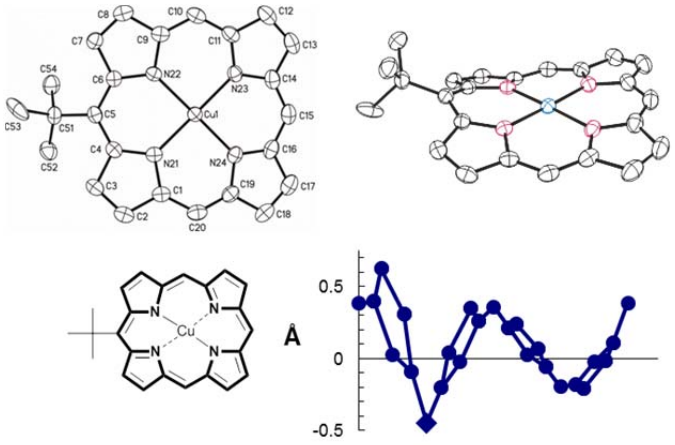


**Fig. 5** Illustration of deriving a skeletal deviation plot to characterize macrocycle non-planarity from the crystal structure of (5-*tert*-butylporphyrinato)copper(II) (top panel);[44] the mean plane defined by the 24-macrocycle atoms (bottom left) from which the individual skeletal deviations are derived (bottom right).

Naturally, the coupling of the conformational data with specific physicochemical properties (*e.g.*, UV/Vis spectra, Resonance Raman vibrational spectra, fluorescence lifetimes, reduction potentials, etc.)[45] is also required to complete the story and give a full measure of the key properties that have been affected.

### Normal structural decomposition method (NSD)

The observation that the commonly observed *ruf*, *sad*, *dom* and *wav* conformers (*vide infra*, Fig. 6) were very similar to static displacements along the lowest-energy normal-modes of vibration of the macrocycle led to the development of a new technique for the more detailed quantitative structural analysis of tetrapyrroles based on a normal-coordinate structural decomposition (NSD) by Shelnutt[‡] and coworkers.[29] The NSD procedure describes an observed macrocycle conformation in terms of a linear combination of displacements from a planar reference geometry along so-called normal-coordinates derived from the normal-modes of a planar porphyrin macrocycle.

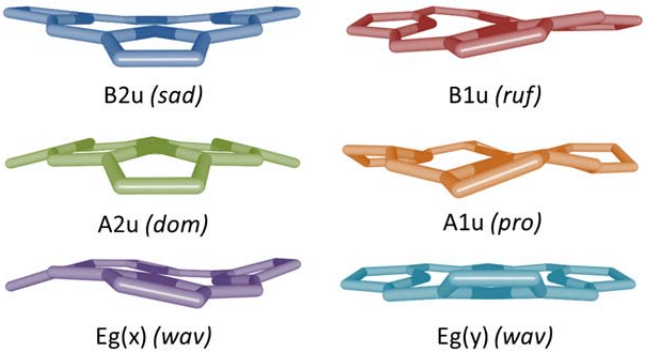


**Fig. 6** Idealizations of the six commonly observed out-of-plane macrocycle conformations. In the *sad* conformations the pyrrole rings are alternately tilted up/down along their $C_a$-$C_a$ axes producing a saddle shape. In the *ruf* conformation, the meso carbons are alternately displaced above and below the mean-plane that could be affected by twisting a planar macrocycle. In the *dom* conformation all of the pyrrole rings are tilted in the same direction with respect to their $C_a$-$C_a$ axes resulting in the characteristic dome shape.

It is a conceptually simple procedure that employs the decomposition of the conformation of the macrocycle by a basis set composed of its various normal-modes of vibration. This technique affords clear separation of the contributing characteristic distortions to the macrocycle conformation in a quantitative yet readily interpretable fashion. Furthermore, often a basis of only the lowest energy normal-mode of each symmetry are necessary (minimum basis) to describe the conformation accurately, affecting reduced dimension compared to specifying the 24 $\Delta z_i$ displacements and therefore allowing the large scale analysis of porphyrinoid crystallographic data. This development represented a turning-point in the structural characterization of porphyrins both from small molecule data and protein crystal structures.[25,46]

The normal-modes for the out-of-plane (OOP) distortions of the minimum basis consist of the lowest energy vibration from each symmetry and comprise the *sad*dle ($B_{2u}$), *ruf*fle ($B_{1u}$), *dom*ed ($A_{2u}$), *pro*pellered ($A_{1u}$) and the degenerate *wav*e modes [$E_g$(x) and $E_g$(y)] (Fig. 6).[29] The in-plane (IP) modes that compose the minimum basis are the *mesostr*etching ($B_{2g}$), *N*-

*str*etching ($B_{1g}$), pyr-*tra*nslation [$E_u$(x) and $E_u$(y)], *bre*athing ($A_{1g}$) and pyr-*rot*ation ($A_{2g}$).

A typical NSD analysis is shown in Fig. 7 and is used to illustrate the influence of the substituent regiochemistry on the conformation. It compares two crystal forms of 5,15-diphenylporphyrin **12**[47] with 5,10-diphenylporphyrin **13**.[48] The 5,15-diphenylporphyrin is characterized by large $B_{1u}$ and $B_{2g}$ distortions and a significant contribution from $A_{1g}$. This is indicative of out-of-plane ruffling, and in-plane macrocycle *m*-stretching, and breathing. $B_{1u}$ and $A_{1g}$ contributions are present to a similar extent in the 5,10-regioisomer, while the stretching contribution is much smaller. While only a minor saddle ($B_{2u}$) distortion is present in the 5,15 derivative, this is noticeably more pronounced in compound **13**. The main conformational difference between the two regioisomers is found in the contribution from $E_g(x)$. This is indicative of a wave distortion and is only present in the 5,10-isomer. Thus, this free base macrocycle 'relaxes' more through out-of-plane than in-plane distortion.[49]

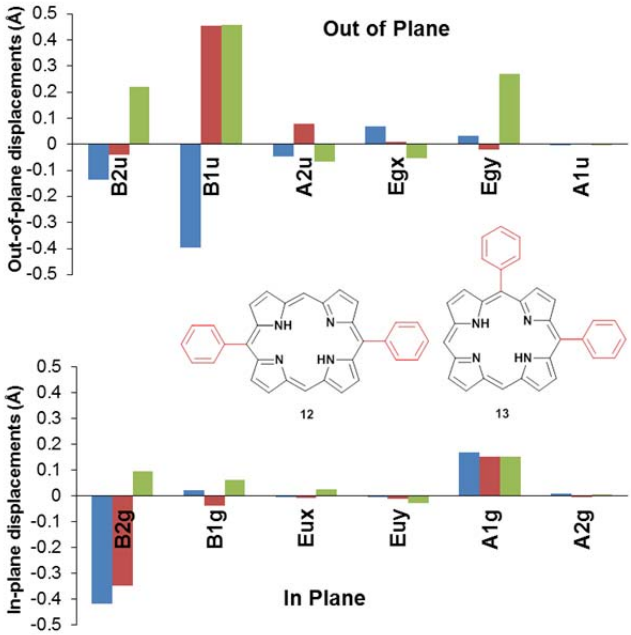


**Fig. 7** Normal-coordinate structural decomposition analysis of free base diphenylporphyrins [■ 5,15A = **12**, ■ 5,15B = **12**·$CH_2Cl_2$, ■ 5,10 = **13**].[49]

## Computational methods

**Statistical analysis.** Through the vast wealth of tetrapyrrole X-ray diffraction structural data available,[50] both of isolated small molecules and biologically embedded cofactors, as well as the structural assessment afforded by the NSD method, it is now possible to perform large scale quantitative comparative analyses and to extract the salient features of tetrapyrrole conformational flexibility using multivariate statistical analyses. For example, cluster analyses of subsets or even the entire body of structural data will doubtless elucidate the general tetrapyrrole conformers (including those of mixed distortion pattern) as well as the chemical substituents, protein environments or crystal packing effects that cause them. Cluster analysis is a statistical technique that may be used to reveal the relationships between observations in a multivariate dataset (*e.g.*, the NSD coefficients for protein-bound cofactors).[51] An example for using agglomerative hierarchical clustering (AHC) of NSD data to find groups of cofactors that possessed similar conformations to test the idea that the individual binding-sites imparted distinct conformations on the bound cofactors is given in the section on bacterial photosynthetic reactions centers (*vide infra*).

Other modes of analysis, such as the extraction of factors or principle components and kernel density estimation of the NSD data, can also assist the process and provide additional insight into the conformational space that has been explored so far and which may determine the true extent of conformational flexibility in a way akin to Ramachandran plots for protein residue conformations. If successful this aspect will allow the prediction of tetrapyrrole conformation from chemical structure and environment, and would also be capable of providing lead structures (or mutant candidates for cofactors) for any desired conformation.

**Quantum molecular modeling.** The selection of an appropriate method for the theoretical modelling of molecular systems and properties of interest is a delicate decision requiring simultaneous consideration of the required accuracy of the theoretical formalism alongside the availability of computational resources. The latter consideration is particularly relevant to porphyrins and their biological derivatives since the simplest compound (*i.e.*, unsubstituted porphyrin) contains 24 non-hydrogen atoms, whilst full models of hemes and chlorophylls have around 43 (290 electrons) and 66 (418 electrons) non-hydrogen atoms, respectively. Additionally, heme is a transition metal derivative and so the presence of d-electrons necessitates further consideration. Semi-empirical, *ab-initio* and DFT have all been applied to predict and explain macrocycle conformations and to determine their contribution to molecular properties.[52]

Calculation of spectroscopic properties of porphyrins using the popular INDO/S method has a well-established precedent in porphyrins and their metal complexes.[32,34,53,54] INDO/S correctly reproduces the non-planarity induced red-shifts of sterically encumbered non-planar porphyrins, providing a realistic geometry is provided (*i.e.*, either from a crystallographic study or suitable *in silico* optimization).[32,34] Work using geometries obtained from MM optimizations (*e.g.*, a porphyrin specific DRIEDING II) has shown that INDO/S calculations may often systematically overestimate the $Q_y$ wavelength, whilst the Soret band is underestimated, but crucially relative differences amongst compounds are very well modelled.[32,54]

Linnanto and Korppi-Tommola[55,56,57] have performed extensive comparisons of the accuracy of semi-empirical and *ab initio* methods for the calculation of geometries and excitation energies of chlorophylls and bacteriochlorophylls. These studies have ranged from isolated molecules and solvent complexes all the way to full models of reaction center and

 

light-harvesting complexes.[57] In general, exceptionally good performance of the PM5//ZINDO/S scheme (*i.e.*, PM5 geometry optimization followed by a ZINDO/S single-point energy calculation) is found for the Mg complexes of unsubstituted porphyrin, chlorin and bacteriochlorin as well as Chls and BChls.[56] The PM5 optimized structures of unligated and 6-coordinate complexes predicts a planar porphyrin with the Mg in the 4N-plane, whilst 5-coordinate species show a substantial out-of-plane displacement of the Mg atom, in line with both B3LYP and HF/6-31g*. Additionally, all methods correctly predict that the Mg-N bond(s) to the reduced rings are longer than those from non-reduced rings. Partial atomic charges were also found to be consistent amongst the semi-empirical, HF and DFT methods.[56] Overall, the best transition energies were obtained using the B3LYP/6-31g*//ZINDO/S scheme. However, PM5//ZINDO/S was also considered to perform well and was recommended for use in large calculations where the more accurate and expensive B3LYP/6-31g* optimizations are impractical.

It has long been known that some form of treatment of the correlation energy is necessary to provide adequate description of the first-row transition metal complexes due to the near degeneracy of the 4s and 4p orbitals as well as amongst the 3d orbitals.[58] Moreover, larger errors typically result from uncorrelated calculations upon metals with incompletely filled d-shells to the right of the d-block (*i.e.*, Fe – Cu)[59] and porphyrins also display significant electronic correlation,[60] as a result of the near degeneracies of the frontier orbitals and the many electrons that are present in the delocalized π-system.

For example, uncorrelated HF optimizations of porphyrin were shown to yield structures with severe framework bond length alternation or "frozen resonance forms" of $C_{2v}$ symmetry, whereas inclusion of electron correlation *via* MP2 or LDF optimization provided the correct $D_{2h}$ structure; notably, the severity of the bond-length alternation in the HF converged structure increased with larger basis sets.[60] The comparisons were also relevant to chlorin and moreover, vibrational calculations of chlorin implied that it is more flexible with respect to out-of-plane distortions than porphyrin, with low-energy vibrational energies for the *sad* and *ruf* modes plus an even softer mode involving a localized torsion of the saturated $C_b$-$C_b$ bond.[60]

Since then, Density Functional Theory (DFT) has found significant application in the modelling of biologically relevant porphyrin and related compounds,[61] and the efficient way in which DFT explicitly incorporates electron correlation within its theoretical formalism is certainly a major contributor to this success.

## Conformationally designed porphyrins

Whilst the aromatic π-system of porphyrins may at first imply planar compounds, it has long been known that the macrocycle possesses considerable conformational flexibility. A number of factors conspire to induce these distortions such as coordinated metals with small ionic radii (*e.g.*, Ni(II); modification of the core by substituents on the pyrrole nitrogen atoms (protonation or alkylation) and steric crowding at the periphery.[31] In the case of the so-called 'highly substituted porphyrins' that are characterized by a high-degree of peripheral substitution with sterically demanding substituents,[27,31] distortion occurs to alleviate the strain imposed by the substituent interactions whereas in metal complexes the M-N bonds place restrictions on the core size of the macrocycle and can lead to distortion in order to maintain optimal bond lengths. After many structural studies, it was noticed that symmetrically substituted porphyrins often exhibited characteristic, symmetric distortions including the saddled, ruffled and domed conformations.[6,31,43] Physicochemical associations of these distortions also had become apparent and included the bathochromic shift of the Q-bands, decreased reduction potentials (easier oxidation, hindered reduction) and a shortening of the fluorescence lifetime of the molecule's excited states.[31,32]

The idea that macrocycle distortion is a mediator of biological function is not new,[7,24,26,34] and considering the associated physicochemical effects of distortion summarized above, in our opinion neither should it be surprising. Indeed, that chemically identical species are able to perform such distinct functions *in vivo* participating in numerous biochemical processes *via* fundamentally distinct chemical reactions is quite unique. However, whilst model-compound studies proved the validity of the concept,[24] the first confirmation of these ideas began with the large-scale NSD analysis of hemes (*vide infra*),[25,29] which demonstrated the existence of functionally conserved conformations.

Even so, whilst the last large-scale analysis of the phenomenon was successful in obtaining recognition for the phenomenon in heme proteins,[25,29] the time lapse between those studies and the present has left the concept of conformational control lacking compared to other protein-cofactor modulatory methods (*e.g.*, H-bonds). Furthermore, whilst there has been significant follow-up in recent times for heme proteins (*vide infra*) there has been very little equivalent consideration of the effect in photosynthetic proteins, with the exception of the contributions from our groups.

### Classic structural studies

It all began 50 years ago with Fleischer's crystal structure determinations of (2,7,12,17-methyl-3,8,13,18-ethylporphyrinato)nickel(II) and (5,10,15,20-tetraphenylporphyrinato)copper(II) [**16**; Cu(II)TPP], which revealed that both macrocycles were considerably non-planar.[62] In a follow-up comparison of these and related metalloporphyrins he concluded that differences in crystal packing and chemical structure were responsible for the dispositions of porphyrins to adopt planar or non-planar conformations.[63] This work is notable as it may be considered the first comparative analysis of tetrapyrrole conformations in general. Shortly after, Hoard and coworkers presented similar results with the crystallographically isomorphous 5,10,15,20-tetraphenylporphyrin [**15**; $H_2$TPP] together with a theoretical rationale for the observations that perhaps could be said to

mark the beginning of the concept of conformational control.[64] The ideas that were put forward in this work were seminal and are worth summarizing as despite the intervening half century the crux would appear to remain relevant today.

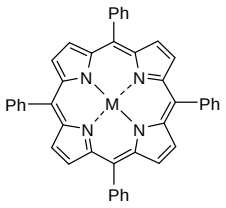

**14** M(II)TPP
**15** M = 2H, $H_2$TPP
**16** M = Cu(II), Cu(II)TPP
**17** M = Zn(II), Zn(II)TPP
**18** M = Ni(II), Ni(II)TPP

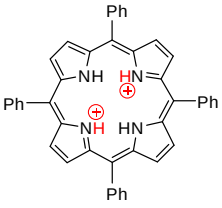

**19** $H_4TPP^{2+}$

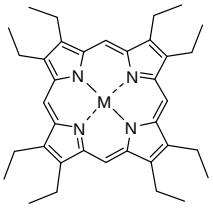

**20** M = 2H, $H_2$OEP
**21** M = Ni(II), Ni(II)OEP
**22** M = Zn(II), Zn(II)OEP

Until then Robertson and Woodward's mid-1930s landmark structure of phthalocyanine,[65] indicating a planar macrocycle, had been taken to indicate that the related porphyrins would too be "naturally planar".[66] However, the crystal structure of $H_2$TPP **15** showed large displacements of the meso carbons above and below the mean-plane (Δ24 = 0.19 Å) (Fig. 8). These did not disrupt the local planarity of several key regions, indicating that the geometric requirements for local π-bonding were retained, but that each pyrrole was not coplanar with the $C_a$-$C_m$-$C_{ipso}$-$C_{a'}$ dihedral, being identified as the *"principal circumstances adverse to ideal π-bonding"*. Ruffling was suggested to allow puckering of the chelate ring between the metal, two adjacent N-atoms and their connecting skeletal carbons to reduce the strain present in the σ-bonding framework resulting from certain bond angles exceeding 120°. Although the affected reduction of such bond-angles was small in magnitude and appreciable only at the meso carbons (as these are not part of a ring), the observed angle of around 125° was said to be sufficiently removed from the ideal for $sp^2$ σ-bonding so that any small reduction would be energetically significant.[64,67]

Subsequently, Silver and Tulinsky's detailed structure of triclinic $H_2$TPP **15** revealed that the same compound could exhibit different conformations, since their crystal form possessed a considerably flatter core (Δ24 = 0.05 Å) – albeit still distorted.[68] In this case, the pyrrole protons were located on fixed and opposite rings and the deformation that remained was attributed to N-H repulsion in the core (*i.e.*, the N(-H)…(H-)N distance was longer by 0.14 Å than the other N…N diagonal).[69] This was complemented by Lauher and Ibers' first β-substituted porphyrin structure, namely that of (planar) 2,3,7,8,12,13,17,18-octaethylporphyrin [**20**; $H_2$OEP], which at the time was useful to assess differences between meso- and β-substitution, with the latter more relevant to natural systems. Their analysis also found lengthened C-C bonds at the substituted positions compared to unsubstituted porphyrin **1** and meso-substituted compounds such as $H_2$TPP.[70]

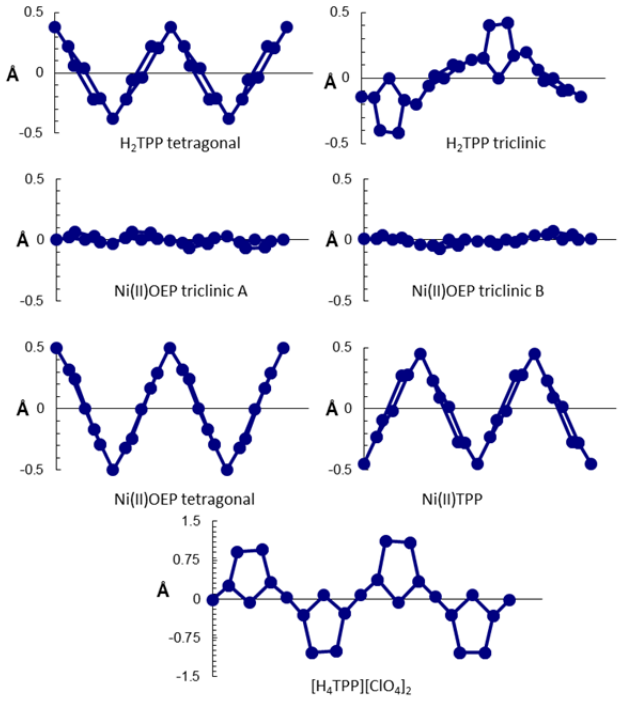


**Fig. 8** View of the skeletal deviations of the macrocycle atoms from the 4N-plane for selected porphyrins.

An important discovery was the structural origin of the red-shifted absorption spectra of porphyrin dications.[71] Crystal structures of some diacid species revealed severe non-planar distortions of the macrocycle that were due to steric interactions of the crowded core as well as electrostatic repulsion of the partially positive pyrrole nitrogen atoms.[72] Moreover, the enhanced red-shifts observed in $H_4TPP^{2+}$ (**19**) (which is green) compared to other dications (which can be purple) were attributed to the rotation of the meso phenyl rings into the macrocycle plane, allowed by the non-planarity of the compounds (Fig. 9).[71,72,73]

Although M-N bond-lengths are the most variable bond-lengths in metalloporphyrins (~1.95 – 2.10 Å), it was noticed early on that they are constrained relative to metal preferences in monodentate complexes by the influence of the macrocycle.[71] Furthermore, despite this variability and the associated (yet reduced) variation in the radius of the central hole, other skeletal parameters were observed[74] to be even less flexible, such as the in-plane center to meso distance (Ct-$C_m$) and the $C_a$-$C_m$-$C_a$ bond-angle. These observations, together with structural data for high-spin Fe(III) complexes, led to the idea that in these species the coordinated Fe was *necessarily* displaced out of the 4N-plane because of size restrictions.[74] Moreover, on this basis it was suggested, and later observed,[75] that low-spin Fe(III) could be accommodated within the 4N-plane. This proved also to be the case in proteins, emphasized for example by the hemes in low-spin ferric cyanomethemoglobin,[76] whilst in contrast, the Fe(II) atom in high-spin deoxyhemoglobin[77] was displaced by ~0.75 Å out of the 4N-plane toward the axial HIS residue.[78]

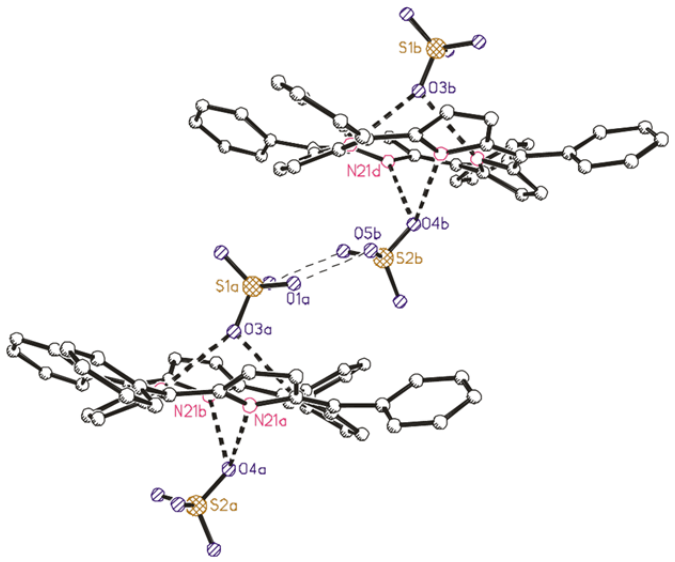


**Fig. 9** View of the molecular structure of the $\{[H_4TPP][HSO_4]_2\}_n$ polymer in the crystal illustrating the degree of distortion in the macrocycle, the rotation of the meso phenyl rings and the intricate H-bonding network which is observed in such compounds.[73b]

Following further advances in the synthesis and characterization of many conformationally distorted porphyrins, Scheidt and Lee[6] gave a systematic evaluation of the contemporary state-of-the-art in 1987 that provided the modern stereochemical classification of non-planarity used today. Here, the terms ruffled (*ruf*) and saddled (*sad*) conformations were formally defined, with *ruf* indicating a twisted macrocycle with meso carbons alternately displaced above and below the mean-plane and *sad*, obtained by a 45° rotation of the *ruf* conformer around the major $C_2$-axis, describing a similar alternate displacement of the pyrrole rings relative to the mean-plane. Additionally, the by then well-known domed (*dom*), waved (*wav*; called "stepping" by Scheidt) and "roof" type conformations were also noted (Fig. 6).

Another key idea developed by Scheidt[79] related the geometric parameters of metalloporphyrin cores (*e.g.*, M-N bond lengths) to the electronic configuration of the central ion. Specifically, any complex in which the "stereochemically active" metal $d_{z2}$ or $d_{x2-y2}$ orbitals were populated, would exhibit greater M-N bond lengths than a complex with the same or a similarly sized metal where these orbitals were empty. This principle could be applied to determine spin-state given structure in ambiguous cases, or else to predict stereochemistry given spin-state, the latter bearing relevance to oxidation state changes during the functioning of heme proteins. Additional constraints on the coordination geometry to be discussed were that axial ligand bonds were generally larger than analogous monodentate complexes, especially with larger ligands, because of the nonbonding repulsion between the ligand and the porphyrin macrocycle. Likewise, the importance in N-heterocyclic ligands (*e.g.*, imidazole and pyridine) of the dihedral angle between the axial ligand plane and the $N_{opp}$-$N_{opp}$ axis and trends in 5- and 6-coordinate complexes were described and served as models for the situation *in vivo*.

**Model compounds and structural correlations**

We have previously reviewed the numerous ways in which conformationally distorted porphyrins are achieved *via* synthetic design as well as the associated physicochemical consequences.[30,31,45] Throughout the following sections only selected examples of the various approaches that have proved successful will be highlighted in order to illustrate the influence of non-planarity on physicochemical properties. An outline of our own involvement in the field and how it developed over the first two decades was given here in 2006.[27]

**Conformational flexibility and multiple crystal forms.** Numerous investigations of Ni(II) derivatives indicated a tendency to *ruf* distortion resulting from core-strain induced by short Ni-N bonds exacerbated in strained or inherently more flexible derivatives, and thus Ni(II) porphyrins are commonly found with substantially distorted macrocycles.[43,80,81,82,83] For instance, non-planar tetragonal and planar triclinic A forms of Ni(II)OEP **21** were known in the 1970s (Fig. 8),[80] the latter with longer Ni-N bonds, and in contrast to the analogous $H_2$TPP (*vide supra*) the tetragonal form was suggested to represent the *unconstrained* structure. A third planar form (triclinic B) was discovered later, distinguished by the presence of significant π-π interactions that appeared to affect two different sets of Ni-N distances, with the shorter pair in-line with the stack.[81]

Ni(II) hydroporphyrins provided an early illustration of the increased flexibility of reduced macrocycles emphasized by considerable deformation compared to the planar porphyrin.[82,84] This characteristic was also present in Fe chlorin derivatives and was suggested to be the result of intrinsically greater core-size in the hydroporphyrins, therefore encouraging ruffling to shorten M-N lengths.[85] Other studies of conformationally distorted chlorins, including our own series of increasingly β-ethyl substituted tetraphenylchlorin derivatives,[86] and compounds with both meso and β-substituents,[87] are in agreement with this observation, as it appears that chlorins have a tendency towards more *ruf* distortion.[87,88]

Many other reports of peripherally crowded Ni porphyrins highlight their status as original models of macrocycle non-planarity.[54,89,90] However, the discovery *via* resonance Raman (RR) spectroscopy by Shelnutt and coworkers that the conformational flexibility of Ni(II)OEP **21** observed amongst the various crystal forms (Fig. 8) was also present in solution deserves special mention, in particular that the non-planar form displayed red-shifted absorptions, which is a characteristic marker of non-planarity.[91] Variable temperature NMR[34,92] experiments and EXAFS[33a,93] measurements had also shown that similar conformations can exist in both solution and solid state, and many other examples[31] are known.

**Highly substituted porphyrins as model compounds.** Many of these studies were based on the synthesis of model compounds specifically designed to impart steric strain and thus conformational distortion on the macrocycle. Often called 'highly substituted porphyrins',[31] the most fundamental design criterion was the presence of both meso and β-substituents to

give rise to *peri* interactions. This is exemplified in 2,3,7,8,12,13,17,18-octaethyl-5,10,15,20-tetraphenylporphyrin [$H_2$OETPP, **27**], which can be envisaged as a chimera of the TPP and OEP frameworks.[94] Compounds such as this can exhibit highly non-planar macrocycle conformations (primarily *sad*, Fig. 10a),[54,89,95] while porphyrins with bulky meso residues, *e.g.*, **32**,[90] or dodecaalkylporphyrins (**33**) are highly ruffled (Fig. 10b).[33a,91,96]

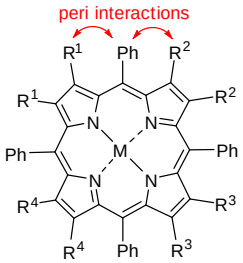


**23** $R^1$ = Et, $R^2$ = $R^3$ = $R^4$ = H 'DETPP'
**24** $R^1$ = $R^3$ = Et, $R^2$ = $R^4$ = H '*t*TETPP'
**25** $R^1$ = $R^2$ = Et, $R^3$ = $R^4$ = H '*c*TETPP'
**26** $R^1$ = $R^2$ = $R^3$ = Et, $R^4$ = H 'HETPP'
**27** $R^1$ = $R^2$ = $R^3$ = $R^4$ = Et 'OETPP'
**28** $R^1$ = $R^2$ = $R^3$ = $R^4$ = Br 'OBrTPP'

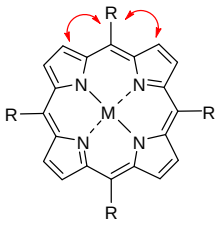


**29** R = alkyl 'TAlkylP'
**30** R = Bu$^n$
**31** R = Pr$^i$
**32** R = Bu$^t$

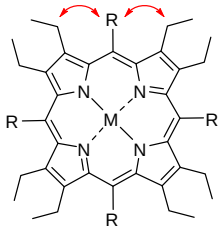


**33** R = alkyl 'OETAP'
**34** R = Bu$^n$ 'OET*n*BuP'

Bending the porphyrin macrocycle not only alters its physicochemistry but also its chemical reactivity. The most fundamental consequences of large *sad* distortions are an increased basicity and faster metalation rates. In fact, some non-planar porphyrins can be protonated by water, while metalation rates can be several orders of magnitude faster. Thus, some standard metalation reactions can be performed by simply stirring the free base with metal salts for a few minutes at room temperature, a property that has considerable relevance for ferrochelatase (*vide infra*). Formation of superstructured cavities above and below the porphyrin core also prevents some reactions that are observed for other porphyrins, *e.g.*, π–π aggregation or the formation of μ-oxo dimers. Similarly, the smaller core size of non-planar porphyrins aids the stabilization of small metal ions but results in lower stability for complexes with larger metal ions.[27,31]

The more non-planar porphyrins yield increasingly unstable chlorins. The steric strain imposed on the systems also gives rise to novel, porphyrin atypical reactions - notably for porphyrins with very large *ruf* distortions, and has led to routes for the formation of porphodimethenes (''calixphyrins'').[97,98] In contrast, the more planar porphyrins, or *sad* distorted porphyrins, undergo ''standard'' porphyrin reactions. This increased reactivity is clearly a consequence of the steric strain at the meso positions.[97] The degree of non-planarity can be further enhanced *via* core protonation or N-substitution.[73a,99]

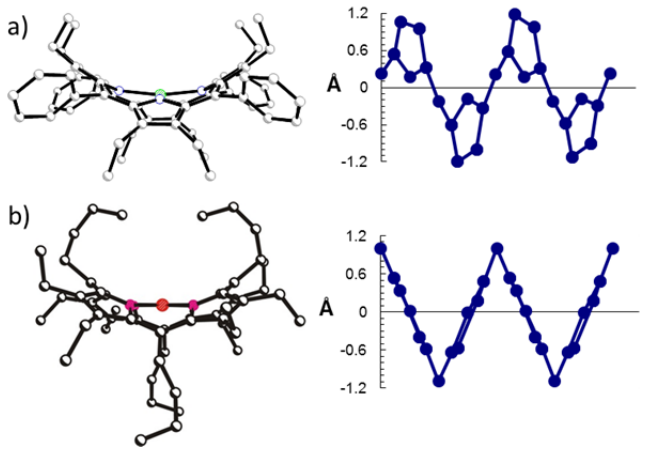


**Fig. 10** View of the molecular structure in the crystal and the skeletal deviations of a) Ni(II)OETPP[93] (top) and b) Ni(II)OET*n*BuP[33a] (bottom).

**Physicochemical correlations.** One of the first direct correlations between non-planarity with both red-shifted absorption spectra and increasing ease of oxidation was made in connection with photosynthetic pigments and immediately associated with the biological function of such chromophores.[34] In particular, experimental observations and INDO/S calculations upon (2,3,7,8,12,13,17,18-octaethyl-5,10,15,20-tetraphenylporphyrinato)zinc(II) [Zn(II)**27**; Zn(II)OETPP)], Zn(II)OEP **22** and Zn(II)TPP **17** demonstrated that non-planarity destabilizes the HOMO and causes the observed differences in absorption and oxidation potentials and is consistent with the insensitivity of their reduction potentials. These results served as a prelude to assessing intrinsic differences caused by conformational variation of the cofactors of the *B. viridis* reaction center[34] and later the pigments of the Fenna-Matthews-Olson (FMO) protein.[53] Expansion of this with the synthesis and characterization of the dodecasubstituted porphyrins just described demonstrated that in these severely *sad* distorted "peripherally crowded" porphyrins the distortion arose from internal steric strain as opposed to crystal-packing effects occurring in dimeric $H_2$TPP π-cation radicals[6] and remained present in solution.[92,100]

The metal's influence upon macrocycle conformation was investigated in detail, revealing that the non-planarity in strained 2,3,7,8,12,13,17,18-octaalkyl-5,10,15,20-tetraphenylporphyrins (*e.g.*, **33**, **34**; OATPPs) can be relaxed (*i.e.*, the opposite effect of small metals) in order to expand the core to accommodate larger metals and that the detailed influence of specific metals are related between the OATPP and the less encumbered OEP series.[90] The macrocycle distortive effects of peripheral steric strain could even be 'prevented' with sufficiently large metal ions.[101]

**Oxidation potentials.** The intriguing interplay between structural and electronic effects in porphyrins was highlighted in the trend in oxidation potentials of the sequentially brominated M($Br_x$TPP) **28** series (*i.e.*, TPP with 1-8 β-bromo).[102] Systematic studies showed that in some cases the

expected increase of the oxidation potentials with increasing bromination due to inductive effects is superseded by the effect of the increasing non-planarity of the macrocycle resulting from the increasing peripheral strain. For example, the Fe(III)(Cl)($Br_x$TPP) series reported by Kadish and coworkers revealed that upon addition of a third bromine the oxidation potential *decreased below* that of the disubstituted product. This trend continued nonlinearly and resulted in the perbrominated compound exhibiting a potential 10 mV *lower* than Fe(III)(Cl)TPP. Estimates of the precise conformational effect were given as 50, 93, 118, 186, 256 and 309 mV for Fe(III)(Cl)($Br_{(3-8)}$TPP) and this corresponds to a linear relationship itself, suggesting an average potential shift of ~53 mV per substituent for the conformational effect ($R^2$ of 0.98).[102a,b] Also, the invariance of the metal-centered reduction with respect to the level of distortion was taken to support the earlier theoretical result[34] that distortion raised the HOMO energy whilst having significantly less effect on that of the LUMO (*vide supra*) and/or to indicate a decreased effect of the conformation on metal-centered processes.

Ochsenbein *et al*. investigated the structures and electrochemistry of 5,10,15,20-tetramesitylporphyins with Cl and Br substituents at the "antipodal positions" (*i.e.,* opposite pyrrole rings tetra-β-halogenated) and the β-octahalogenated derivatives.[102c] Both shifts in the RR spectra and UV/Vis absorptions (both Q- and B-bands) were taken to indicate that the distortions were preserved in solution. The observation that the β-octahalogenated derivatives were both *easier* to oxidize than the corresponding β-tetrahalogenated compounds was accounted for by the excessive distortion of the former (*sad* with some *ruf*).[103] Additionally, although not severely distorted, the β-tetrabrominated compound possesses the relatively less-common *wav* conformation, where substituted pyrrole rings are bent above and below the mean plane. More recent electrochemical studies focused on the identification of metalloporphyrins with high oxidation states. For example, both Ni(III) and Cu(III) porphyrin dications[104,105] and a Ni(III) porphyrin radical cation[106] have now been characterized. Both redox reactions and photoexcitation further modulate the conformational landscape of porphyrins.[107] Likewise, the conformation of non-planar porphyrins can be further fine-tuned *via* axial ligand effects or weak interactions.[108]

**Photophysical correlations.** A number of early studies showed that photophysical properties are significantly affected by the macrocycle conformation, too.[109,110,111,112,113,114] These have revealed that non-planarity results in decreased $S_1$-lifetimes ($\tau_{S1}$) and fluorescence quantum yields ($\phi_F$) as a result of enhanced non-radiative decay rates ($k_{IC}$, $k_{ISC}$ and $k_{CT}$) of the $^1(\pi,\pi^*)$ excited state. Holten and coworkers assessed the influence of *sad* and *ruf* distortion on free base porphyrins using dodecasubstituted porphyrins and 5,10,15,20-tetraalkylporphyrins showing that both distortions affect strongly "perturbed" properties but that the *ruf* mode leads to more drastic consequences.[111,112] These perturbations include enhanced Stokes' shifts of 850 – 975 $cm^{-1}$, decreased $\phi_F$ and $\tau_{S1}$ of 0.003 – 0.009 and 400 – 800 ps, respectively, and shortened IC and ISC lifetimes of around 0.8 – 8.8 ns and 0.4 – 1.7 ns, respectively, for the *sad* compounds (cf. 106 $cm^{-1}$ (Stokes' shift), 0.13 ($\phi_F$), 15 ns ($\tau_{S1}$), 74 ns ($\tau_{IC}$) and 22 ns ($\tau_{ISC}$), averages for planar compounds).[111] For the *ruf* compounds, smaller Stokes' shifts of 478 – 486 $cm^{-1}$ were observed yet only negligible fluorescence was detected with $\phi_F = 1 - 2 \times 10^{-4}$ and $\tau_{S1}$ of 8 – 46 ps.[112]

The relationships between the macrocycle conformation and the observed effects were proposed to arise because of greater conformational flexibility of the non-planar compounds in the excited state.[111,112] This idea was formed on the basis of the large Stokes' shifts that could not be accounted for classically as solvent reorganization dynamics should be similar in all of the porphyrins studied. The increased flexibility would also be manifest in the observed increased $k_{IC}$ and this was further evidenced by the fact that the *ruf* distorted compounds exhibited similar properties to planar analogues at low-temperature.[110,113]

Unique excited state perturbations were found in Ni(II)TBu$^t$P (**32**) that differ considerably from the above owing to the fact that the $^1(\pi,\pi^*)$ excited state immediately decays to a ($d_{z2}$,$d_{x2-y2}$) intermediate, a general feature of low-spin $d^8$ nickel(II) porphyrins.[115] In this case, the (*d,d*) lifetime of the highly ruffled porphyrin (33 ns) was orders of magnitude larger than that of planar complexes (100–300 ps). Furthermore, in Ni(II)T*t*BuP, the lifetime of the (*d,d*) excited state exhibited a dramatic temperature and solvent dielectric dependence, ranging over 2 ps to 50 ns in very polar and nonpolar solvents, respectively, and increased to the microsecond timescale at decreased temperatures.[116] Additionally, the strong solvent dependence was taken to indicate significant polarity of the excited state non-planar conformation and this was suggested to be another feature of some non-planar conformations in general (*e.g.*, *dom*).

Recently, Röder *et al*.[33b] utilized our series of conformationally designed porphyrins exhibiting a graded degree of *sad* distortion[117] to systematically assess the photophysical effects (Fig. 11). This study departs from the "all-or-nothing" approach by assessing the influence of gradually increased non-planarity in a set of closely related compounds and additionally included the effect of metalation by comparing the free-base and zinc(II) derivatives of the $(Et)_x$TPP (x = 2, 4, 6, 8, **23**-**27**) series. It was shown that the singlet excited state properties were more sensitive to the conformation than those of the triplet and that the onset of the conformational effect was faster for the zinc(II) derivatives. Furthermore, both series exhibited gradually decreased $S_1$-liftimes, ISC quantum yields and triplet lifetimes, the latter resulting in dramatically reduced singlet oxygen quantum yields.[33b] Intriguingly, this hints at a potential mechanism for photosynthetic proteins to impart photo-protective abilities on chromophores through induced non-planarity.

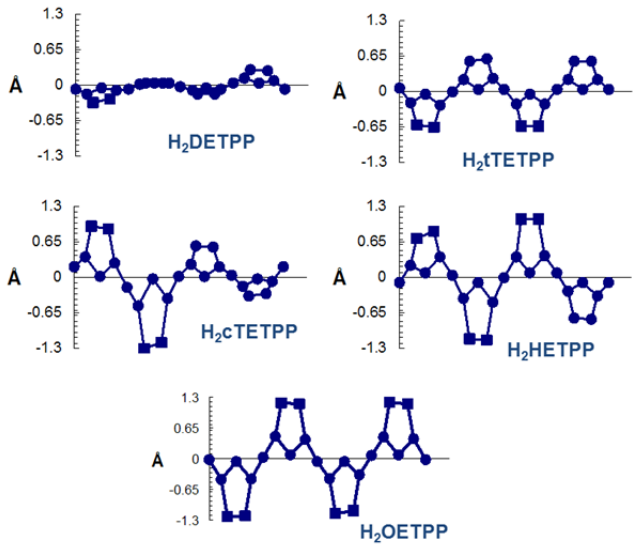


**Fig. 11** View of the skeletal deviation plots (4N-plane) of the XETPP porphyrin series (for $H_2$TPP see Fig. 8).[114b,117]

**Summary of consequences of macrocycle distortion.** Some general trends with regard to the effects of porphyrin macrocycle distortion on various parameters are compiled in Table 1. These are meant to serve as general indicators only; naturally, sometimes significant differences occur between free bases and metal complexes, exact values depend on solvents and experimental conditions and on the mix of distortion modes present.[31,118,119] Additional effects are altered axial ligand affinities in metal complexes and different orbital interactions with coordinated metals.[6,79,120] This simplified picture also neglects the effects of in-plane distortion,[49,69] which has not been studied to the same detail yet as out-of-plane distortions. Nevertheless, all affected parameters are crucial for the *in vivo* function of porphyrins, especially with regard to electron and exciton transfer properties.

**Table 1** Comparison of selected physicochemical parameters for planar and distorted porphyrins.[a)]

| Parameter | Porphyrin distortion planar | saddled | ruffled | Effect |
|---|---|---|---|---|
| Color | red | green | green | |
| Absorption $\lambda_{max}$ Q-band, nm | ~636 | ~710 | ~696 | ↗ |
| Emission $\lambda_{max}$ Q-band, nm | ~640 | ~760 | ~720 | ↗ |
| Stokes shift, $cm^{-1}$ | 26 – 142 | 850 – 975 | 40 – 100 | ↗ |
| $E_{1/2}$ox, V [*e.g.*, Ni(II)] | 0.92-1.15 | 0.85 | 0.55 | ↘ |
| Metalation rate, relative | 1 | >10,000 | n.d. | ↗ |
| $\phi_F$, fluorescence yield | 0.11 – 0.16 | $3 – 9\times10^{-3}$ | $2\times10^{-4}$ | ↘ |
| $\phi_T$, triplet yield | 0.7 | <0.5 | <0.2 | ↘ |
| $\tau_{S1}$ lifetime, ns | 10 – 22 | 0.4 – 1 | 0.008 – 0.05 | ↘ |
| $\tau_{rad}$ lifetime, ns | 128 | 121 | 160 | ↔ |
| $\tau_{ISC}$ lifetime, ns | 22-31 | 0.8 – 1.7 | <0.12 | ↘ |
| $\tau_{IC}$ lifetime, ns | 77 – 155 | 0.8 – 1.5 | <0.03 | ↘ |

[a)] Approximate values and general trends for typical systems only.

Additionally, in some cases the effects of particular deformations (*i.e.*, *sad*, *ruf*, *etc.*), have been distinguished. In relation to electronic absorptions, the higher-frequency deformation modes $B_{1u}(2)$ and $B_{1u}(3)$ that are correlated with the *ruf* conformation are particularly responsible for red-shifted absorption maxima. This observation may also be relevant to oxidation potentials as the red-shift has been shown to occur due to greater destabilization of the macrocycle HOMO compared to the perturbation of the LUMO energy.[121] Another clear cut example was the observation that the perturbations to photophysical properties in non-planar porphyrins were considerably amplified in ruffled compounds.

## Biological aspects and diversity of tetrapyrroles in nature

Porphyrins and their derivatives are an important class of compounds in nature, performing a multitude of biological functions acting as prosthetic groups in proteins. The best-known examples are the hemes and chlorophylls. The hemes are essential to the function of cytochromes, $P_{450}$s, hemo- and myoglobins and the peroxidases,[19a,122,123] in which they provide the active-site where the chemistry takes place (Fig. 12). Likewise, chlorophylls affect the fundamental processes in the light-reactions of photosynthesis by acting as light-harvesting chromophores and the primary agents of charge-separation.[124,125]

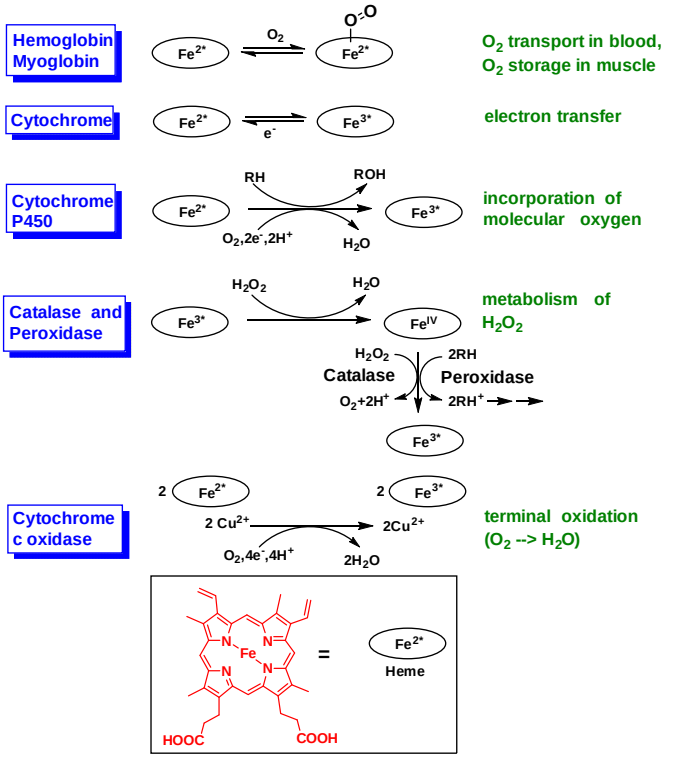


**Fig. 12** The functional flexibility of natural heme proteins.

The employment of heme as $O_2$-transporters, electron transfer agents and the providers of high-valent Fe-oxo intermediates is dependent upon the coordination and redox chemistry of the heme-Fe central substituent. However, the utility of the porphyrin ligand in heme is clearly beyond that of the formation of a stable metal-chelate complex rendering potentially deleterious free Fe less prevalent *in vivo*, or just to provide a 'handle' with which the protein may bind Fe

efficiently. In reality, heme is like all coordination complexes where ligands are crucial modulators of the properties of the metal centers.

In contrast, the macrocycle is the unambiguous site of the photochemical and photophysical processes that are required to affect photosynthesis so that in the chlorophylls the presence of the centrally coordinated Mg is intended to influence the properties of the ligand. This is clear not only because of, for example, the knowledge that charge-separation results in π-cations and -anions or the related fact that the $Mg^{2+}$ ion is redox inert (*i.e.*, does not change oxidation state during Chl redox reactions), but is especially emphasized by the photosynthetic roles of the pheophytins – the free-base derivatives of chlorophylls. Thus, photosynthesis is dependent upon the intense π*←π transitions of the macrocycle to yield broad action spectra (tuned during biosynthetic modification to suit the environment of the particular organism) whilst initial charge-separation is possible due to their capacity for photochemically induced electron transfer.

## Hemes

**Structure of hemes.** There is considerable diversity in the structures of heme-cofactors but the most commonly observed in natural systems are heme b **9**, the Fe-chelate of protoporphyrin IX from which all naturally occurring porphyrin-type hemes are derived, and heme c **35**, which differs from heme b by covalent attachment to its protein *via* thioether linkages formed between the α-vinyl carbons and (typically) cysteine residues in the common CXXCH binding motif (Fig. 13).[122] Heme b is found in the oxygen binding hemo- and myoglobins, the catalases and peroxidases, b-type cytochromes and all $P_{450}$ enzymes,[126] whilst heme c is most prevalent in their namesake, the c-type cytochromes.[127]

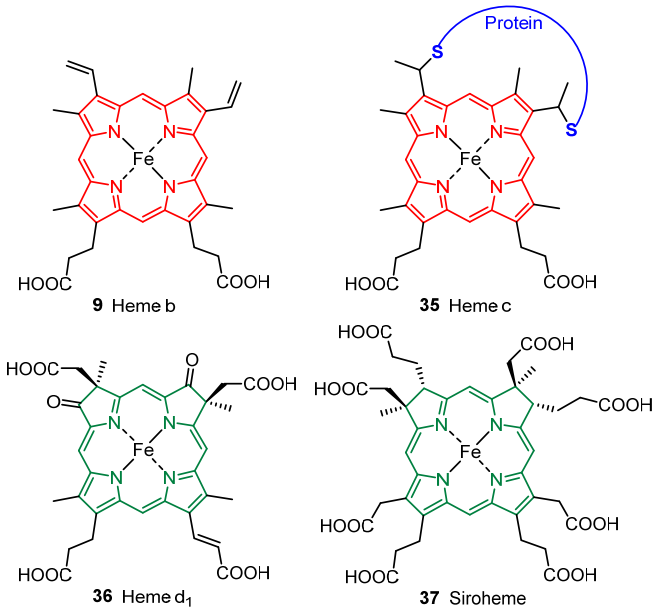


**Fig. 13** Heme b, schematic illustration of protein-bound heme c and two isobacteriochlorin type hemes.

Bound hemes are always at least penta-coordinate and commonly an additional residue provides an octahedral environment for the heme-iron. There are examples of hemes with relatively exotic axial ligands such as N-termini, proline or cysteinate residues,[122] but for heme c at least, usually bis-HIS, HIS-MET and (less often) MET-MET axial ligation is observed,[19a] whilst additional aquo ligands may lead to octahedral coordination in otherwise penta-coordinate HIS ligated hemes. A detailed analysis of the axial ligand preferences of hemes b and c revealed key differences including the greater prevalence of exchangeable small-ligands in hemes b and stereochemical constraints imposed on HIS orientation in hemes c.[128]

Additionally, there is a range of naturally occurring reduced "hemes" where two neighboring pyrrole rings are reduced at the $C_b$-$C_b$ bond. Formally that makes these compounds isobacteriochlorins and the two main classes are heme $d_1$ **36**[129] and siroheme **37**.[130] Both are found as cofactors in various sulfur and nitrogen reductases.

**Heme-protein functions.** Heme-containing proteins are well-known for their involvement in respiration, metabolism and small-molecule sensing across the bacteria, plants and higher organisms. Yet despite their early discovery, new functions continue to be uncovered including roles in gene regulation, cholesterol homeostasis and antibiotic synthesis.[122]

Hemo- and myoglobin are perhaps the best-known examples and function as the transport and storage vehicles (respectively) for the supply of $O_2$. The quaternary structure of hemoglobin consists of four subunits, each of which contains a single HIS-ligated heme that is capable of reversibly binding $O_2$ at the heme-Fe. In an impressive achievement for structural biology, the mechanism of heme co-operativity,[77,131] wherein initial binding of $O_2$ at one site increases the affinity of the rest, was uncovered to be the result of a substantial decrease in the Fe-HIS bond length upon $O_2$ binding associated with the altered oxidation level and spin-state of the heme-Fe. This results in the heme 'pulling' on the protein and induces a global conformational change that is communicated to the other sub-units and is responsible for the increased $O_2$ affinities of the remaining deoxyhemes.

In eukaryotic bacteria and mitochondrial membranes the respiratory electron transport chain (ETC) generates the proton gradient that drives metabolic oxidative phosphorylation and produces adenosine triphosphate (ATP).[132] Four of the five protein complexes in the sequence between the primary electron donors (NADH and FADH) and the terminal acceptor ($O_2$) utilize hemes as redox centers. In Complex II, the role of the heme (when present) is not fully understood and has been ascribed a structural function in maintaining the fold of the protein.[133] Mechanistic detail is available for cyt $bc_1$,[134] which accepts electrons from a soluble ubiquinol into heme-$B_L$ of the cyt b subunit directly whilst cyt $c_1$ is reduced via the 2Fe/2S-center simultaneously as electron transfer occurs from heme-$B_L$ to heme-$B_H$. Subsequently, heme-$B_H$ reduces a bound ubiquinone, which is released after a second reduction, and cyt $c_1$ reduces soluble cyt c. Cyt c

oxidase (or complex IV), the terminal enzyme in the ETC, accepts four electrons from four molecules of reduced cyt c and uses them to reduce molecular $O_2$ to water.

Although the precise mechanism of $O_2$ reduction is not closed to debate, it roughly proceeds as follows:[135] When fully reduced, cyt c oxidase binds $O_2$ at the heme $a_3$ / $Cu_b$ heterobinuclear site where a series of intra-protein electron transfer events and the uptake of two protons results in loss of $H_2O$ and the production of an oxyferryl intermediate ($Fe(IV)=O^{2-}$); Subsequently, another electron and proton are delivered to the heme $a_3$ – $Cu_b$ site producing a hydroxyferryl species (Fe(III)OH) which yields a second $H_2O$ molecule after receiving an additional proton. This leaves the $a_3$-$Cu_b$ site in the fully oxidized state which can be re-reduced by cyt c *via* $Cu_a$ and then heme a.

**Modulation of properties.** The modulation of heme reduction potentials is of utmost importance for establishing the position of cytochromes in inter-protein ETCs as well as the direction of ET in multi-heme cytochromes. In general, heme-protein reduction potentials exhibit an impressive range spanning 1 V from -550 mV to +450 mV *versus* SHE[136] and are a key-determinant of their function.[137] Considerable success has been achieved with respect to defining the effect of the axial ligand on key-properties such as reduction potentials. For instance, the horse heart mitochondrial cyt c M80H and *Desulfovibrio vulgaris* cyt $c_3$ H70M variants, both of which interconvert HIS-MET and bis-HIS heme coordination, reported a 200-220 mV lower potential for the bis-HIS ligated form.[138] This agrees with the isolated heme model compounds, which show a 150 mV decrease resulting from bis-HIS coordination relative to HIS-MET,[139] which is itself remarkably close to the 160 mV, found to best describe the difference in a study of 96 heme-proteins containing 141 hemes.[137]

There is also a significant influence of the peripheral substituents on the porphyrin ligand.[123] For example, a 50 mV decrease in the midpoint potential of bis-imidazole ligated heme b is observed simply by reduction of the 3,8-vinyl groups, which serves as a basic model for heme c. Moreover, through the *cis*-effect the donation characteristics of the porphyrin may alter the Fe's affinity for axial ligands as well as redox potentials.[123,140] Reconstitution experiments of native hemeproteins[141] with exogenous model porphyrins show clearly that these effects are relevant *in vitro*, too. For instance, a study that investigated the oxygen affinities of a series of reconstituted hemoglobins with heme derivatives bearing altered substituents at the 3,8 positions (vinyl in heme b) found that $O_2$ affinity was inversely proportional to the substituents inductive effects.[142] There are many more examples and this field has been recently reviewed by Hayashi.[141]

In addition to the effects of the porphyrin and axial ligands noted above, many other factors conspire to produce the large potential range, equivalent to a ~100 $kJ.mol^{-1}$ shift in the free-energy of reduction, and at this point they are quite well understood.[137] These include the protonation state and solvent exposure of the heme propionates, electrostatic effects of charged-residues in the binding-site and the inter-heme redox coupling (*i.e.,* the dependence of individual heme potentials on the redox state of nearby hemes in multi-heme complexes).[137,143] Thus, whilst variations in chemical structure are important when present, it is most commonly the particular construction of the binding site that serves as the most flexible modulator of heme properties *in vivo*.

### Heme $d_1$ and siroheme

Isobacteriochlorin type hemes ($d_1$ **36** and siroheme **37**) are involved in the cycling of sulfur and nitrogen. For example, the crystal structure of a sulfite reductase from *E. coli* revealed a hexacoordinated siroheme, the Fe center bound to a CYS thiolate and a phosphate anion. The siroheme-cofactor exhibits a distinctive non-planar conformation which has been traced to specific protein-cofactor interactions, and it was rationalized that the saturated ring system and its flexibility accounts for the specificity of sirohemes for sulfite reduction.[144] In a more recent structure of the dissimilatory sulphite reductase for a hyperthermophilic archaeon, two siroheme-cofactors are present, a functional and structural one. Both have similar conformations but are less distorted than the cofactor on the assimilatory sulphite reductase from *E. coli*.[145]

Similarly, non-planar macrocycles have also been implied in nitrite reductases. For example, the structure of oxidized cyt $cd_1$ (nitrite reductase) from *Thiosphaera pantotropha* showed a covalently bound, hexacoordinated (HIS, HIS) type c cytochrome and a planar, hexacoordinated (TYR, HIS) heme $d_1$.[146] The latter is in contrast to the distorted conformations of most other isobacteriochlorin-cofactors. Since macrocycle distortion favors ring oxidation, this has been initially interpreted by Fülöp and coworkers to indicate that the catalytic cycle of sulfite reductase involves ring oxidation whereas that of nitrite reductase does not. However, the reduction of nitrite reductase triggers a conformational change in $d_1$ making it non-planar,[147] and this reduction is thought to be responsible for the structural movements observed upon reduction of the protein.[148]

### Chlorophylls

**Photosynthesis and chlorophylls.** One of the most important biological processes for life on Earth is that by which plants, bacteria and algae harness the energy of the sun and store it in energy-rich reduced carbon compounds; the fundamental building blocks for all the naturally occurring organic matter that surrounds us. Furthermore, oxygenic photosynthesis (PS) was, and is, responsible for the appearance and continual regeneration of oxygen in the atmosphere that allows the efficient release of this stored energy by life *via* aerobic respiration and allowed the appearance of surface life by eliminating much of the harmful UV radiation. The main photosynthetic cofactors are the chlorophylls found in oxygenic PS plants (Chl a **7** and Chl b **38**), and the bacteriochlorophylls present in purple bacteria such as *Rhodobacter sphaeroides* (BChl a; **8**) and *Blastochloris viridis* (BChl b; **39**).[149,150]

 

At the heart of the initial stages of photosynthesis are the light-harvesting complexes (LHCs)[151] and the reaction centers (RCs),[21a] both of which contain numerous Chls or BChls that are crucial to their functions.[152] In LHCs,[153] light is captured by these cofactors in π*←π excitations and is 'funneled' *via* non-radiative energy transfer,[2,21a,152] toward the RC complex where electron transfer is initiated. Indeed, that the processes of light-harvesting, charge-separation and photo-protection all involve and depend upon numerous tetrapyrrole-cofactors is a true testament to their versatility. We have recently given an overview of the role of chlorophylls in photosynthesis and the various protein complexes involved, which covers these aspects in detail.[125]

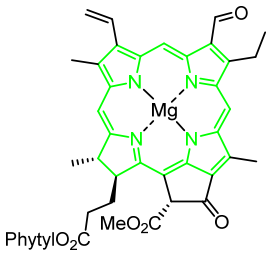


**38** Chlorophyll b (Chl b)

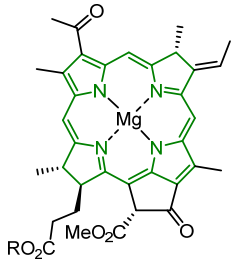


**39** Bacteriochlorophyll b (BChl b)

Over the years many crystal structures of chlorophyll derivatives have been reported.[88] In the context of the present discussion the most significant result of these was the observation of a wide range of conformations for chemically closely related pheophorbides and rhodochlorins.[34,87a,88,154] To highlight only one study, the high-precision structure of the BChl *a* derivative methyl bacteriopheophorbide *a* provides interesting details regarding the pigment's conformation.[155] The core bond lengths are largely symmetric around the $N_A$-$N_C$ axis and are well suited to the specific bond-order pattern indicated for BChl *a* above. The C3-acetyl is orientated significantly out-of-plane with respect to ring A (~23°), with the carbonyl oxygen closer to ring B, and the keto oxygen is evidently conjugated to the macrocycle on the basis of bond-lengths in ring E.

**Chlorophyll-protein interactions.** Aside from general architectural considerations, a number of specific protein-Chl interactions are known to influence their properties. Unlike heme, the axial ligand is not always a particularly dominant factor in determining the key-properties of protein-bound Chls as in the majority of cases the usual 5-coordination is fulfilled by HIS, the major function of which is to affect stable attachment to the protein. In detail, around 50% of protein-bound Chls are believed to be coordinated by HIS, although examples of coordination by GLN, ASN, backbone carbonyls and water are known, and the substitution of such a well-conserved feature is likely to be of importance.[156] However, the most exceptionally unique coordination yet observed appears in photosystem I (PSI) where both second accessory Chls are ligated by the sulfur atoms of MET residues, a feature that has been suggested to allow these Chls to act as the low potential electron acceptors in PSI.[157]

All Chls, and BChls in particular, possess carbonyl groups that are capable of acting as H-bond donors. In Chls, this is most important with respect to the keto oxygen on the cyclopentanone ring whilst additionally in BChls the acetyl provides another H-bond donor that is also strongly conjugated to the aromatic system. The presence of suitable acceptors in binding-sites is therefore one way in which a protein may regulate cofactor properties. Site-directed mutagenesis has been exploited to add and remove H-bonds to the C3-acetyl and $C13^1$-keto groups of the BChls comprising the special-pair dimer in the *Rhodobacter sphaeroides* RC and have shown that their individual effects on the BChl dimer's midpoint potential are additive at about +90 mV per new H-bond.[158]

Another important feature of binding-sites is the presence of any charged residues in the vicinity of the pigment that induce an electrostatic perturbation upon the cofactor. Positively charged residues stabilize the reduced form relative to the oxidized form, whilst the converse is true for negatively charged amino acids.[19b,159] Slightly more complex is the effect upon excitation energies, where the charge and its placement relative to the transition-induced charge-redistribution of the cofactor, may affect either blue-shifted or red-shifted absorptions.[19b,53] Likewise, the charged cofactors associated with intermediate states of charge-separations in RCs have a similar effect on neighboring cofactors.[160] Additionally, the energetic influence of dielectric relaxation of the protein occurring due to Coulomb interactions with the charged chromophores has been shown to stabilize the charge-separation intermediates.[161]

Note, some bacteria, *e.g.*, the green sulfur bacteria (*Chlorobiaceae*), contain chlorosomes as LHCs. Here, self-organized aggregates of the bacteriochlorophylls c-e (**40**-**42)** are utilized as antenna pigments *without* a structural protein matrix.[125,162] These pigments often exist as complex mixtures of homologues and can exhibit different macrocycle conformations.[34,88] As they are not directly bound to protein they are less important for our discussion here. Nevertheless, conformational differences between, *e.g.*, the BChl c **40** and e **42** *versus* d **41** series and different degrees of alkylation have been discussed in the context of light adaptation.[154e,163,164]

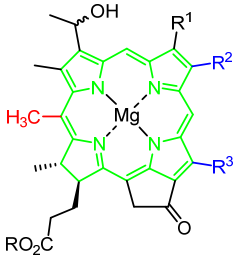


**40** $R^1$ = Me (BChl c)
**42** $R^1$ = CHO (BChl e)

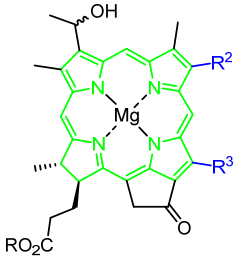


**41** (BChl d)

**Coenzyme $B_{12}$**

Cobalamins are ubiquitous natural compounds and their most prominent representative is coenzyme $B_{12}$ **11**. Chemically they belong to the class of corrins, *i.e.* lack one methine bridge and are highly reduced, nonaromatic tetrapyrroles. They typically contain a central cobalt ion which can form reactive Co-C bonds and are biosynthesized only in microorganisms.

Coenzyme $B_{12}$ is found in various isomerases, methyltransferases, and dehalogenases.[165]

Isolated corrins show a variety of often non-planar conformations and, due to the high degree of saturation in corrins, the basic framework is quite flexible.[43] Indeed, Geno and Halpern showed that this flexibility is a necessary requirement for the enzymatic reaction of vitamin $B_{12}$-dependent enzymes.[166] Additionally, the nucleotide base has been shown to contribute to the conformational distortion of the corrin ring in Coβ-cyanoimidazolylcobamide.[167]

By now, a number of crystal structures of protein-bound cobalamins are available.[167] These include a methylmalonyl-CoA and a glutamate mutase,[168] dehydrases, lysases and aminomutases,[169] a ribonucleotide reductase,[170] a bacterial shell protein bound to a cobalamin-cofactor and a human intrinsic factor with vitamin $B_{12}$.[171,172] All structures show very tight binding of the cofactor and steric effects are clearly involved in the cleavage of the Co-C bond. However, while protein-induced macrocycle distortions have often been discussed, clear cut evidence from protein crystals structures is still lacking in this case. For a full discussion of the various complexes see Gruber *et al.*[11]

**Factor $F_{430}$**

Other highly reduced tetrapyrroles such as $F_{430}$ show a very significant degree of conformational flexibility, too. $F_{430}$ **10** is the active cofactor of methyl coenzyme M reductase involved in methanogenesis and is the most highly reduced natural tetrapyrrole involved in enzymatic reactions.[12,13,173] Here, the central metal is a nickel species and a Ni(I) state functions prominently in the catalytic cycle.

Initial molecular mechanics calculations indicated that $F_{430}$, due to the presence of two saturated meso carbon atoms, can easily accommodate both high- and low-spin Ni(II) and Ni(I) ions.[174] EXAFS studies of low- and high-spin $F_{430}$ derivatives showed a span of Ni-N bond lengths in the range of 1.9-2.1 Å, indicating conformations ranging from planar to severely distorted.[175] The macrocycle conformation of the isolated cofactor $F_{430}$ is highly non-planar (Fig. 14) and the importance of the nickel ion in regulating the conformation of $F_{430}$, and vice versa, has been recognized early on.[176]

In contrast to the *sad* and *ruf* distorted conformations in the isolated $F_{430}$ complex,[12a] crystal structures of intact methyl-coenzyme M reductase show a very tightly bound cofactor with a relatively planar macrocycle conformation (Fig. 14).[12b,177,178,179,180] Here we have a situation where a non-planar macrocycle is made more planar by the apoprotein, with $F_{430}$ being sterically constrained against out-of-plane distortions in the native complex.[181] This interplay between protein constraints, macrocycle flexibility, core geometry and its effect on the chemical reactivity of the central metal ion was investigated in detail with NSD and various physicochemical methods by Zimmer and coworkers.[182] Recently, Cedervall *et al.* reported the structure of a chemically generated Ni(III) $F_{430}$ protein complex.[178] For comparison we have analyzed all available $F_{430}$ structures *via* NSD (Fig. 14). All protein-bound cofactor structures exhibit relatively similar out-of-plane distortions while the isolated compound exhibits significantly larger $B_{2u}$, $B_{1u}$ and $A_{1g}$ distortions.

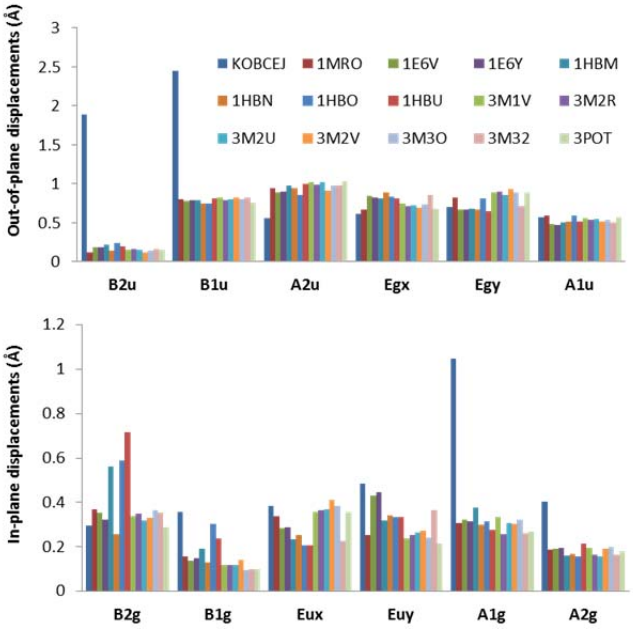


**Fig. 14** Mean out-of-plane complete basis NSD of isolated $F_{430}$ (KOBCEJ)[12a] and the $F_{430}$ cofactor in the various protein structures.[12b,177,178,179,180] Data for the latter were retrieved from the Protein Data Bank (PDB)[183] and analyzed with the NsdGUI Vers. 1.3α.[29,184]

**Linear tetrapyrroles**

Similar to porphyrins, a whole cornucopia of linear tetrapyrroles occurs in nature. All of them are derived from cyclic tetrapyrroles *via* ring-opening reactions of either porphyrins or chlorins. In many cases the *raison d'etre* is as a breakdown product of the cyclic precursor compounds to prevent photosensitizing reactions *in vivo* and for excretion from the body. Classic examples are the formation of bilirubin **43** and biliverdin **44** as heme catabolites[185] and related reactions in the degradation of chlorophylls.[186] However, except potentially for transport and linkage with serum proteins, these compounds are not protein bound.

Nevertheless, conformational aspects do play a role. Bilirubin is a classic example of a flexible molecule where the simple 2D representation of the molecular structure **43** is misleading and does not correlate with the *in vivo* situation. Only a specifically folded ridge-tile conformation with intramolecular hydrogen bonds **45** can explain its low solubility and the need for subsequent glucuronidation as part of the detoxification process.[187,188]

On the other hand, photosynthetic organisms contain functional linear tetrapyrrole protein complexes. Firstly, the photosensory phytochromes contain a phytochromobilin **46**. These are photoswitchable photosensors and regulate photomorphogenesis.[18,189] Similar to the visual process in animals, a *cis/trans* isomerization changes the shape of the

 

molecule and gives rise to conformational changes in the protein, which is the first step in the various signaling cascades.[190]

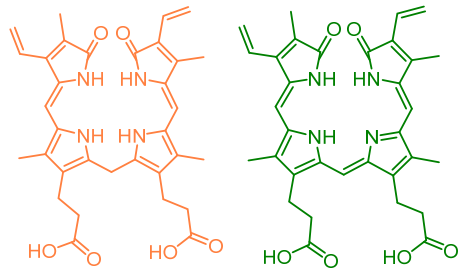

**43** Bilirubin **44** Biliverdin

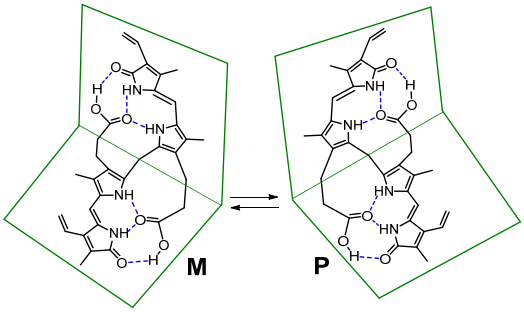


**45** Bilirubin (ridge-tile conformation of M and P enantiomers with H-bonds)

More recently, the bacteriophytochromes have been discovered as photochromic kinases in non-photosynthetic bacteria. They utilize biliverdin **44** as a photoreceptor in two-component sensor histidine kinases.[191] The emerging picture on their structures,[192] mechanisms and photoresponses reveals in detail the structural changes that follow photoisomerization and include nm scale movements of the bilins, significant changes in protein structure and folding, and their ultimate impact on the signal output domains.[193]

Secondly, linear tetrapyrroles function as accessory light-harvesting pigments in photosynthesis. They are parts of the phycobilisomes, highly organized pigment-protein complexes which act as antenna systems for photosystem II in cyanobacteria and red algae, amongst others.[16] More specifically, the phycobilins (*e.g.*, phycocyanobilin **47**, phycoerythrobilin **48**, and others) are part of the pigment protein complexes allophycocyanins, phycocyanins, phycoerythrins or phycoerythrocyanins, which are then assembled into phycobilisomes.[194] Individual phycobiliproteins have specific absorption maxima and their number, type and arrangement in the phycobilisomes allows for absorption and unidirectional energy transfer to Chl a in PSII. In this way the organisms can utilize light in the 500-650 nm range which is not possible directly with Chls.

The biosynthesis of the phycobilins involves ring-opening of heme b by heme oxygenase to yield biliverdin IX α **44**, which is then enzymatically converted into the various phycobilin pigments.[195] They have photophysical and stereochemical properties which are highly susceptible to the protein environment.[196] For example, their highly efficient chromatic adaptation[197] appears to be modulated in part *via* pigment-protein interactions (*vide infra*).

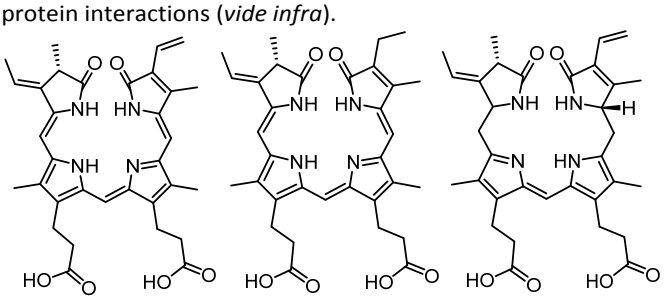

**46** Phytochromobilin **47** Phycocyanobilin **48** Phycoerythrobilin

## Case studies on tetrapyrrole non-planarity in biology

A complete analysis of all porphyrin-protein interactions in the various functional complexes is outside the scope of this article. Thus, in the following we illustrate the current state of the art by focusing on selected cases where the interplay between protein backbone and cofactor conformation has been studied using the methodological approaches outlined above.

### Shelnutt's systematic assessment of heme conformations

In 1995 Hobbs and Shelnutt demonstrated that the hemes in a diverse set of c-type cytochromes exhibited a conserved *ruf* conformation by a comparative structural analysis of the then available X-ray structural data.[26] It was shown that the distortion was predominantly induced *via* the CYS thioether linkages to the macrocycle and that this affected an asymmetric distribution of the pyrrole tilt angles with respect to the mean-plane. Additionally, on the basis of an earlier resonance Raman study that indicated a reluctance of metalloporphyrins with core-sizes ≥2 Å to ruffle,[198] they suggested that the distortion occurred at significant energetic cost to the protein. Together with the emerging knowledge that porphyrin conformation influenced redox potentials, these results were proposed to imply a functional significance of the conserved conformation. Moreover, they suggested that the oxidation state of the heme-Fe could be communicated through the heme's conformation *via* its protein-contacts, to potentially mediate the protein's interaction with its redox-partners.

In a series of landmark publications,[25,28,29] this study was expanded extensively by considering the heme conformations from a diverse set of crystal structures encompassing dozens of proteins and hundreds of crystal structures (including significant redundancy, albeit using case by case analyses). These advances were greatly assisted by the introduction of the normal-coordinate structural decomposition procedure for the analysis of porphyrin macrocycle conformations described above.[29,46] Structures of globins, cytochromes c, cytochromes $P_{450}$ and peroxidases, amongst many others, were included, and both species conservation of heme conformations in related proteins as well as new heme-specific structural differences within multi-heme proteins were revealed.[25,28,29]

For example, subtle differences were uncovered between the α- and β-hemes in human deoxyhemoglobin, with the former possessing mostly *dom* and *ruf* deformations and the latter *sad* and *dom* distortions.[29] In comparison, the predominance of the *dom* distortion remained evident in sperm whale deoxymyoglobin – although a unique contributing *wav* component was also observed.[28] The analysis of several cytochromes $c_3$ lent further credence to the notion that the segment between covalently linked CYS residues was crucial for determining heme conformation since only changes in this region were accompanied by cross-species conformational differences between equivalent hemes.[25] Notably, no systematic differences between reduced and oxidized cytochromes could be detected. Another result was that the non-covalently bound hemes b in peroxidases were all very strongly distorted with mostly *sad* conformations plus additional *ruf* contributions.[25,29]

A general result for nearly all proteins was that the heme conformations were well described by only a few of the normal-coordinates of the macrocycle alone (*i.e.*, to within the experimental error), suggesting that the distortions arose from an overall energetic perturbation from the binding-site as opposed to specific localized contacts.[29] In support of the reliability of the protein structural data for the purposes of comparing detailed macrocycle conformations, it was also reported for some examples that deviations in the NSD results amongst redundant structures resembled the coordinated error of a single atom in the resolved structures.[29]

**Chelatases**

Chelatases are enzymes which insert either Ni, Co, Fe or Mg ions into biosynthetic precursors of native porphyrins (Fig. 15). The best understood systems are ferrochelatase and magnesium chelatase which incorporate iron and magnesium into protoporphyrin IX, respectively. These enzymes are located at crucial crossroads in the biosynthesis of tetrapyrroles leading to committed intermediates and function as focal points for signaling pathways.[199]

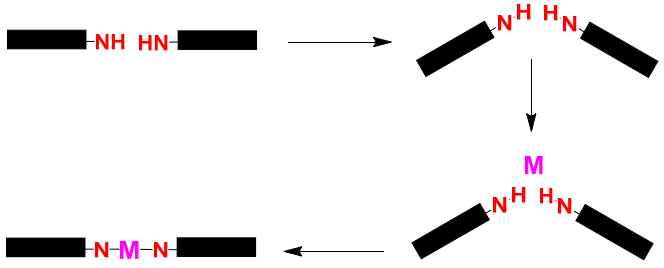


**Fig. 15** Illustration of the metal chelatase enzyme reaction.

The gradual unravelling of the distortion mediated mechanism of metalation exploited by chelatase enzymes represents a widely accepted example of conformational control.[15,200,201,202] Aside from the fundamental nature of this research, it is also biomedically relevant as mutations in ferrochelatase can lead to erythropoietic protoporphyria.[203] The idea that macrocycle deformation was a key step in the mechanism of metal insertion in general was originally based on the observation that *N*-alkylporphyrins, which have a distorted macrocycle,[204] underwent metalation 3-5 orders of magnitude faster than non-methylated derivatives.[205,206] Soon after it was discovered that such compounds are potent inhibitors of ferrochelatase[207] and it was suggested that the sterically imposed non-planar conformation was similar to a reaction intermediate. This idea was subsequently supported by the generation of an efficient antibody metalation catalyst that had been raised against *N*-methyl mesoporphyrin IX (*N*-MeMP, **49**).[208]

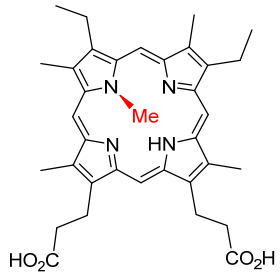


**49** *N*-Methyl mesoporphyrin IX *N*-MeMP

The structure of the active-site of ferrochelatase was first identified by Lecerof *et al.*[209] who obtained the crystal structures of the protein bound with both an *N*-MeMP substrate as well as the metallated product Cu(II)*N*-MeMP. The enzyme bound the ring A methylated isomer alone, similar to the antibody bound structure, although with greater distortion, indicating that tilting of pyrrole ring A contributed to the catalytic mechanism. Pyrrole rings B, C and D were each fixed by numerous contacts with the protein, described as "vice-like", and remained relatively in the mean-plane, although a general mix of *ruf*/*sad* conformation was apparent. Ring A, on the other hand, was tilted substantially by ~36° - which is greater than that observed in isolated *N*-MeMPs. Additionally, the structural similarity of ferro- and cobalt chelatases was cited as indicating a ubiquitous mechanism of chelation for all variants (Fig. 16)[210].

Sigfridsson and Ryde have performed a theoretical study that specifically addresses the importance of distortions for metal insertion by ferrochelatase.[211] They assessed the energetics of the macrocycle distortion of $H_2P$ (**1**) and a series of metalloporphyrins and found that not only were such distortions energetically feasible but that the distortions also provided a release mechanism for the product. They also confirmed that ring A of *N*-MeMP was distorted further by the protein rather than as a result of the steric crowding caused by the methyl protruding into the core. They also revealed that the dianionic deprotonated form of porphyrin was even easier to distort, implying that this intermediate would be energetically stabilized by the distortion imposed by the binding-site.

Comparison of the distortion energies of various MPs established an ordering of Co > Cu > Zn > Fe that was concordant with the fact that ferrochelatase can catalyze the insertion of these other metals into the porphyrin *in vitro* (the high-specificity *in vivo* is believed to arise because ferrous iron is most probably delivered directly to the enzyme by a molecular chaperone). Consideration of the same property of

 

CdP led to the conclusion that it was easier to distort than $H_2P$, providing a mechanistic possibility for the mode of inhibition by Cd. Optimization of protoporphyrin IX (*i.e.*, the free-base of heme b) in the ferrochelatase binding-site demonstrated that ring A of the natural substrate was also tilted by the protein in the same direction as the *N*-MeMP structure and that rings B-D were also (slightly) tilted to form a *sad* conformation.

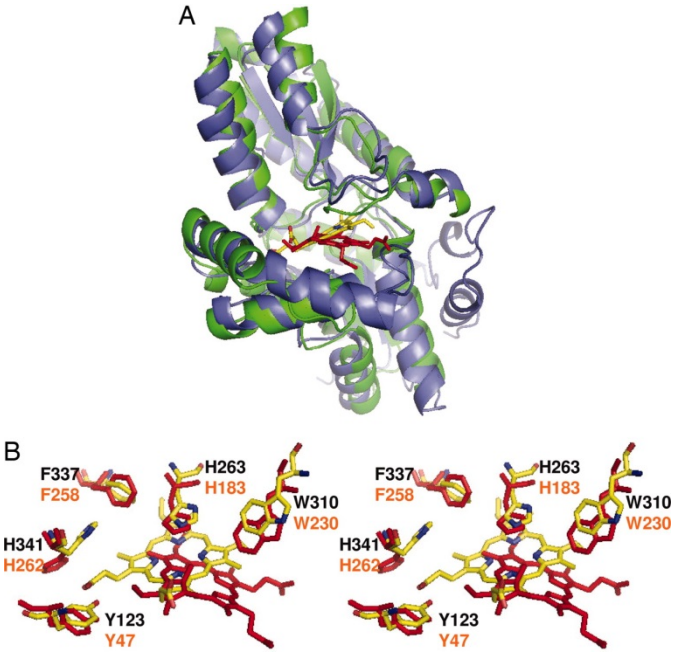


**Fig. 16** Comparison of the protoporphyrin IX and *N*-MeMP binding modes for human and *B. subtilis* ferrochelatase, respectively.[210] (*A*) Structural alignment of the E343K human ferrochelatase model containing protoporphyrin IX (blue) with the *B. subtilis* ferrochelatase model containing *N*-MeMP (green; PDB ID code 1C1H). (*B*) Stereoview showing the relative positions of protoporphyrin IX, *N*-MeMP, and the side chains of strictly conserved amino acids within the active sites. Reproduced from reference 210, © by the National Academy of Sciences.

The proposed mechanism received definitive validation when a Raman mode sensitive to the extent of non-planarity was shown to be directly correlated with catalytic affinity.[212] Lastly, Ferreira and coworkers[201] have taken these ideas a step further by employing directed evolution to create ferrochelatase variants that have greater selectivity for nickel over iron. These new proteins were shown to induce less saddling than the wild-type protein, and thus, their previous suggestion that "chelatases distort to select"[15] has proven to be correct.

### Chlorophylls in photosynthesis

Tetrapyrroles play many critical roles in photosynthetic pigment-protein complexes. They are the primary donors and acceptors in initial photosynthetic charge-separation,[21,152] the chromophores of the light-harvesting complexes,[151,153b,213] and the redox-cofactors responsible for the re-reduction of the primary donor[21,214] once their energetic excess has driven subsequent stages of the photosynthetic machinery. The simplicity of this description belies the beautifully intricate and complicated processes involved, and the many efforts to utilize this for biomimetic solar energy conversion.[9,215] However, at this point it suffices to say that these individual events demand drastically different behaviors from the cofactors, and although both hemes and chlorophylls are involved, the complexes that perform these tasks can do so only by exploiting their architectural utility as scaffolds and their ability to tune cofactor physicochemical properties through protein-cofactor interactions.

From the onset of our involvement in this area we were interested in studying conformational control in photosynthesis in more detail.[24] However, in the early 1990s only a few crystal structures of photosynthetic protein complexes were available. This situation has changed significantly since, and we have thus come back to our initial idea to study the role of chlorophyll macrocycle conformations in photosynthesis using a combination of conformational analysis, statistical methods and computational techniques.

**Functional tetrapyrrole conformations in bacterial photosynthetic reaction centers.** The largest body of structural information related to chlorophyll-protein complexes in photosynthesis is now available for the reaction center electron transfer chains (RC-ETC) from two species of purple photosynthetic bacteria, *Rhodobacter sphaeroides* and *Blastochloris viridis*. At the time of our initial analysis (2011)[216] 92 such protein crystal structures were accessible, and these served as the starting point for a statistically reliable analysis of the interrelationship between the biological function and macrocycle conformation of (bacterio)chlorophylls in photosynthesis.[216]

The bacteriochlorin-cofactors of the ETC are bound by one of two reaction center proteins (branches are denoted by L or M; synonymous with A and B, respectively), *via* numerous interactions including axial ligation by HIS residues in the case of the four bacteriochlorophylls, and are arranged in pairs of approximate $C_2$-symmetry (Fig. 17).[21,217,218] Once P (primary donor) is excited to P*, an electron is transferred to the primary acceptor BPheo ($H_A$) in ~2 ps and ~3-5 ps, for *B. viridis* and *R. sphaeroides*, respectively, the beginning of the formation of the cross-membrane electron gradient that drives PS.[152,219] This takes place through a scarcely detectable $P^+B_L^-$ intermediate that is formed rapidly after photo-excitation. Subsequent reduction of $Q_A$ by $H_A^-$ is followed by electron transfer from $Q_A^-$ to $Q_B$ (Q denotes quinones). After re-reduction of $P^+$, either directly by cyt $c_2$ in *R. sphaeroides* or by the RC-cyt in *B. viridis*, a second ET cycle takes place culminating in the reduction of $Q_B^-$ to $Q_B^{2-}$. At this point, the fully reduced and protonated $QH_2$ dissociates from its binding-site in the RC and is replaced by another oxidized quinone from the cytoplasmic pool.[220] A crucial feature of the RC is that electron transfer occurs only along the L-branch despite the apparent $C_2$-symmetry.[221]

There are two striking differences between the RCs from *R. sphaeroides* and *B. viridis*. Specifically, the RC from *B. viridis* utilizes BChl b and is in possession of a bound tetraheme cytochrome, whilst that from *R. sphaeroides* contains BChl a and does not have a bound cyt.[152] Other differences include the identity of the carotenoid close to the ET inactive

accessory BChl ($B_B$) and of the quinones (1,2-dihydroneurosporene, menaquinone-9 ($Q_A$) and ubiquinone-9 ($Q_B$) in *B. viridis* and sphereoidene and ubiquinone-10 in *R. sphaeroides*), as well as the detailed binding interactions of the pigments with the chromophores. There are also significant differences in the static physical properties of the RCs (*e.g.*, P960 in *B. viridis vs*. P865 in *R. sphaeroides*) as well as the kinetic parameters with respect to photo-induced charge-separation between the two species.[152,219]

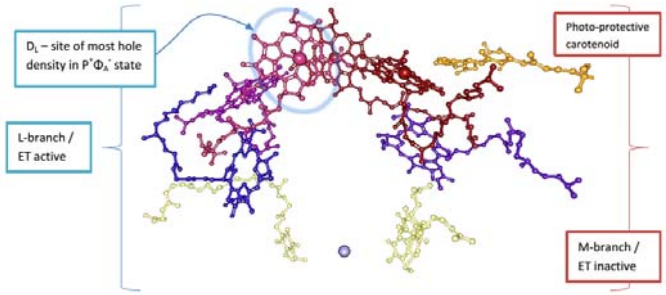


**Fig. 17** The prosthetic groups of the ETC of *R. sphaeroides*. Top left (pink; circled) $D_L$, top right (red) $D_M$, middle left (purple) $B_A$, middle right (dark red) $B_B$, bottom middle left (blue) $H_A$, bottom middle right (indigo) $H_B$, bottom left (yellow) $Q_A$, bottom right (yellow) $Q_B$ bottom middle (grey) $Fe^{2+}$ and top far right (orange) carotenoid. Note that each L, M (equivalent to A, B) pair is approximately related by a $C_2$ rotation about an axis which is located in the plane of the page and bisects the ETC into two halves.[218]

In our analysis of the RC pigments we determined the NSD for every BChl and BPheo from crystal structures of the RCs from *R. sphaeroides* and *B. viridis* obtained from the Protein Data Bank (PDB). The data was then analyzed *via* a methodical statistical route which included the investigation of the nature and reliability of each structure with respect to their description of the BChl and BPheo conformations.[216,222]

The initial analyses of the NSD data showed that many RC crystal structures exhibited consistent skeletal conformations for each individual BChl in the ETC, demonstrating that the conformations provided by many of the structure determinations were consistent with the idea that the individual binding-sites imposed distinct conformation on each cofactor. Moreover, there were both cross-species conservation of the conformations at particular sites as well as distinct differences at others, and many of the implied conformational differences represented a departure from the apparent $C_2$-symmetry of the ETC (Fig. 18).

Finally, we investigated whether it was possible to find validated best estimates of the conformation at each site by considering every RC crystal structure that was published in the PDB. This analysis ultimately provided the best experimentally determined macrocycle conformations of the cofactors to date and will hopefully be of use to computational chemists and crystallographers alike in modelling RC structure and function.[216]

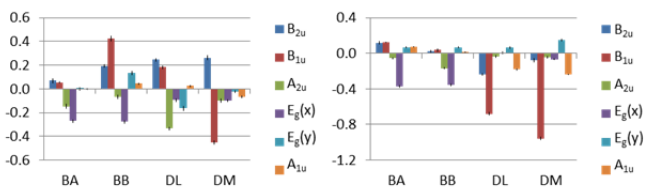


**Fig. 18** Mean out-of-plane minimum basis NSD of each ETC bacteriochlorin-cofactor in *R. sphaeroides* derived from crystal structures (left; subset RBC4, $n$ = 32) and *B. viridis* (right; subset BBC1, $n$ = 13). Y-axes in Å; error bars indicate two standard errors.

The conformations, together with the current understanding of the effects of non-planarity, tie in with the observed physical properties of ET in photosynthetic systems such as the species variant extent of the bathochromic shift of the special-pair, the preference for L-branch ET or the photo-protective action of $B_B$ in *R. sphaeroides*, amongst others, and therefore provide a new chemical rationale for understanding these processes.[223] An initial assessment of the energetic consideration of the distortions indicates that the conformational effects are likely on a par with both H-bonding and electrostatic effects. The concept of conformational control of tetrapyrrole-cofactors can clearly be used to address questions of functional significance in the bacterial photosynthetic RC in a statistically reliable manner. This indicates the general validity of this concept and shows that it can be extended to hemes, among other systems, and serve as a model for structural cofactor modulation in general.

**Photosystems I and II.** As there have been only a few reported crystal structures of PSI, a large-scale statistical analysis analogous to that performed for the bacterial RCs is not possible at present. Except for the structure of PSI from the cyanobacteria *Synechococcus elongatus,*[157] most of these are of such low resolution as to preclude a discussion of the chlorophyll conformations.[224] In contrast, more structures are available for PSII. However, these structures again are of low resolution, with many in the range 3 – 7 Å.[225] Amongst the remaining ones, there are two particularly interesting candidates, namely structures 3ARC and 4IL6 at 1.9 and 2.1 Å resolution, respectively.[226,227]

The NSDs of the cofactors from the highest-resolution crystal structure of PSI[157] (PDB ID: 1JB0), taking into account the error estimates for this structure, indicate that there are almost no significant conformational differences between $C_2$-related pairs of cofactors aside from the greater *sad* deformation of $P_B$ compared to $P_A$ (Fig. 19a).[228] In general contrast to the bacterial RCs (and also PSII, described later), the cofactors with the largest degree of non-planarity in the PSI ETC are the first accessories, $Chl_{A1}$ and $Chl_{B1}$. Quite uniquely, both cofactors possess a very large *sad* distortion, which is one of the largest single-mode deformations of all the ETC BChls and approached only by the ~1 Å *ruf* of the *B. viridis* $D_M$. This is complemented with a comparatively minor *ruf* component that is identical to that of the special-pair Chls and is also comparable to $B_B$, $D_L$ or $D_M$ from *R. sphaeroides* (*i.e.* 0.4, 0.2 or −0.4 Å), within the margin of error. These Chls also exhibit a small, yet likely significant degree of the *dom* mode in the direction of their

 

HIS ligands, whilst in terms of their in-plane conformations they have a larger *N-str* ($B_{1g}$) than the other PSI ETC Chls. Additionally, $Chl_{B1}$ exhibits a moderate core contraction relative to the rest, as indicated by the decreased *bre* deformation ($A_{1g}$) and, although technically not significant with respect to the estimated error for the IP normal-deformations (0.23 Å), is worth mentioning because of the relative consistency of the other Chls' *bre* distortions as well as this modes usual association with increased non-planarity.

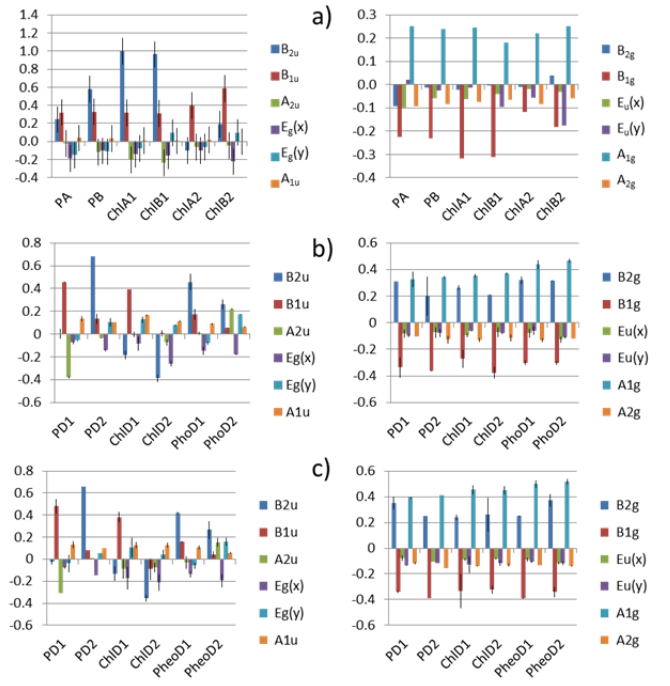


**Fig. 19** a) Out-of-plane min. basis NSDs (left) of the ETC cofactors in PSI (PDB ID: 1JB0);[157] error bars show ± one half of the Luzzati error; $\delta_{oop}$ = 0.0203, 0.0247, 0.0422, 0.0389, 0.0120 and 0.0149 (left-to-right). In-plane minimum basis NSDs (right); error bars are not shown as the required $\pm\pi/4$ times Luzzati error (0.23 Å) overwhelms the plot; $\delta_{ip}$ = 0.0484, 0.0443, 0.0548, 0.0571, 0.0492 and 0.0513 (left-to-right). b) Mean out-of- (left) and in-plane (right) minimum basis NSDs of the ETC cofactors in PSII (PDB ID: 3ARC);[226] error bars show ±s.d. between the two corresponding cofactors in the asymmetric unit. Mean $\delta_{oop}$ = 0.0410, 0.0300, 0.0364, 0.0332, 0.0294 and 0.0354 (left-to-right); mean $\delta_{ip}$ = 0.0648, 0.0644, 0.0637, 0.0670, 0.0679 and 0.0698 (left-to-right); e.s.u. based on $R_{free}$ = 0.090 Å. c) Mean out-of- (left) and in-plane (right) minimum basis NSDs of the ETC cofactors in PSII (PDB ID: 4IL6);[227] error bars show ±s.d. between the two corresponding cofactors in the asymmetric unit. Mean $\delta_{oop}$ = 0.0409, 0.0308, 0.0328, 0.0439, 0.0249 and 0.0341 (left-to-right); mean $\delta_{ip}$ = 0.0653, 0.0685, 0.0677, 0.0677, 0.0700 and 0.0738 (left-to-right); e.s.u. based on $R_{free}$ = 0.154 Å.[228]

The conformational asymmetry of $P_A$ and $P_B$ of the special-pair heterodimer, in the form of a dominant *sad* conformation for $P_B$., is somewhat reminiscent of the situation in both the RCs where the M-branch BChl was generally more non-planar than the other. Aside from this feature, both Chls are characterized by the same *ruf* distortion as the first accessories. Finally, the second accessory Chls may possess a slightly greater *ruf* conformation and very nearly display significant differences across the $C_2$-axis, with $Chl_{B2}$ exhibiting larger *ruf* and *sad* deformations. Taken together, the analysis suggests that two PsaB Chls may be only slightly more distorted than their PsaA counterparts, if at all, which is in stark contrast to the purple bacterial RCs where the M-branch BChls were consistently more non-planar. However, this result could be significant, re-calling that in PSI both branches participate in ET.[229] It can also be noted that the greater distortion of the accessory chlorophylls of this RC compared to both RCs and PSII in light of the fact that these Chls have been implicated as the primary donors.[230]

The normal-deformations for the cofactors obtained from the two highest resolution structures of PSII are rather similar (Fig. 19b and c). However, there are small differences between the resolved conformations from each which indicates that atomic configurations in structure 4IL6 were allowed to deviate from the starting model 3ARC. In contrast to PSI, the high resolution structure of PSII[226] indicates considerable asymmetry of the cofactor conformations across the $C_2$-axis. $P_{D2}$ possesses the most distortion with a well-defined *sad* conformation. A striking feature is that $P_{D1}$ displays a similar degree of the *dom* distortion compared to $D_L$ of the *R. sphaeroides* RC, although $P_{D1}$ has a greater contribution from the *ruf* mode than this BChl. The $C_2$-asymmetry continues with $Chl_{D1}$ displaying a *ruf* conformation quite dissimilar to $Chl_{D2}$'s mixed *sad* and *wav* deformations. The pheophytins are also suggested to be distinguishable with PheoD1 possessing substantial *sad* and some *ruf* contributions to its conformations, whilst PheoD2 has about half the degree of *sad*, and also similar contributions from *dom* and *wav*. In common with the bacterial RCs, PSII displays considerable branch-asymmetry with respect to ET. It is perhaps significant that the active branch cofactors exhibit greater *ruf* distortion than their counterparts.

Saito *et al*. have already addressed the influence of differences in the PSII ETC Chls *a* conformations, as revealed by the 1.9 Å crystal structure[226] using a modified NSD and a MM/QM approach.[231] They found that the dominant *dom* conformation of the $P_{D1}$ cofactor (conserved from certain RCs) could stabilize the oxidation of HIS-ligated Chls generally, but not in the RC specifically. Also, whereas doming was induced by axial ligands alone in $P_{D2}$ and $Chls_{D1/D2}$, an interaction between the peripheral substituents of $P_{D1}$ and the protein affected its conformation. Additionally, greater ruffling of the RC-cofactors of the D1 branch (*i.e.*, the active branch) was observed to potentially contribute to ET asymmetry in the RC. However, whilst all these points were noted to be correspondent with the charge-distribution in $P_{D1/D2}^{+\bullet}$ and ET asymmetry in general, it was suggested that the conformations were likely only indicative of the local steric environment of the cofactor and that the dynamics were affected by the electrostatic influences of the protein. This was based on an earlier study regarding the determinants of the hole distribution of $P_{D1/D2}^{+\bullet}$ in PSII where they had found only slight charge asymmetry (favoring $P_{D1}^{+\bullet}$) when calculated without the protein environment, which was attributed in part to differing phytol conformations.[232]

**Quantifying conformational control – Conformational modulation of heme redox potentials in the *B. viridis* reaction center cytochrome subunit.** If the examples presented so far are taken to indicate the validity of the concept of

conformational control then the question arises to what extent changes in the conformation contribute to the overall modulation of a cofactor's properties as opposed to other 'forces' such as H-bonding, changes in dielectric constant, etc.? Our analysis of the bacterial photosynthetic reaction centers[216] allowed the development of a systematic method for an unbiased critical analysis of the reliability of entire RC crystal structures, and sets thereof, with respect to their appropriateness for the detailed comparison of the cofactor conformations displayed at different sites. Next, we attempted to take this further by *quantitatively* assessing the role of conformational control in modulating the reduction potentials of the hemes in the RC tetraheme cytochrome subunit (RC-cyt) of *Blastochloris viridis*.[233]

This subunit is tethered to the RC in the periplasmic space above the membrane and serves the purpose of re-reducing the oxidized special-pair of the electron transfer chain.[21] The four hemes are grouped into pairs of low- and high-potential cofactors and these pairs are arranged such that a chain of alternating low/high redox potentials is created through to the special-pair (*i.e.*, low, high, low, high, SP; Fig. 20).[234]

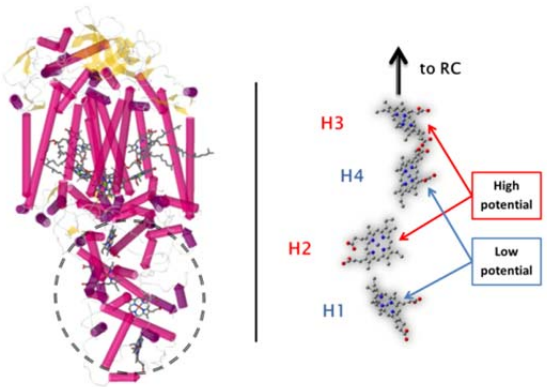


**Fig. 20** Illustration of the tetraheme cytochrome subunit in the reaction center of *B. viridis*; image adapted from the coordinates of PDB ID: 1PRC.[233]

Again, our investigation required a statistical analysis of the heme conformations afforded by the available crystal structure data, although in this case, the effect on reduction potentials was not inferred; instead it was explicitly calculated using an experimentally calibrated computational procedure.[235] This method utilized heme-Fe partial atomic charges and proved useful with the computationally inexpensive B3LYP/3-21g method calculated for simplified heme models extracted from the PDB,[183] incorporating only the effects of varying macrocycle conformations and thereby delineating their physicochemical effects. The method was successfully calibrated using the atomic coordinates and published midpoint potentials from the heme-cofactors in wild-type and mutant heme-NO and -$O_2$ binding domains which confirmed the sole conformational modulation of the redox potentials in these complexes. This procedure was then applied to the RC-cyt indicating that 'conformational control' may account for up to 70% (54 mv) of the observed differences in the reduction potentials of the four hemes. This approach was validated using larger basis sets up to and including the triple-ζ, doubly polarized and augmented 6-311+g** basis.[235]

**FMO protein and other light-harvesting complexes.** The success in quantifying structure-function relationships in RC and heme complexes prompted us to return to the more light-harvesting complexes. For initial studies in this area we chose the Fenna-Matthews-Olson protein (Fig. 21). Historically, this is the first crystal structure of a chlorophyll-containing protein and remains the most widely investigated protein-Chl complex.[236,237] It functions as the excitation energy transfer (EET) intermediate between the chlorosome baseplate and the RCs of the photosynthetic green sulphur bacteria and contains seven BChl a pigments.[125,213,237,238]

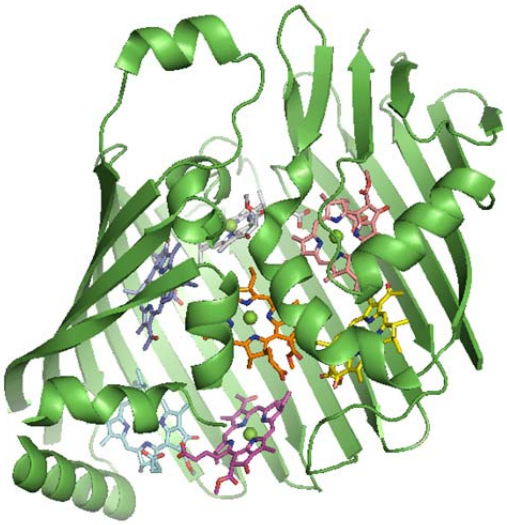

**Fig. 21** Illustration of the FMO protein monomeric asymmetric unit. From bottom left to center *via* an approximate '9'-shaped spiral: BChl 1 (pale blue), 2 (purple), 3 (yellow), 4 (pink), 5 (grey), 6 (blue) and 7 (orange). The image was created from the crystallographic coordinates found in PDB ID: 4BCL[238] using PyMol.

The available structural data for the FMO protein indicate that the BChls display a significant degree of conformational heterogeneity of both their peripheral substituents and the non-planar skeletal deformations of their tetrapyrrole macrocycles. While modulation of the site-energies[239] of specific pigments and thus of the EET dynamics is fairly well characterized for the dihedral angle of BChl a's C3-acetyl substituent, the situation is not so clear when considering the effects of the protein-induced non-planarity of the tetrapyrrole macrocycle. Initial results indicate that this is partly the result of an inability of the molecular models usually employed to delineate framework and substituent effects (*i.e.,* sequential truncation studies) to account for interactions between the macrocycle conformation and the effects of the substituents. We are currently developing an alternative approach that can account for this phenomenon and will use it to assess the conformational effects upon site-energy distribution amongst the BChls in the FMO complex.[240,241]

Zucchelli *et al*. have attempted to use NSD directly to determine the *intrinsic* site-energy distributions[239] of Chl pigments in light-harvesting complexes.[242] In this approach,

 

the four-orbitals of Chl that have greatest influence over the $Q_y$ transition are considered to be perturbed in proportion to the extent of macrocycle deformations that possess the same symmetry. In this scheme then, both $E_g$ (*wav*) distortions affect blue-shifts whilst the $A_{2u}$ (*dom*) and $A_{1u}$ (*pro*pellering) modes affect red-shifts; it produces site-energy distributions in remarkable agreement with other methods.[242b]

**H-NOX, cytochromes and other hemeproteins**

**Bioengineering of hemeproteins: H-NOX, a prototype for rational protein design?** The heme nitric oxide and oxygen binding domain (H-NOX) has become the subject of active research for its endogenous biological regulatory role in small-molecule sensing,[243] its potential as a tunable model system for biomimetic applications[244,245] and in particular, for the highly non-planar conformation imposed by the protein on its single heme-cofactor.[246,247,248,249,250,251,252] This is one of the most distorted heme-cofactors to be observed in natural systems,[247] and this feature has been linked to its uncommonly high midpoint potential[248] and is likely crucial to its biological function.

H-NOX proteins are proving to be particularly fruitful model systems that are being well explored. Aside from the physical characteristics that render them attractive for potential uses (*e.g.*, exceptionally high thermal stability), their biomedical importance with respect to the crucial role of the NO–sGC–cGMP signaling pathway in humans, and thus related pathologies,[253] gives research in this area an additional impetus.

The crystal structure of the H-NOX domain isolated from the obligate anaerobe *Thermoanaerobacter tengcongensis* (Fig. 22) revealed an exceptionally distorted heme, whose degree of distortion was shown to be related to global structural changes on the surface of the protein, providing a potential link to heme conformation and signal transduction. This work by Kuriyan and coworkers was ground breaking as this crystal structure provided the first atomic resolution picture of a heme binding-site with significant sequence homology to the soluble guanylyl cyclase heme domain in vertebrates.[247]

**Fig. 22** View of the H-NOX domain structure from *Thermoanaerobacter tengcongensis* (PDB ID: 1U56; image created using PyMol).[247]

Recently, Marletta's group at UC Berkeley showed that mutation of the conserved PRO115 residue present in very close proximity to the heme (van der Waals contact) to the less sterically demanding ALA residue affected heme relaxation to a more planar conformation in both the solid state *via* crystallography[248] and in solution using resonance Raman spectroscopy.[249] This structural change also led to increased oxygen affinity and lower midpoint potentials of the complex. The generation of other mutants with intermediate degrees of macrocycle distortion demonstrated that the redox potential was systematically modulated by the heme conformation (Fig. 23).[246] Other important developments include recent conformation of the connection between heme flattening and signal transduction in further mutational studies,[252] and an early technological application that involved the replacement of a single tyrosine residue to affect loss of the heme's oxygen binding ability for the creation of a NO sensor.[250]

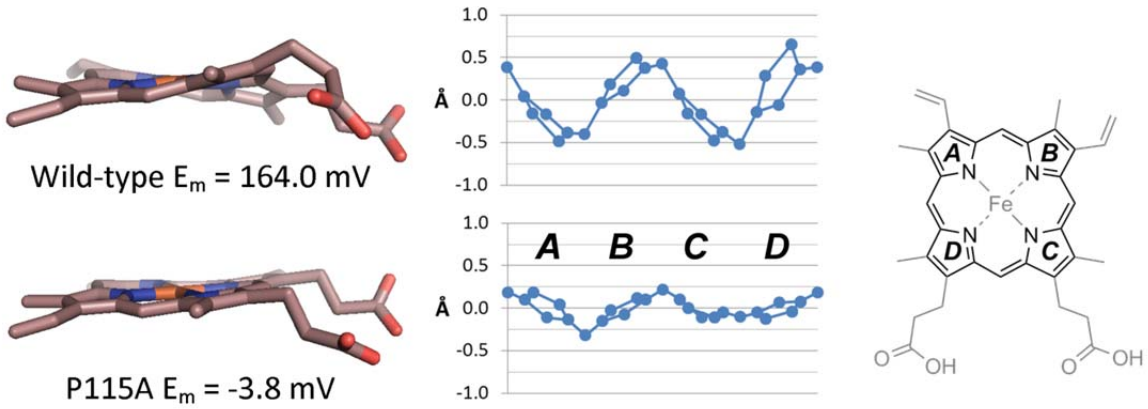


**Fig. 23** The heme conformations in the wild-type[247] and P115A[248] mutant H-NOX complexes (PDB IDs: 1U56 and 3EEE, molecules A and D, both respectively) illustrated by side-on views and skeletal deviation plots, which indicate core macrocycle atoms vertical displacements from the mean plane.

Clearly, H-NOX provides an excellent system for understanding how and why nature exploits conformational control but it is also becoming a prototype complex for the artificial exploitation of the effect to fine-tune physicochemical properties and to go beyond. Marletta has begun to apply another major design principle, that of substitution of the native heme-cofactor with other porphyrin molecules.[254] Cofactor reconstitution experiments involve substitution of the native cofactor by either a stepwise approach first employing the removal of the native ligand or in a concerted approach relying on stoichiometric saturation with the desired replacement compound. A more modern method is to express the protein in a system that has access only to the exogenous ligand.[255] In any case, the original motivations for the procedure in general were analytical and indeed some noteworthy results have been obtained from reconstitution experiments involving photosynthetic RCs.[256]

The first example of such a heme-substituted H-NOX unit was reported recently and involved the incorporation of (CO)(mesoporphyrinato IX)ruthenium(II) into the heme site using the expression methodology with the goal being the creation of a useful molecular oxygen sensor based on phosphorescence quenching.[244] The results indicated a clear success as emphasized by the complexes steady-state absorption/emission spectra in the presence and absence of $O_2$ and, moreover, exited-state dynamics that yielded an $O_2$ detection precision comparable to that of commercial sensors. The same communication reported an analogous complex formed using myoglobin (Mb) as the protein scaffold and a comparison of its photophysical parameters to those of the H-NOX Ru mesoporphyrin complex indicated wholly different pigment conformations and/or chemical environments. The authors concluded with a forward-thinking, yet in practice likely reachable, statement regarding potential further tailoring of photophysical properties using other porphyrins or protein modification; biological targeting using genetically encoded tags and enhancing biocompatibility *via* additional derivatization.

The latest application of heme-substituted H-NOX proteins is as a contrast agent for the burgeoning and broadly impacting method of magnetic resonance imaging (MRI).[245] Here, Winter *et al.* first noted that the H-NOX complex containing its native high-spin Fe(III) heme possessed significantly higher longitudinal and transverse proton relaxivities than Mb. To further enhance this property, they then generated a series of reconstituted H-NOX complexes using Mn(II) and Mn(III) complexes of protoporphyrin IX and a Gd(III) mesoporphyrin IX complex, since these paramagnetic metals are known to be highly effective in this regard. Although modest in their report, their results for the Gd complex are truly astounding as emphasized by relaxivities approximately 10 times greater than those of the current commercially available Gd(III) chelate based contrast agents. The Mn(III) substituted H-NOX also showed improved values compared to a commercial equivalent (approximately 4 times greater for the longitudinal relaxivity), whilst the reduced Mn(II) form was only marginally better.

Although not an example of an H-NOX application, a related study by Jasanoff and coworkers reporting a Mn-substituted cytochrome serves to show the potential benefits of further protein design.[257] Here the choice of protein scaffold was the heme domain found in cytochrome $P_{450}$ BM3 (BM3h) and they inserted Mn-PPIX by co-expression of the scaffold with the heme transporter ChuA. Crucially, they also generated their complex with a series of mutated forms of the cytochrome and demonstrated that each possessed distinctly different proton relaxivities and changes therein upon substrate binding.

**Contemporary studies on other hemeproteins.** Bren and coworkers have performed a number of studies on the effects of non-planarity in cytochromes.[258,259,260] One of their recent achievements in this field has been the development of NMR as a technique for assessing the impact of ruffling on the electronic structure of heme on a per atom basis.[259] This multi-faceted and impressively thorough study combined site-specific mutations[261] to vary the extent of heme ruffling and to control the heme MET axial ligand's binding mode in *Hydrogenobacter thermophiles* cytochrome $c_{552}$, with NMR, EPR and DFT to assess the resultant spin-density distributions and the heme-Fe orbital energies. They confirmed that the mutation affected decreased *ruf* distortion *via* $^{1}$H NMR and were then able to identify new $^{13}$C chemical-shift – ruffling correlations. The specific changes indicated that the spatial extent of the spin-density distribution was decreased at both the heme's $C_m$ and $C_b$ positions as a result of ruffling. Notably, EPR suggested that the relative energies and contributions to the HOMO of the Fe *d*-orbitals did not change appreciably, indicating a distinct difference of the effect of *ruf* distortion in this cytochrome compared to other *ruf* distorted model compounds containing strong π-acceptor ligands where configurations change from $(d_{xy})^2(d_{xz},d_{yz})^3$ to $(d_{xz},d_{yz})^4(d_{xy})^1$. This highlights the complicated relationship between the effects of distortion in concert with other environmental aspects.

In a follow-up focused upon delineating the influence of *ruf* distortion *vs*. Fe(III)-HIS bond strength on the EPR spectra of *H. thermophiles* cyt $c_{552}$ and *Pseudomonas aeruginosa* cyt $c_{551}$, it was again suggested that heme ruffling was correlated with decreased reduction potentials.[260] However, here the results were confounded by the fact that the reduction potentials of the mutants could also be explained by a change in the Fe(III)-HIS bond strength. However, the effects were considered separable on the basis that the observed change in the EPR axial ligand field term was opposite to what would be expected from changes in the axial HIS bond strength. As a result, the decrease of the axial term was shown to be consistent with increased *ruf* distortion and thus it was concluded that the axial bond strength was mostly invariant across the mutants so that the observed changes in spectral features and reduction potential were attributed to the effects of heme ruffling.

The observation that the heme degrading proteins IsdI and IsdG (iron-regulated surface determinant) produce oxidation products that are very different to those from the typical heme oxygenase enzymes (HOs)[262] has been attributed to the

 

extremely large ruffling induced in the protein bound substrate heme.[263,264] Takayama *et al*. found that IsdIFe$^{3+}$(CN) possessed exceptionally small average methyl proton chemical shifts and large paramagnetic shifts of the meso hydrogens.[263] This indicated greater delocalization of the heme-Fe's unpaired electron onto the meso carbons compared to the β-pyrrole carbons and was suggested to result from the dominance of the $(d_{xy},d_{yz})^4(d_{xy})^1$ configuration over the $(d_{xy})^2(d_{xz},d_{yz})^3$ state. This was rationalized as a result of the ruffling allowed overlap of the macrocycle $2a_{2u}(\pi)$ orbital with the Fe $3d_{xy}$, the former having large values at the meso and nitrogen skeletal atoms. Such a change in the electronic configuration has been observed in ruffled FeP model compounds only when strong π-acceptor axial ligands are present although it was posited here to exist in dynamic exchange in the native protein, on the basis of the methyl proton resonances; it is highlighted that the $(d_{xy},d_{yz})^4(d_{xy})^1$ configuration may facilitate oxidative susceptibility of the heme meso positions.

Additionally, the structural consequence of the excessive ruffling appeared to present the heme β- and meso carbons to the oxygen binding site.[263] It was also suggested that ruffling works against differences in the H-bonding and dielectric properties of IsdI compared to typical HOs, which are predicted to raise the potential of IsdI relative to HOs. However, because the observed $E_m$s are similar, it was also suggested that the increased ruffling lowers the reduction potential, similar to the situation in *H. thermophiles* cyt $c_{552}$ and *P. aeruginosa* cyt $c_{551}$ noted above.

Following this study was a report of a mutant IsdI, with reduced heme ruffling and substantially diminished activity.[264] Since the $E_m$ of the mutant was similar to wild-type, the decreased activity was suggested to occur entirely due to the removal of the ability of the protein to substantially ruffle the heme. The TRP66 residue is noted to be conserved in both IsdG and IsdI and is in direct contact with the heme's β-meso carbon, and therefore contributes substantially to the conformation. Mutations in this position were previously shown to reduce the catalytic activity of IsdG.

In this study, the IsdI variants exhibited macrocycle distortions ranged over 1.3 – 2.3 Å, most likely a significantly greater energetic variation than in the H-NOX study (in which the range was up to ~1 Å) and supposed to be enough to alter the electronic configuration. Importantly, the TRP66 residue was shown not to be required for substrate binding, although heme degradation activity was dependent on AAs with large side-chains being present in this position. The electronic spectra and the p$K_a$s of the distal water ligand of two of the variants contrasted with the wild-type such that they were more similar to classic HOs. These changes were attributed to the decreased ruffling, confirmed for W66Y by X-ray crystallography. In particular, the Soret and Q-bands of the variants were blue-shifted relative to WT, in agreement with expectations but also lending more credence to the distortion / red-shift theory, as these conformation alterations were achieved without chemical modification of the heme. $^1$H NMR indicated a significantly smaller contribution of the $(d_{xy},d_{yz})^4(d_{xy})^1$ electronic state in W66Y. W66F was neither crystallized nor were its methyl resonances assigned, however, on the basis of the nature of the mutation and the fact that all corresponding paramagnetic shifts were lower field than those in the W66Y, it was suggested that this variant possessed even less ruffling. This is consistent with the idea that ruffling is essential for degradation as the W66F mutant was kinetically slower than W66Y.

Another recent study demonstrated that $O_2$ affinities in protoglobin are affected differently by non-planar and in-plane distortions so that increasing *ruf* distortion is correlated with decreased affinity (in line with the results from H-NOX studies discussed earlier), whilst core contraction also results in decreased affinity.[265] This effect is not surprising since core contraction is itself correlated with increased *ruf*, yet interestingly compression (or expansion) along a single $N_{opp}$-$N_{opp}$ axis also decreases the $O_2$ affinity. A similar non-planarity / $E_m$ correlation to that found in H-NOX (*i.e.*, that is somewhat at odds with the result of the previous few conclusions) is suspected in *E. coli* succinate dehydrogenase (a complex II homolog), where its high $E_m$ has been attributed partially to the substantial *sad* deformation of the heme b cofactor.[266] Additionally, it was speculated that the heme conformation may play a regulatory role by exhibiting sensitivity to the redox state of the quinone pool.

**Linear tetrapyrroles – Phycobilins**

Some conformational aspects of linear tetrapyrroles were outlined above in the brief discussion of natural bilins. The rapidly increasing number of crystal structures of components of the phycobilisome now allows taking an initial look at the native conformation of linear tetrapyrroles as photosynthetic pigments, especially in comparison to our studies related to chlorophylls.

Taking the (bacterio)phytochromes and light-harvesting phycobiliproteins into account as well, a general picture is emerging.[193] On one hand we have the classic photochemical *cis/trans* isomerization with subsequent conformational changes in the protein acting as a signal output for the various signaling cascades. The majority of known (bacterio)phytochromes, including the one from *Aradinopsis,*[267] shows the bilin in a *ZZZssa* configuration in the dark.[193,268] Herein, the A–C rings are relatively coplanar and the D-ring is rotated out of the mean plane. The classic mechanistic proposal then involves a photochemical *Z* → *E* isomerization of the C15=C16 double bond (to yield the bilin in *ZZEssa* configuration),[269] which results in a flipping of ring D with associated changes in bilin-protein interactions, movement of the chromophore and protein conformational changes.[270]

Most intriguing is the wide range of absorption which can be covered by the totality of the bilin chromophores (Fig. 24).[271] Depending on bilin type and the mode of protein attachment, almost the whole visible spectrum and the near UV region are covered. Attachment to the protein and protein-chromophore interactions can shift the absorption maxima up to 100 nm.[17,272] For example, phycocyanobilin linked to β-155 in C-phycocyanin has an absorption maximum at 590 nm, while the

same bilin dye absorbs at 670 nm in the terminal emitters of the phycobilisomes.[17] The structural rational for this was recently traced by Peng *et al.* to the degree of co-planarity of the four pyrrole rings, which correlates with the absorption maximum.[273] Other effects may contribute to this, *e.g.*, conformational differences in the A/B system. In any case, the degree of coplanarity in the tetrapyrrole unit is adjusted by the apoprotein to yield photoactive complexes with absorption and emission properties specifically tailored to the environment and "need" of the organism (for example, adaptation to different light conditions).

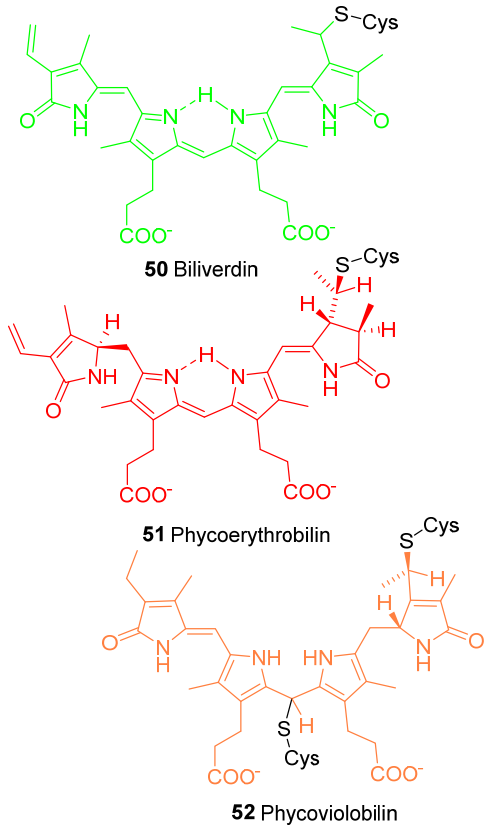


**Fig. 24** Protein-bound biliverdin **50**, PEB **51**, and PVR **52**.

Similar to the discussion given above for H-NOX, this field is rapidly moving towards bioengineered photoresponsive proteins with novel properties. The wide range of available mutant structures and those reconstituted with different chromophores offers significant potential to develop new cell biological reporter molecules and in optogenetics.[17,193] An example for the former is the use of small phytochrome fragments with mutations which result in highly fluorescent molecules.[274] Together with the ability to tune the specific absorption and emission wavelength, this leads to new fluorescent tag molecules with more scope for use than the commonly used green fluorescent proteins.[193] Recent reviews by Scheer *et al.*[17] and Burgie and Vierstra[193] further illuminate this use of biliproteins as bioimaging agents and the path to designer photoresponsive proteins.

**Non-tetrapyrrole cofactors**

The concept of conformational control is not restricted to tetrapyrrole-containing proteins. There are many established and a few more emerging manifestations of similar processes in biochemistry that are worth consideration as they help to generalize the phenomena. Broadly speaking, such effects may be classified as those that involve the control of protein conformational dynamics *via* cofactor associated parameters or else the functional control of cofactor properties *via* direct modification of its conformation. These two classifications are illustrated in our context by contrasting, for example, heme cooperativity in hemoglobin with the maintenance of a high midpoint potential by excessive distortion in the wild-type H-NOX complex.

A classic example is the visual sensing protein rhodopsin, wherein the photo-isomerization of an 11-*cis*-retinal to the all-*trans* form initiates the visual photo-transduction cascade (Fig. 25).[275] However, whilst it has long been known that the apoprotein affects substantially increased yields of the active agonist,[275] a computational study demonstrated that the structural mechanism responsible is the protein-induced distortion of the C11-C12 and C12-C13 dihedral angles in the ground state.[276] Moreover, recent reports have indicated that deleterious mutations in the binding-site known to cause *Retinitis pigmentosa*, a condition associated with blindness, result in substantial changes in the C11-C12 dihedral angle and significant spectral-shifts of the chromophore.[277]

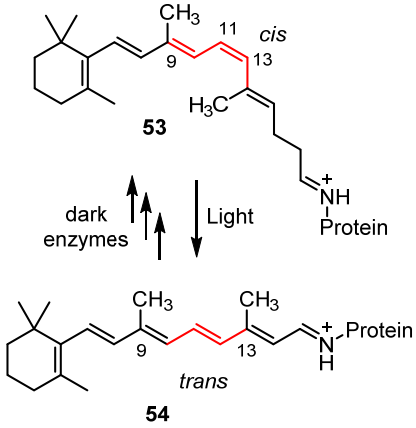


**Fig. 25** *cis-trans* Isomerization of protein-bound retinal.

In another twist, ubiquinone redox potentials have been attributed to the orientation of their methoxy substituents.[278] It was revealed that the reason only ubiquinones with methoxy substituents may function as both $Q_A$ and $Q_B$ in photosynthetic RCs (*i.e.*, 1 and 2-electron acceptors, respectively) is because the protein distorts the $Q_B$'s methoxy by around 20 – 25° out of the aromatic plane, which contributes ~50 mV (65 – 80%) to the observed potential difference. This result is particularly interesting in our context as it extends the notion of conformational control to other cofactors in RCs.

## Outlook

To summarize, aspects of conformational control are now established for almost any class of tetrapyrrole-containing proteins. These range from the initial observations on oxygen binding in hemoglobin, the identification of conformational changes associated with the heme-cofactors of cytochromes by Shelnutt, to the more recent studies on cytochromes in the bacterial photosynthetic reaction center, H-NOX and IsdI. An in depth look at chlorophylls in RC complexes has added significant detail to the analysis of photosynthetic systems and identified key aspects of the involvement of conformation control in EET.

Many avenues remain for further work along these lines. For heme, an in depth analysis of cyt $P_{450}$ might help with development of new catalysts or drug candidates and to deepen our understanding of the reaction mechanisms of peroxidases and other enzymes involving high-valent metalloporphyrin intermediates. In photosynthesis the increasing number of high resolution structures for the RCs from higher organisms and for large LHC puts a statistical analysis of hydroporphyrin conformations within reach. Likewise, new computational methods, together with emerging structural data on phycobiliproteins and (bacterio)phytochromes, should advance our understanding of the photochemical and signaling processes involving bilins.

Potential also exists for a revisit of non-planar porphyrins in terms of small molecule chemistry. While they have been used for the development of, *e.g.*, oxidation catalysts[279] and for chiral recognition,[280] detailed studies on their use as molecular receptors, optical materials, or organocatalysts are lacking.[281]

The progress made in synthetic methods to prepare unsymmetrically (highly) substituted porphyrins now makes it possible to utilize specific macrocycle conformations as a design principle for chromophores or receptors with tailor made properties. This will involve fine-tuning the optical properties of chromophores in intelligent photochromic and electro-optical materials, for use as NLO materials and novel sensors.

For example, applications of non-planar porphyrins for specialized PDT treatment,[282] as building blocks in supramolecular chemistry and nanomaterials,[283] or as biomimetic solar energy convertors *via* readily photo-oxidizable molecules with fine-tuned absorbance maxima[284] are now under scrutiny. The development of compounds with improved performance in such applications is, in essence, a problem of multiple optimizations where desired and unwanted properties are both linked to structure. This is the challenge: how does one optimize a few properties simultaneously whilst ameliorating unwanted effects when the methods used in their control are usually closely entangled with both? Here, 'conformational control' adds to the canon of methods for fine-tuning porphyrin properties.

However, rather than such step-wise advances, a view is emerging that the underlying concept can be used for wider, more far-reaching goals and two examples may serve to highlight this in the final section.

The data-driven critique of the tetrapyrrole conformations in bacterial photosynthetic RC afforded by particular crystal structures could serve as a prototype for the validation of small-molecule structures found in the PDB. The use of crystallographic co-ordinates in modern theoretical studies of protein function is increasing and should one wish to assess the electronic structure of a molecule in its experimental conformation (*i.e.,* without quantum mechanical optimization) structure selection is a key consideration. A common approach is to choose the highest resolution, most recent, or in some cases the most well-known structure. However, these criteria are not necessarily relevant to the intended use of the structure – especially in cases when the purpose of the original crystallographic study was different from that which the theoretical study intends to address. Likewise, small-changes in bond-lengths and angles can have a disproportionate impact on the outcome of a theoretical calculation. It is important therefore to give adequate thought to the relevance of the structure to the study in hand, and if possible to perform an unbiased (quantitative) critique and comparison of structures to ensure that this source of error is minimized.

Lastly, contemporary molecular biology allows the rational design or modification of proteins with new or tailor-made properties, perhaps in a more facile fashion than synthetic organic chemistry approaches. We have highlighted conclusive reports of the successful modification of protein-bound porphyrin-cofactor conformations to affect altered properties above: The redox modulation of the H-NOX complex *via* site-specific mutations chosen to allow the heme to relax into a less non-planar conformation,[246] the retardation of the heme degrading activity of IsdI by a mutation that decreased *ruf,*[264] and the directed evolution of ferrochelatase Ni-variants to show further specificity for Ni that was associated with decreased *sad* distortion.[201]

Especially the first two examples involving heme proteins indicate that, in a controlled experimental situation, modification of the conformation of a protein-bound porphyrin effects substantially altered properties. It is considered that with further development, the advances described here will contribute to the provision of a framework in which the effects of conformational control could be efficiently exploited in protein engineering, for example in the development of designer enzymes. One can almost intuit a general approach based on the recent works with H-NOX (Fig. 26) and the suggestions made by Scheer *et al.*[17] with regard to the design of photoresponsive proteins.

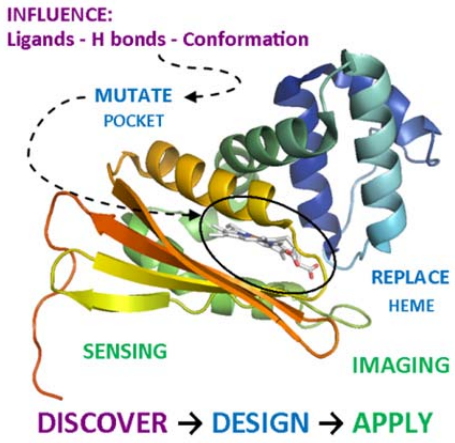


**Fig. 26** This is only the beginning… Fundamental research on the H-NOX domain has culminated in the development of protein-porphyrin complexes destined to represent prototypes for next generation MRI contrast agents and small-molecule sensors and also illustrates the path to designer photoresponsive proteins.

The first step will involve the recognition of a highly distorted cofactor, perhaps as well conservation of the conformation in related complexes, or else at least the discovery of interesting conformational features. The next step is to try to understand the role or consequences of this observation in a biological context. The final step is to harness the mechanism as a design principle and if successfully achieved, marks the transition from fundamental to applied research. One may envisage then that the ubiquity, versatility, diversity and specificity of tetrapyrrole-protein complexes in nature may also one day be mirrored in our own uses of them.

## Acknowledgements

Our recent work in this area was supported by Science Foundation Ireland (SFI IvP 13/IA/1894). Past support by Science Foundation Ireland, the Deutsche Forschungsgemeinschaft, and the many collaborators and co-workers is gratefully acknowledged.

## Notes and references

‡ Science is not driven by discoveries but by the researchers who make them and who enable others to do so as well. Both holds true for the late Prof. John Shelnutt (1946-2014), one of the main driving forces of this field. John was an author on many of the seminal contributions described herein and his contributions are ground breaking, fundamental and substantial. Not only did he develop many of the spectroscopic and computational methods and applied them to answer crucial questions, he was also a constant supportive and inquisitive colleague and friend to all of us in the field.

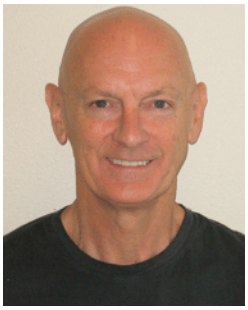

1 P. Tompa, *Trends Biochem. Sci.*, 2002, **27**, 527.
2 R. Huber, *Eur. J. Biochem.*, 1990, **187**, 283.
3 K. M. Kadish, K. M. Smith and R. Guilard (Eds.), *The Porphyrin Handbook*, Academic Press, San Diego, 2000.
4 S. Fukuzumi, *Bull. Chem. Soc. Jpn.* 2006, **79**, 177.
5 H. E. Toma and K. Araki, *Coord. Chem. Rev.* 2000, **196**, 307.
6 W. R. Scheidt and Y. J. Lee, *Struct. Bonding (Berlin, Ger.)*, 1987, **64**, 1.
7 A. Forman, M. W. Renner, E. Fujita, K. M. Barkigia, M. C. W. Evans, K. M. Smith and J. Fajer, J. *Isr. J. Chem.* 1989, **29**, 57.
8 *(a)* B. M. J. M. Suijkerbuijk and R. J. M. K. Gebbink, *Angew. Chem. Int. Ed.* 2008, **47**, 7396; *(b)* M. O. Senge, *Chem. Commun.*, 2011, **47**, 1943.
9 A. A. Ryan and M. O. Senge, *Photochem. Photobiol. Sci.*, 2015, **14**, 638.
10 A. R. Battersby, *Nat. Prod. Rep.*, 2000, **17**, 507.
11 K. Gruber, B. Puffer and B. Kräutler, *Chem. Soc. Rev.*, 2011, **40**, 4346.
12 *(a)* A. Pfaltz, B. Jaun, A. Fassler, A. Eschenmoser, R. Jaenchen, H. H. Gilles, G. Diekert and R. K. Thauer, *Helv. Chim. Acta*, 1982, **65**, 882; *(b)* U. Ermler, W. Grabarse, S. Shima, M. Goubeaud and R. K. Thauer, *Science*, 1997, **278**, 1457.
13 F.-P. Montforts, B. Gerlach and F. Hoper, *Chem. Rev.*, 1994, **94**, 327.
14 T. Matsui, S. Nambu, Y. Ono, C. W. Goulding, K. Tsumoto and M. Ikeda-Saito, *Biochemistry*, 2013, **52**, 3025.
15 S. Al-Karadaghi, R. Franco, M. Hansson, J. A. Shelnutt, G. Isaya and G. C. Ferreira, *Trends Biochem. Sci.*, 2006, **31**, 135.
16 A. N. Glazer, *Biochim. Biophys. Acta*, 1984, **768**, 29.
17 H. Scheer, X. Yang and K.-H. Zhao, *Procedia Chem.*, 2015, **14**, 176.
18 N. C. Rockwell, Y.-S. Su and J. C. Lagarias, *Ann. Rev. Plant Biol.*, 2006, **57**, 837.
19 *(a)* S. K. Chapman, S. Daff and A. W. Munro, in *Metal Sites in Proteins and Models Iron Centres*, eds. H. A. O. Hill, P. J. Sadler and A. J. Thomson, Springer, Berlin, 1997, **vol. 88**, p. 39; *(b)* J. P. Allen and J. C. Williams, in *Chlorophylls and Bacteriochlorophylls*, eds. B. Grimm, R. J. Porra, W. Rüdiger and H. Scheer, Springer, Dordrecht, 2006, p. 283.
20 S. Jones and J. M. Thornton, *Proc. Natl. Acad. Sci. U.S.A.*, 1996, **93**, 13.
21 J. Deisenhofer, O. Epp, K. Miki, R. Huber and H. Michel, *J. Mol. Biol.*, 1984, **180**, 385; *Nature*, 1985, **318**, 618.
22 *(a)* R. H. Felton, in *The Porphyrins*, ed. D. Dolphin, Academic Press, New York, 1978, **vol. 5**, p. 53; C. E. Castro, in *The Porphyrins*, ed. D. Dolphin, Academic Press, New York, 1978, **vol. 5**, p. 1; *(b)* D. Mauzerall, in *The Porphyrins*, ed. D. Dolphin, Academic Press, New York, 1978, **vol. 5**, p. 29; *(c)* M. P. Johansson, M. R. A. Blomberg, D. Sundholm and M. Wikström, *Biochim. Biophys. Acta*, 2002, **1553**, 183.
23 M. Gouterman, *J. Mol. Spectrosc.*, 1961, **6**, 138.
24 M. O. Senge, *J. Photochem. Photobiol. B: Biol.*, 1992, **16**, 3.
25 J. A. Shelnutt, X.-Z. Song, J.-G. Ma, S.-L. Jia, W. Jentzen and C. J. Medforth, *Chem. Soc. Rev.*, 1998, **27**, 31.
26 J. D. Hobbs and J. A. Shelnutt, *J. Protein Chem.*, 1995, **14**, 19.
27 M. O. Senge, *Chem. Commun.*, **2006**, 243.
28 W. Jentzen, J.-G. Ma and J. A. Shelnutt, *Biophys. J.*, 1998, **74**, 753.
29 W. Jentzen, X.-Z. Song and J. A. Shelnutt, *J. Phys. Chem. B*, 1997, **101**, 1684.
30 Some examples will be given below in the discussion on conformationally designed porphyrins. For a thorough analysis of the data up to 2000 see ref. 31.

 

31 M. O. Senge, in *The Porphyrin Handbook*, eds. K. M. Kadish, K. M. Smith and R. Guilard, Academic Press, San Diego, 2000, **vol. 1**, p. 239.

32 R. E. Haddad, S. Gazeau, J. Pecaut, J. C. Marchon, C. J. Medforth and J. A. Shelnutt, *J. Am. Chem. Soc.*, 2003, **125**, 1253.

33 *(a)* M. O. Senge, M. W. Renner, W. W. Kalisch and J. Fajer, *J. Chem. Soc., Dalton Trans.*, **2000**, 381; *(b)* B. Röder, M. Büchner, I. Rückmann and M. O. Senge, *Photochem. Photobiol. Sci.*, 2010, **9**, 1152.

34 K. M. Barkigia, L. Chantranupong, K. M. Smith and J. Fajer, *J. Am. Chem. Soc.*, 1988, **110**, 7566.

35 D. E. Koshland, *Proc. Natl. Acad. Sci. U.S.A.*, 1958 **44**, 98; *Angew. Chem., Int. Ed. Engl.*, 1994, **33**, 2375.

36 E. Fischer, *Ber. Dtsch. Chem. Ges.*, 1894, **27**, 2985.

37 *(a)* L. Pauling, *Nature*, 1948, **161**, 707; *(b)* T. L. Amyes and J. P. Richard, *Biochemistry*, 2013, **52**, 2021.

38 C. J. Cramer, *Essentials of Computational Chemistry: Theories and Models*, Wiley, West Sussex, England, 2004.

39 However, a small protein structure was recently solved to a resolution of 0.48 Å, PDB ID: 3NIR. A. Schmidt, M. Teeter, E. Weckert and V. S. Lamzin, *Acta Cryst.*, 2011, **F67**, 424.

40 While this limits the information that can be derived from protein crystal structures with regard to the conformation of individual chromophores and how they are affected by cofactor-protein interplay related macromolecular structures have proven to be landmark achievements in the field. Examples are the Nobel prizes for the structures determinations of sperm whale myoglobin[41] and the bacterial photosynthetic reaction center.[21]

41 J. C. Kendrew, G. Bodo, H. M. Dintzis, R. G. Parrish, H. Wyckoff and D. C. Phillips, *Nature*, 1958, **181**, 662.

42 G. J. Kleywegt, *Acta Cryst.*, 2007, **D63**, 94.

43 C. Kratky, R. Waditschatka, C. Angst, J. E. Johansen, J. C. Plaquevent, J. Schreiber and A. Eschenmoser, *Helv. Chim. Acta*, 1985, **68**, 1312.

44 M. O. Senge, *Acta Cryst.*, 2011, **C67**, m39.

45 M. Ravikanth and T. K. Chandrashekar, *Struct. Bonding (Berlin, Ger.)*, 1995, **83**, 105.

46 X.-Z. Song, W. Jentzen, S.-L. Jia, L. Jaquinod, D. J. Nurco, C. J. Medforth, K. M. Smith and J. A. Shelnutt, *J. Am. Chem. Soc.*, 1996, **118**, 12975.

47 A. D. Bond, N. Feeder, J. E. Redman, S. J. Teat and J. K. M. Sanders, *Crystal Growth Des.*, 2002, **2**, 27.

48 *(a)* S. Hatscher and M. O. Senge, *Tetrahedron Lett.*, 2003, **44**, 157; *(b)* C. Ryppa, M. O. Senge, S. S. Hatscher, E. Kleinpeter, P. Wacker, U. Schilde and A. Wiehe, *Chem. Eur. J.*, 2005, **11**, 3427.

49 M. O. Senge, K. Dahms, H.-J. Holdt and A. Kelling, *Z. Naturforsch.*, 2015, **70b**, 119.

50 M. O. Senge, in *The Porphyrin Handbook*, eds. K. M. Kadish, K. M. Smith and R. Guilard, Academic Press, San Diego, 2000, **vol 10**, p. 1.

51 *(a)* B. S. Everitt, S. Landau, M. Leese and D. Stahl, *Cluster Analysis*, Wiley, West Sussex, England, 2011; *(b)* A. C. Rencher and W. F. Christensen, *Methods of Multivariate Analysis*, Wiley, Hoboken, NJ, 2012.

52 A. Ghosh and P. R. Taylor, *Curr. Opin. Chem. Biol.*, 2003, **7**, 113.

53 E. Gudowska-Nowak, M. D. Newton and J. Fajer, *J. Phys. Chem.*, 1990, **94**, 5795.

54 W. Jentzen, M. C. Simpson, J. D. Hobbs, X. Song, T. Ema, N. Y. Nelson, C. J. Medforth, K. M. Smith, M. Veyrat, M. Mazzanti, R. Ramasseul, J.-C. Marchon, T. Takeuchi, W. A. Goddard and J. A. Shelnutt, *J. Am. Chem. Soc.*, 1995, **117**, 11085.

55 *(a)* J. Linnanto and J. Korppi-Tommola, *Phys. Chem. Chem. Phys.*, 2006, **8**, 663; *(b)* J. Linnanto, J. E. I. Korppi-Tommola and V. M. Helenius, *J. Phys. Chem. B*, 1999, **103**, 8739; *(c)* J. Linnanto and J. Korppi-Tommola, *Phys. Chem. Chem. Phys.*, 2000, **2**, 4962; *(d)* J. Linnanto and J. Korppi-Tommola, *J. Phys. Chem. A*, 2001, **105**, 3855; *(e)* J. Linnanto and J. Korppi-Tommola, *J. Phys. Chem. A*, 2004, **108**, 5872.

56 J. Linnanto and J. Korppi-Tommola, *J. Comput. Chem.*, 2004, **25**, 123.

57 J. Linnanto, A. Freiberg and J. Korppi-Tommola, *J. Phys. Chem. B*, 2011, **115**, 5536.

58 *(a)* M. Guse, N. S. Ostlund and G. D. Blyholder, *Chem. Phys. Lett.*, 1979, **61**, 526; *(b)* T. H. Dunning, B. H. Botch and J. F. Harrison, *J. Chem. Phys.*, 1980, **72**, 3419; *(c)* B. H. Botch, T. H. Dunning and J. F. Harrison, *J. Chem. Phys.*, 1981, **75**, 3466.

59 K. Raghavachari and G. W. Trucks, *J. Chem. Phys.*, 1989, **91**, 1062.

60 J. Almlof, T. H. Fischer, P. G. Gassman, A. Ghosh and M. Haeser, *J. Phys. Chem.*, 1993, **97**, 10964.

61 *(a)* T. Vangberg and A. Ghosh, *J. Am. Chem. Soc.*, 1999, **121**, 12154; *(b)* A. Ghosh and E. Steene, *J. Biol. Inorg. Chem.*, 2001, **6**, 739; *(c)* K. E. Thomas, A. B. Alemayehu, J. Conradie, C. M. Beavers and A. Ghosh, *Acc. Chem. Res.*, 2012, **45**, 1203.

62 E. B. Fleischer, *J. Am. Chem. Soc.*, 1963, **85**, 146; *J. Am. Chem. Soc.*, 1963, **85**, 1353.

63 E. B. Fleischer, C. K. Miller and L. E. Webb, *J. Am. Chem. Soc.*, 1964, **86**, 2342.

64 *(a)* J. L. Hoard, M. J. Hamor and T. A. Hamor, *J. Am. Chem. Soc.*, 1963, **85**, 2334; *(b)* M. J. Hamor, T. A. Hamor and J. L. Hoard, *J. Am. Chem. Soc.*, 1964, **86**, 1938.

65 *(a)* J. M. Robertson, *J. Chem. Soc.*, **1935**, 615; *(b) J. Chem. Soc.*, **1936**, 1195; *(c)* J. M. Robertson and I. Woodward, *J. Chem. Soc.*, **1937**, 219.

66 An early analysis of the various concepts in porphyrin structural chemistry was given in: J. L. Hoard, *Ann. N. Y. Acad. Sci.*, 1973, **206**, 18.

67 A crucial observation presented later was that a $S_4$ ruffled conformation would not necessarily be the only non-planar conformation likely to be found, *"A convex form ($C_4$ or $C_{4v}$ symmetry) of the skeleton becomes plausible with longer M-N bonds, by allowing the metal atom to lie far enough outside the plane of the four nitrogens to take care of the added dimensional constraint. This configuration, moreover, could be induced by the additional coordination of an externally constrained ligand to M. The high spin $Fe^{+2}$ and $Fe^{+3}$ derivatives are outstanding candidates for such configurations. Thus Kendrew's observation that, in myoglobin, the iron atom lies more than 0.25 Å out of the mean plane of the haem group is interpretable in simple fashion."* This foresight predicts the presence of macrocycle doming in 5-coordinate complexes, which had not yet been directly observed, and moreover suggests that it should accompany the vertical displacement of the heme-Fe that had been observed in myoglobin. They also identify the deeper meaning of their suggestion by stating that, in the

context of the myoglobin structure, *"…the easy deformability of the porphine skeleton is one of its useful biological characteristics"*.[64]

68 S. J. Silvers and A. Tulinsky, *J. Am. Chem. Soc.*, 1967, **89**, 3331.

69 Today this is interpreted as an example of in-plane distortion and described by a core elongation along a meso-meso axis. See: C. J. Medforth, M. O. Senge, T. P. Forsyth, J. D. Hobbs, J. A. Shelnutt and K. M. Smith, *Inorg. Chem.*, 1994, **33**, 3865; M. O. Senge, T. P. Forsyth and K. M. Smith, *Z. Kristallogr.*, 1996, **211**, 176; M. O. Senge, C. J. Medforth, T. P. Forsyth, D. A. Lee, M. M. Olmstead, W. Jentzen, R. K. Pandey, J. A. Shelnutt and K. M. Smith, *Inorg. Chem.*, 1997, **36**, 1149.

70 J. W. Lauher and J. A. Ibers, *J. Am. Chem. Soc.*, 1973, **95**, 5148.

71 *E.g.*, an increase of only 0.04 Å is observed in palladium(II) compared to nickel(II) complexes): E. B. Fleischer, *Acc. Chem. Res.*, 1970, **3**, 105.

72 A. Stone and E. B. Fleischer, *J. Am. Chem. Soc.*, 1968, **90**, 2735.

73 This was later confirmed in comparative analyses of many different porphyrin dications, *e.g.*: *(a)* M. O. Senge, T. P. Forsyth, L. T. Nguyen and K. M. Smith, *Angew. Chem. Int. Ed. Engl.*, 1994, **33**, 2485; *(b)* M. O. Senge and W. W. Kalisch, *Z. Naturforsch.*, 1999, **54b**, 943; *(c)* M. O. Senge, *Z. Naturforsch.*, 2000, **55b**, 336; *(d)* B. S. Cheng, O. Q. Munro, H. M. Marques and W. R. Scheidt, *J. Am. Chem. Soc.*, 1997, **119**, 10732.

74 *(a)* J. L. Hoard, M. J. Hamor, T. A. Hamor and W. S. Caughey, *J. Am. Chem. Soc.*, 1965, **87**, 2312; *(b)* T. A. Hamor, W. S. Caughey and J. L. Hoard, *J. Am. Chem. Soc.*, 1965, **87**, 2305.

75 *(a)* R. P. Countryman, D. M. Collins and J. L. Hoard, *J. Am. Chem. Soc.*, 1969, **91**, 5166; *(b)* L. J. Radonovich, A. Bloom and J. L. Hoard, *J. Am. Chem. Soc.*, 1972, **94**, 2073.

76 W. A. Hendrickson, W. E. Love and J. Karle, *J. Mol. Biol.*, 1973, **74**, 331.

77 M. F. Perutz, *Nature*, 1970, **228**, 726.

78 D. M. Collins, R. Countryman and J. L. Hoard, *J. Am. Chem. Soc.*, 1972, **94**, 2066.

79 *(a)* W. R. Scheidt, *Acc. Chem. Res.*, 1977, **10**, 339; *(b)* W. R. Scheidt and C. A. Reed, *Chem. Rev.*, 1981, **81**, 543.

80 *(a)* E. F. Meyer Jr., *Acta Cryst.*, 1972, **B28**, 2162; *(b)* D. L. Cullen and E. F. Meyer, *J. Am. Chem. Soc.*, 1974, **96**, 2095.

81 T. D. Brennan, W. R. Scheidt and J. A. Shelnutt, *J. Am. Chem. Soc.*, 1988, **110**, 3919.

82 *(a)* A. Ulman, J. Gallucci, D. Fisher and J. A. Ibers, *J. Am. Chem. Soc.*, 1980, **102**, 6852; *(b)* C. Kratky, C. Angst and J. E. Johansen, *Angew. Chem. Int. Ed. Engl.*, 1981, **20**, 211.

83 For other examples for planar nickel(II) porphyrins see: *(a)* M. O. Senge, *Acta Cryst.*, 2012, **E68**, m1191; *(b)* M. O. Senge and M. Davis, *Acta Cryst.*, 2010, **E66**, m790; *(c)* M. Davis, M. O. Senge and O. B. Locos, *Z. Naturforsch.*, 2010, **65b**, 1472.

84 A. M. Stolzenberg, P. A. Glazer and B. M. Foxman, *Inorg. Chem.*, 1986, **25**, 983.

85 S. H. Strauss, M. E. Silver, K. M. Long, R. G. Thompson, R. A. Hudgens, K. Spartalian and J. A. Ibers, *J. Am. Chem. Soc.*, 1985, **107**, 4207.

86 M. O. Senge, W. W. Kalisch and S. Runge, *Tetrahedron*, 1998, **54**, 3781.

87 *(a)* M. O. Senge and K. M. Smith, *Photochem. Photobiol.*, 1991, **54**, 841; *(b)* K. M. Barkigia, M. A. Thompson, J. Fajer, R. K. Pandey, K. M. Smith and M. G. H. Vicente, *New J. Chem.*, 1992, **16**, 599; *(c)* M. O. Senge, W. W. Kalisch and K. Ruhlandt-Senge, *Chem. Commun.*, **1996**, 2149; *(d)* K. M. Shea, L. Jaquinod, K. G. Richard and K. M. Smith, *Chem. Commun.*, **1998**, 759.

88 For an analysis of all small molecule crystal structures related to chlorophylls see: M. O. Senge and S. A. MacGowan, in *Handbook of Porphyrin Science*, eds. K. M. Kadish, K. M. Smith and R. Guilard, World Scientific, Singapore, 2011, **vol. 13**, p. 253.

89 C. J. Medforth, M. O. Senge, K. M. Smith, L. D. Sparks and J. A. Shelnutt, *J. Am. Chem. Soc.*, 1992, **114**, 9859.

90 L. D. Sparks, C. J. Medforth, M. S. Park, J. R. Chamberlain, M. R. Ondrias, M. O. Senge, K. M. Smith and J. A. Shelnutt, *J. Am. Chem. Soc.*, 1993, **115**, 581.

91 W. Jentzen, E. Unger, G. Karvounis, J. A. Shelnutt, W. Dreybrodt and R. Schweitzer-Stenner, *J. Phys. Chem.*, 1996, **100**, 14184.

92 K. M. Barkigia, M. D. Berber, J. Fajer, C. J. Medforth, M. W. Renner and K. M. Smith, *J. Am. Chem. Soc.*, 1990, **112**, 8851.

93 K. M. Barkigia, M. W. Renner, L. R. Furenlid, C. J. Medforth, K. M. Smith and J. Fajer, *J. Am. Chem. Soc.*, 1993, **115**, 3627.

94 B. Evans, K. M. Smith and J.-H. Fuhrhop, *Tetrahedron Lett.*, 1977, 443.

95 A. Regev, T. Galili, C. J. Medforth, K. M. Smith, K. M. Barkigia, J. Fajer and H. Levanon, *J. Phys. Chem.*, 1994, **98**, 2520.

96 W. W. Kalisch and M. O. Senge, *Angew. Chem. Int. Ed. Engl.*, 1998, **37**, 1107.

97 *(a)* T. Ema, M. O. Senge, N. Y. Nelson, H. Ogoshi and K. M. Smith, *Angew. Chem., Int. Ed. Engl.*, 1994, **33**, 1879; *(b)* M. O. Senge, I. Bischoff, N. Y. Nelson and K. M. Smith, *J. Porphyrins Phthalocyanines*, 1999, **3**, 99.

98 I. Bischoff, X. Feng and M. O. Senge, *Tetrahedron*, 2001, **57**, 5573.

99 M. O. Senge, W. W. Kalisch and S. Runge, *Liebigs Ann. Chem.*, 1997, 1345.

100 In contrast to the conclusion for dications, the concomitant in-plane rotation of the meso-phenyl groups in these species were suggested *not* to affect increased conjugation since meso-phenyl bond-lengths remained unchanged relative to planar compounds.[92]

101 M. O. Senge, *J. Chem. Soc., Dalton Trans.*, **1993**, 3539.

102 *(a)* K. M. Kadish, F. D'Souza, A. Villard, M. Autret, E. Van Caemelbecke, P. Bianco, A. Antonini and P. Tagliatesta, *Inorg. Chem.*, 1994, **33**, 5169; *(b)* K. M. Kadish, J. Li, E. Van Caemelbecke, Z. Ou, N. Guo, M. Autret, F. D'Souza and P. Tagliatesta, *Inorg. Chem.*, 1997, **36**, 6292; *(c)* P. Ochsenbein, K. Ayougou, D. Mandon, J. Fischer, R. Weiss, R. N. Austin, K. Jayaraj, A. Gold, J. Terner and J. Fajer, *Angew. Chem., Int. Ed. Engl.*, 1994, **33**, 348.

103 D. Mandon, P. Ochenbein, J. Fischer, R. Weiss, K. Jayaraj, R. N. Austin, A. Gold, P. S. White and O. Brigaud, *Inorg. Chem.*, 1992, **31**, 2044.

104 K. M. Kadish, E. Van Caemelbecke, P. Boulas, F. D'Souza, E. Vogel, M. Kisters, C. J. Medforth and K. M. Smith, *Inorg. Chem.*, 1993, **32**, 4177.

105 Y. Fang, M. O. Senge, E. Van Caemelbecke, K. M. Smith, C. J. Medforth, M. Zhang and K. M. Kadish, *Inorg. Chem.*, 2014, **53**, 10772.

106 R. J. Cheng, C. H. Ting, T. C. Chao, T. H. Tseng and P. P. Y. Chen, *Chem. Commun.*, 2014, **50**, 14265.

 

107 M. W. Renner, K. M. Barkigia and J. Fajer, *Inorg. Chim. Acta*, 1997, **263**, 181.

108 K. M. Barkigia, M. W. Renner, M. O. Senge and J. Fajer, *J. Phys. Chem. B*, 2004, **108**, 2173.

109 Note, that many of the early studies in this area utilized "strapped" and basket-handle-type porphyrins as conformationally distorted systems which gave results complementary to those discussed here.[45,110]

110 N. C. Maiti and M. Ravikanth, *J. Chem. Soc., Faraday Trans.*, 1995, **91**, 4369; 1996, **92**, 1095.

111 S. Gentemann, C. J. Medforth, T. P. Forsyth, D. J. Nurco, K. M. Smith, J. Fajer and D. Holten, *J. Am. Chem. Soc.*, 1994, **116**, 7363.

112 S. Gentemann, C. J. Medforth, T. Ema, N. Y. Nelson, K. M. Smith, J. Fajer and D. Holten, *Chem. Phys. Lett.*, 1995, **245**, 441.

113 These ideas were confirmed and extended in a follow-up study that demonstrated that the *sad* distorted compounds also tended toward more "normal" behavior at low-temperatures, albeit to a lesser extent than the *ruf* compounds; the trends were also shown to be present in the corresponding zinc(II) complexes: S. Gentemann, N. Y. Nelson, L. Jaquinod, D. J. Nurco, S. H. Leung, C. J. Medforth, K. M. Smith, J. Fajer and D. Holten, *J. Phys. Chem. B*, 1997, **101**, 1247.

114 *(a)* C. M. Drain, C. Kirmaier, C. J. Medforth, D. J. Nurco, K. M. Smith and D. Holten, *J. Phys. Chem.*, 1996, **100**, 11984; *(b)* S. Michaeli, S. Soffer, H. Levanon, M. O. Senge and W. W. Kalisch, *J. Phys. Chem. A*, 1999, **103**, 1950; *(c)* J. L. Retsek, C. M. Drain, C. Kirmaier, D. J. Nurco, C. J. Medforth, K. M. Smith, I. V. Sazanovich, V. S. Chirvony, J. Fajer and D. Holten, *J. Am. Chem. Soc.*, 2003, **125**, 9787; *(d)* A. Y. Lebedev, M. A. Filatov, A. V. Cheprakov and S. A. Vinogradov, *J. Phys. Chem. A*, 2008, **112**, 7723; *(e)* F. Nifiatis, W. Su, J. E. Haley, J. E. Slagle and T. M. Cooper, *J. Phys. Chem. A*, 2011, **115**, 13764.

115 C. M. Drain, S. Gentemann, J. A. Roberts, N. Y. Nelson, C. J. Medforth, S. Jia, M. C. Simpson, K. M. Smith, J. Fajer, J. A. Shelnutt and D. Holten, *J. Am. Chem. Soc.*, 1998, **120**, 3781.

116 These results were rationalized in terms of the M-N repulsion affected by population of the $d_{x^2-y^2}$ orbital that requires expansion of the core for its relief, a process that is hindered in *ruf* distorted porphyrins (see earlier). It was postulated then that a *dom* or mixed-mode conformer forms in the excited state, which therefore has a large barrier for deactivation to the pure *ruf* ground state, resulting in a kinetically trapped excited state.

117 *(a)* W. W. Kalisch and M. O. Senge, *Tetrahedron Lett.*, 1996, **37**, 1183; *(b)* M. O. Senge and W. W. Kalisch, *Inorg. Chem.*, 1997, **36**, 6103.

118 *(a)* M. O. Senge, V. Gerstung, K. Ruhlandt-Senge, S. Runge and I. Lehmann, *J. Chem. Soc., Dalton Trans.*, 1998, 4187; *(b)* M. O. Senge and I. Bischoff, *Eur. J. Org. Chem.*, 2001, 1735.

119 M. O. Senge, W. W. Kalisch and I. Bischoff, *Chem. Eur. J.*, 2000, **6**, 2721.

120 *(a)* M. Nakamura, *Coord. Chem. Rev.*, 2005, **250**, 2271; *(b)* M. Nakamura, A. Ikezaki and M. Takahashi, *J. Chin. Chem. Soc.*, 2013, **60**, 9.

121 One could also speculate that the higher-frequency deformation modes generally hold greater influence over properties on the basis that they introduce a larger energetic perturbation to be distributed amongst the orbitals and that the greater conformational strain may alter dynamic properties (*e.g.*, relaxation after excitation or oxidation).

122 A. W. Munro, H. M. Girvan, K. J. McLean, M. R. Cheesman and D. Leys, in *Tetrapyrroles - Birth, Life and Death*, eds. M. Warren and A. Smith, Springer, New York, 2009, p. 160.

123 C. J. Reedy and B. R. Gibney, *Chem. Rev.*, 2004, **104**, 617.

124 B. Grimm, R. J. Porra, W. Rüdiger and H. Scheer, eds., *Chlorophylls and Bacteriochlorophylls*, Springer, Dordrecht, The Netherlands, 2006.

125 M. O. Senge, A. A. Ryan, K. A. Letchford, S. A. MacGowan and T. Mielke, *Symmetry*, 2014, **6**, 781.

126 *(a)* S. Schneider, J. Marles-Wright, K. H. Sharp and M. Paoli, *Nat. Prod. Rep.*, 2007, **24**, 621; *(b)* N. Mochizuki, R. Tanaka, B. Grimm, T. Masuda, M. Moulin, A. G. Smith, A. Tanaka and M. J. Terry, *Trends Plant Sci.*, 2010, **15**, 488; *(c)* I. G. Denisov and S. G. Sligar, in *Handbook of Porphyrin Science*, eds. K. M. Kadish, K. M. Smith and R. Guilard, World Scientific, Singapore, 2010, **vol. 5**, p. 165.

127 *(a)* I. Bertini, G. Cavallaro and A. Rosato, *Chem. Rev.*, 2006, **106**, 90; *(b)* J. M. Stevens and S. J. Ferguson, in *Handbook of Porphyrin Science*, eds. K. M. Kadish, K. M. Smith and R. Guilard, World Scientific, Singapore, 2012, **vol. 19**, p. 371.

128 C. Fufezan, J. Zhang and M. R. Gunner, *Proteins*, 2008, **73**, 690.

129 W. Wu and C. K. Chang, *J. Am. Chem. Soc.*, 1987, **109**, 3149.

130 M. J. Murphy and L. M. Siegel, *J. Biol. Chem.*, 1973, **248**, 6911.

131 *(a)* M. F. Perutz, *Nature*, 1970, **228**, 734; *(b)* M. F. Perutz, A. J. Wilkinson, M. Paoli and G. G. Dodson, *Ann. Rev. Biophys. Biomol. Struct.*, 1998, **27**, 1.

132 Y. Hatefi, *Ann. Rev. Biochem.*, 1985, **54**, 1015.

133 C. Hägerhäll, *Biochim. Biophys. Acta.*, 1997, **1320**, 107.

134 A. R. Crofts, J. T. Holland, D. Victoria, D. R. Kolling, S. A. Dikanov, R. Gilbreth, S. Lhee, R. Kuras and M. G. Kuras, *Biochim. Biophys. Acta.*, 2008, **1777**, 1001.

135 *(a)* H. Michel, J. Behr, A. Harrenga and A. Kannt, *Ann. Rev. Biophys. Biomol. Struct.*, 1998, **27**, 329; *(b)* S. Yoshikawa and A. Shimada, *Chem. Rev.*, 2015, **115**, 1936.

136 C. J. Reedy, M. M. Elvekrog and B. R. Gibney, *Nucleic Acids Res.*, 2008, **36**, D307.

137 Z. Zheng and M. R. Gunner, *Proteins*, 2009, **75**, 719.

138 *(a)* A. L. Raphael and H. B. Gray, *Proteins*, 1989, **6**, 338; *(b)* I. Mus-Veteau, A. Dolla, F. Guerlesquin, F. Payan, M. Czjzek, R. Haser, P. Bianco, J. Haladjian, B. J. Rapp-Giles and J. D. Wall, *J. Biol. Chem.*, 1992, **267**, 16851.

139 G. S. Wilson, *Bioelectrochem. Bioenerg.*, 1974, **1**, 172.

140 *(a)* W. S. Caughey, W. Y. Fujimoto and B. P. Johnson, *Biochemistry*, 1966, **5**, 3830; *(b)* F. A. Walker, M.-W. Lo and M. T. Ree, *J. Am. Chem. Soc.*, 1976, **98**, 5552.

141 *(a)* T. Hayashi, in *Handbook of Porphyrin Science*, eds. K. M. Kadish, K. M. Smith and R. Guilard, World Scientific, Singapore, 2010, **vol. 5**, p. 1; *(b)* T. Hayashi, Y. Sano and A. Onoda, *Isr. J. Chem.*, 2015, **55**, 76.

142 Y. Sugita and Y. Yoneyama, *J. Biol. Chem.*, 1971, **246**, 389.

143 *(a)* G. Tollin, L. K. Hanson, M. Caffrey, T. E. Meyer and M. A. Cusanovich, *Proc. Natl. Acad. Sci. U.S.A.*, 1986, **83**, 3693; *(b)* M. R. Gunner and B. Honig, *Proc. Natl. Acad. Sci. U.S.A.*, 1991, **88**, 9151; *(c)* J. Mao, K. Hauser and M. R. Gunner, *Biochemistry*, 2003, **42**, 9829; *(d)* P. Voigt and E. W. Knapp, *J. Biol. Chem.*, 2003, **278**, 51993.

144 B. R. Crane, L. M. Siegel and E. D. Getzoff, *Biochemistry*, 1997, **36**, 12101.
145 A. Schiffer, K. Parey, E. Warkentin, K. Diederichs, H. Huber, K. O. Stetter, P. M.H. Kroneck and U. Ermler, *J. Mol. Biol.*, 2008, **379**, 1063.
146 *(a)* V. Fülöp, J. W. B. Moir, S. J. Ferguson and J. Hajdu, *Cell,* 1995, **81**, 369-377; *(b)* S. C. Baker, N. F. W. Saunders, A. C. Willis, S. J. Ferguson, J. Hajdu and V. Fülöp, *J. Mol. Biol.*, 1997, **268**, 440-455.
147 P. A. Williams, V. Fülöp, E. F. Garman, N. F. W. Saunders, S. J. Ferguson and J. Hajdu, *Nature*, 1997, **389**, 406.
148 D. Nurizzo, F. Cutrussola, M. Arese, D. Bourgeois, M. Brunori, C. Cambillau and M. Tegoni, *J. Biol. Chem.*, 1999, **274**, 14997.
149 H. Scheer, ed., *Chlorophylls*, CRC Press, Boca Raton, USA, 1991.
150 M. O. Senge, A. Wiehe and C. Ryppa, in *Chlorophylls and Bacteriochlorophylls*, eds. B. Grimm, R. J. Porra, W. Rüdiger and H. Scheer, Springer, Dordrecht, 2006, p. 27.
151 G. McDermott, S. M. Prince, A. A. Freer, A. M. Hawthornthwaite-Lawless, M. Z. Papiz, R. J. Cogdell and N. W. Isaacs, *Nature*, 1995, **374**, 517.
152 A. J. Hoff and J. Deisenhofer, *Phys. Rep.*, 1997, **287**, 1.
153 *(a)* T. Renger, *Photosynth. Res.*, 2009, **102**, 471; *(b)* M. Sener, J. Strumpfer, J. Hsin, D. Chandler, S. Scheuring, C. N. Hunter and K. Schulten, *ChemPhysChem*, 2011, **12**, 51871.
154 *(a)* M. O. Senge and K. M. Smith, *Z. Kristallogr.*, 1992, **199**, 239; *(b)* M. O. Senge and K. M. Smith, *Photochem. Photobiol.*, 1994, **60**, 139; *(c)* M. O. Senge, K. Ruhlandt-Senge and K. M. Smith, *Z. Naturforsch.*, 1995, **50b**, 139; *(d)* M. O. Senge and K. M. Smith, *Acta Cryst.*, 1997, **C53**, 1314; *(e)* M. O. Senge, N. W. Smith and K. M. Smith, *Inorg. Chem.*, 1993, **32**, 1259.
155 K. M. Barkigia, D. S. Gottfried, S. G. Boxer and J. Fajer, *J. Am. Chem. Soc.*, 1989, **111**, 6444.
156 H. Scheer, in *Chlorophylls and Bacteriochlorophylls*, eds. B. Grimm, R. J. Porra, W. Rüdiger and H. Scheer, Springer, Dordrecht, 2006, p. 1.
157 P. Jordan, P. Fromme, H. T. Witt, O. Klukas, W. Saenger and N. Krauss, *Nature*, 2001, **411**, 909.
158 *(a)* X. Lin, H. A. Murchison, V. Nagarajan, W. W. Parson, J. P. Allen and J. C. Williams, *Proc. Natl. Acad. Sci. U.S.A.*, 1994, **91**, 10265; *(b)* J. Rautter, F. Lendzian, C. Schulz, A. Fetsch, M. Kuhn, X. Lin, J. C. Williams, J. P. Allen and W. Lubitz, *Biochemistry*, 1995, **34**, 8130; *(c)* J. P. Allen, K. Artz, X. Lin, J. C. Williams, A. Ivancich, D. Albouy, T. A. Mattioli, A. Fetsch, M. Kuhn and W. Lubitz, *Biochemistry*, 1996, **35**, 6612.
159 H. Ishikita, W. Saenger, J. Biesiadka, B. Loll and E. W. Knapp, *Proc. Natl. Acad. Sci. U.S.A.*, 2006, **103**, 9855.
160 L. K. Hanson, J. Fajer, M. A. Thompson and M. C. Zerner, *J. Am. Chem. Soc.*, 1987, **109**, 4728.
161 H. Treutlein, K. Schulten, A. T. Brünger, M. Karplus, J. Deisenhofer and H. Michel, *Proc. Natl. Acad. Sci. U.S.A.*, 1992, **89**, 75.
162 *(a)* J. M. Olson, *Photochem. Photobiol.*, 1998, **67**, 61; *(b)* J. Psencik, T. P. Ikonen, P. Laurinmaki, M. C. Merckel, S. J. Butcher, R. E. Serimaa and R. Tuma, *Biophys. J.*, 2004, **87**, 1165; *(c)* T. Miyatake and H. Tamiaki, *J. Photochem. Photobiol., C: Photochem. Rev.*, 2005, **6**, 89; *(d)* T. S. Balaban, *Acc. Chem. Res.*, 2005, **38**, 612.
163 *(a)* M. S. Huster and K. M. Smith, *Biochemistry*, 1990, **29**, 4348; *(b)* C. M. Borrego and L. J. Garcia-Gill, *Photosynth. Res.*, 1995, **45**, 21.
164 Note, that C20 methylation of BChl d to BChl c results in a 10 nm red-shift of the absorption maxima which is more efficient for low-light conditions.[163]
165 B. Kräutler, *Biochem. Soc. Trans.*, 2005, **33**, 806.
166 M. K. Geno and J. Halpern, *J. Am. Chem. Soc.*, 1987, **109**, 1238.
167 B. Kräutler, R. Konrat, E. Stupperich, G. Färber, K. Gruber and C. Kratky, *Inorg. Chem.*, 1994, **33**, 4128.
168 *(a)* F. Mancia, N. H. Keep, A. Nakagawa, P. F. Leadlay, S. McSweeney, B. Rasmussen, P. Bosecke, O. Diat and P. R. Evans, *Structure*, 1996, **4**, 339; *(b)* R. Reitzer, K. Gruber, G. Jogl, U. G. Wagner, H. Bothe, W. Buckel and C. Kratky, *Structure*, 1999, **7**, 891.
169 *(a)* J. Masuda, N. Shibata, Y. Morimoto, T. Toraya and N. Yasuoka, *Struct. Fold. Des.*, 2000, **8**, 775; *(b)* M. Yamanishi, M. Yunoki, T. Tobimatsu, H. Sato, J. Matsui, A. Dokiya, Y. Iuchi, K. Oe, K. Suto, N. Shibata, Y. Morimoto, N. Yasuoka and T. Toraya, *Eur. J. Biochem.*, 2002, **269**, 4484; *(c)* F. Berkovitch, E. Behshad, K. H. Tang, E. A. Enns, P. A. Frey and C. L. Drennan, *Proc. Natl. Acad. Sci. U.S.A.*, 2004, **101**, 15870; *(d)* N. Shibata, H. Tamagaki, N. Hieda, K. Akita, H. Komori, Y. Shomura, S. Terawaki, K. Mori, N. Yasuoka, Y. Higuchi and T. Toraya, *J. Biol. Chem.*, 2010, **285**, 26484; *(e)* K. R. Wolthers, C. Levy, N. S. Scrutton and D. Leys, *J. Biol. Chem.*, 2010, **285**, 13942.
170 M. D. Sintchak, G. Arjara, B. A. Kellogg, J. Stubbe and C. L. Drennan, *Nat. Struct. Biol.*, 2002, **9**, 293.
171 *(a)* M. C. Thompson, C. S. Crowley, J. Kopstein, R. A. Bobik and T. O. Yeates, *Acta Cryst.*, 2014, **F70**, 1584; *(b)* F. S. Mathews, M. M. Gordon, Z. Chen, K. R. Rajashankar, S. E. Ealick, D. H. Alpers and N. Sukumar, *Proc. Natl. Acad. Sci. U.S.A.*, 2007, **104**, 17311.
172 *(a)* M. L. Ludwig and R. G. Matthews, *Ann. Rev. Biochem.*, 1997, **66**, 269; *(b)* E. N. G. Marsh and G. D. R. Melendez, *Biochim. Biophys. Acta*, 2012, **1824**, 1154.
173 U. Ermler, *Dalton Trans.*, 2005, 3451.
174 *(a)* M. Zimmer and R. H. Crabtree, *J. Am. Chem. Soc.,* 1990, **112**, 1062; *(b)* M. Zimmer, *J. Biomolecular Struct. Dynamics,* 1993, **11**, 203.
175 L. R. Furenlid, M. W. Renner and J. Fajer, *J. Am. Chem. Soc.,* 1990, **112**, 8987.
176 *(a)* G. Färber, W. Keller, C. Kratky, B. Jaun, A. Pfaltz, C. Spinner, A. Kobelt and A. Eschenmoser, *Helv. Chim. Acta,* 1991, **74**, 697; *(b)* A. Eschenmoser, *Ann. N. Y. Acad. Sci.*, 1986, **471**, 108.
177 W. Grabarse, F. Mahlert, E. C. Duin, M. Goubeaud, S. Shima, R. K. Thauer, V. Lamzin and U. Ermler, *J. Mol. Biol.*, 2001, **309**, 315.
178 P. E. Cedervall, M. Dey, X. H. Li, R. Sarangi, B. Hedman, S. W. Ragsdale and C. M. Wilmot, *J. Am. Chem. Soc.*, 2011, **133**, 5626.
179 P. E. Cedervall, M. Dey, A. R. Pearson, S. W. Ragsdale and C. M. Wilson, *Biochemistry*, 2010, **49**, 7683.
180 W. Grabarse, F. Mahlert, S. Shima, R. K. Thauer and U. Ermler, *J. Mol. Biol.*, 2000, **303**, 329.
181 A. Ghosh, T. Wondimagegn and H. Ryeng, *Curr. Opin. Chem. Biol.*, 2001, **5**, 744.

 

182 *(a)* L. N. Todd and M. Zimmer, *Inorg. Chem.*, 2002, **41**, 6831; *(b)* C. Mbofana and M. Zimmer, *Inorg. Chem.*, 2006, **45**, 2598.

183 H. M. Berman, J. Westbrook, Z. Feng, G. Gilliland, T. N. Bhat, H. Weissig, I. N. Shindyalov and P. E. Bourne, *Nucleic Acids Res.*, 2000, **28**, 235.

184 J. A. Shelnutt, NSDGUI, Version 1.3 Alpha Version, Sandia National Laboratory, Albuquerque, AZ, 2000-2001.

185 D. A. Lightner, *Bilirubin: Jekyll and Hyde Pigment of Life,* Springer, Wien, Austria, 2013.

186 *(a)* S. Hörtensteiner and B. Kräutler, *Biochim. Biophys. Acta*, 2011, **1807**, 977; *(b)* B. Kräutler, *Chem. Soc. Rev.*, 2014, **43**, 6227.

187 For more details on the biomedical relevance of conformational aspects in bilirubin photomedicine see: A. F. McDonagh and D. A Lightner, *Pediatrics*, 1985, **75**, 443.

188 R. V. Person, B. R. Peterson and D. A. Lightner, *J. Am. Chem. Soc.*, 1994, **116**, 42.

189 H. A. Borthwick, S. B. Hendricks, M. W. Parker, E. H. Toole and V. K. Toole, *Proc. Natl. Acad. Sci. U.S.A.*, 1952, **38**, 662.

190 *(a)* J. R. Wagner, J. S. Brunzelle, K. T. Forest and R. D. Vierstra, *Nature*, 2005, **438**, 325; *(b)* X. Yang, J. Kuk and K. Moffat, *Proc. Natl. Acad. Sci. U.S.A.*, 2008, **105**, 14715; *(c)* L. O. Essen, J. Mailliet and J. Hughes, *Proc. Natl. Acad. Sci. U.S.A.*, 2008, **105**, 14709.

191 S. H. Bhoo, S. J. Davis, J. Walker, B. Karniol and R. D. Vierstra, *Nature*, 2001, **414**, 776.

192 J. R. Wagner, J. R. Zhang, J. S. Brunzelle, R. D. Vierstra and K. T. Forest, *J. Biol. Chem.*, 2007, **282**, 12298.

193 E. S. Burgie and R. D. Vierstra, *Plant Cell*, 2014, **26**, 4568.

194 *(a)* A. R. Grossman, M. R. Schaefer, G. G. Chiang and J. L. Collier, *Microbiol. Rev.*, 1993, **57**, 725; *(b)* R. MacColl, *J. Struct. Biol*., 1998, **124**, 311.

195 T. Dammeyer and N. Frankenberg-Dinkel, *Photochem. Photobiol. Sci.*, 2008, **7**, 1121.

196 H. Scheer, *Angew. Chem. Int. Ed. Engl.,* 1981, **20**, 241.

197 L. Bogorad, *Ann. Rev. Plant Physiol. Plant Mol. Biol.,* 1975, **26**, 369.

198 K. K. Anderson, J. D. Hobbs, L. Luo, K. D. Stanley, J. M. E. Quirke and J. A. Shelnutt, *J. Am. Chem. Soc.*, 1993, **115**, 12346.

199 *(a)* F. J. Leeper, *Nat. Prod. Rep.*, 1985, **2**, 19; *(b)* H. A. Dailey, T. A. Dailey, C. K. Wu, A. E. Medlock, K. F. Wang, J. P. Rose and B. C. Wang, *Cell. Mol. Life Sci.*, 2000, **57**, 1909; *(c)* E. Raux, H. L. Schubert and M. J. Warren, *Cell. Mol. Life Sci.*, 2000, **57**, 1880; *(d)* J. D. Reid and C. N. Hunter, *Biochem. Soc. Trans.*, 2002, **30**, 643; *(e)* R. Tanaka and A. Tanaka, *Ann. Rev. Plant Biol.*, 2007, **58**, 321.

200 *(a)* R. Franco, J.-G. Ma, Y. Lu, G. C. Ferreira and J. A. Shelnutt, *Biochemistry*, 2000, **39**, 2517; *(b)* Z. Shi, R. Franco, R. Haddad, J. A. Shelnutt and G. C. Ferreira, *Biochemistry*, 2006, **45**, 2904.

201 N. R. McIntyre, R. Franco, J. A. Shelnutt and G. C. Ferreira, *Biochemistry*, 2011, **50**, 1535.

202 S. Shipovskov, T. Karlberg, M. Fodje, M. D. Hanson, G. C. Ferreira, M. Hansson, C. T. Reimann and S. Al-Karadaghi, *J. Mol. Biol.*, 2005, **352**, 1081.

203 *(a)* I. A. Magnus, T. A. Prankerd, A. Jarrett and C. Rimington, *Lancet*, 1961, **2**, 448; *(b)* D. J. Todd, *Br. J. Dermatol.*, 1994, **131**, 751.

204 *(a)* W. K. McEwen, *J. Am. Chem. Soc.*, 1946, **68**, 711; *(b)* S. P. C. Cole and G. S. Marks, *Mol. Cell. Biochem.*, 1984, **64**, 127.

205 M. J. Bain-Ackerman and D. K. Lavallee, *Inorg. Chem.*, 1979, **18**, 3358.

206 Note, that highly substituted, very nonplanar porphyrins can exhibit metalation rates several orders of magnitude faster than those of planar porphyrins. J. Takeda, T. Ohya and M. Sato, *Inorg. Chem.*, 1992, **31**, 2877.

207 H. A. Dailey and J. E. Fleming, *J. Biol. Chem.*, 1983, **258**, 11453.

208 A. G. Cochran and P. G. Schultz, *Science*, 1990, **249**, 781.

209 D. Lecerof, M. Fodje, A. Hansson, M. Hansson and S. Al-Karadaghi, *J. Mol. Biol.*, 2000, **297**, 221.

210 A. Medlock, L. Swartz, T. A. Dailey, H. A. Dailey and W. N. Lazilotta, *Proc. Natl. Acad. Sci. U.S.A.*, 2007, **104**, 1789.

211 E. Sigfridsson and U. Ryde, *J. Biol. Inorg. Chem.*, 2003, **8**, 273.

212 S. Venkateshrao, J. Yin, A. A. Jarzecki, P. G. Schultz and T. G. Spiro, *J. Am. Chem. Soc.*, 2004, **126**, 16361.

213 B. W. Matthews and R. E. Fenna, *Acc. Chem. Res.*, 1980, **13**, 309.

214 H. L. Axelrod, E. C. Abresch, M. Y. Okamura, A. P. Yeh, D. C. Rees and G. Feher, *J. Mol. Biol.*, 2002, **319**, 501.

215 D. Gust, T. A. Moore and A. L. Moore, *Acc. Chem. Res.*, 2009, **42**, 1890.

216 S. A. MacGowan and M. O. Senge, *Chem. Commun.*, 2011, **47**, 11621.

217 J. Deisenhofer and H. Michel, *Science*, 1989, **245**, 1463.

218 There are a few nomenclatures for the individual pigments in the ETC and here the components of the special-pair dimer (P) will be distinguished by the addition of a subscript indicating the protein to which it is attached (*i.e.* $D_L$ and $D_M$). This formality is continued for both the monomeric 'accessory' BChls ($B_A$ and $B_B$) and the BPheos ($H_A$ and $H_B$) noting the distinction that in bacterial RCs it is conventional to describe the monomers of P using the L/M nomenclature and the accessories using the equivalent A/B labels.

219 W. W. Parson and A. Warshel, in *The Purple Phototrophic Bacteria*, eds. C. N. Hunter, F. Daldal, M. C. Thurnauer and J. T. Beatty, Springer, Dordrecht, 2009, p. 355.

220 C. R. Lancaster and H. Michel, *Structure*, 1997, **5**, 1339.

221 M. E. Michel-Beyerle, M. Plato, J. Deisenhofer, H. Michel, M. Bixon and J. Jortner, *Biochim. Biophys. Acta*, 1988, **932**, 52.

222 This was necessary in order to ensure that subsequent aggregation of the experimental data by averaging was appropriate, so that best estimates of the actual conformations present in the crystal were extracted.

223 For a detailed description of individual aspects and the biological implications thereof see our original publication.[216]

224 *(a)* A. Amunts, O. Drory and N. Nelson, *Nature*, 2007, **447**, 58; *(b)* A. Amunts, H. Toporik, A. Borovikova and N. Nelson, *J. Biol. Chem.*, 2010, **285**, 3478; *(c)* H. N. Chapman, P. Fromme, A. Barty, T. A. White, R. A. Kirian, A. Aquila, M. S. Hunter, J. Schulz, D. P. DePonte, U. Weierstall, R. B. Doak, F. R. Maia, A. V. Martin, I. Schlichting, L. Lomb, N. Coppola, R. L. Shoeman, S. W. Epp, R. Hartmann, D. Rolles, A. Rudenko, L. Foucar, N. Kimmel, G. Weidenspointner, P. Holl, M. Liang, M. Barthelmess, C. Caleman, S. Boutet, M. J. Bogan, J. Krzywinski, C. Bostedt, S. Bajt, L. Gumprecht, B. Rudek, B. Erk, C. Schmidt, A. Homke, C. Reich, D. Pietschner, L. Struder, G. Hauser, H. Gorke, J. Ullrich, S. Herrmann, G. Schaller, F. Schopper, H. Soltau, K. U. Kuhnel, M.

Messerschmidt, J. D. Bozek, S. P. Hau-Riege, M. Frank, C. Y. Hampton, R. G. Sierra, D. Starodub, G. J. Williams, J. Hajdu, N. Timneanu, M. M. Seibert, J. Andreasson, A. Rocker, O. Jonsson, M. Svenda, S. Stern, K. Nass, R. Andritschke, C. D. Schroter, F. Krasniqi, M. Bott, K. E. Schmidt, X. Wang, I. Grotjohann, J. M. Holton, T. R. Barends, R. Neutze, S. Marchesini, R. Fromme, S. Schorb, D. Rupp, M. Adolph, T. Gorkhover, I. Andersson, H. Hirsemann, G. Potdevin, H. Graafsma, B. Nilsson and J. C. Spence, *Nature*, 2011, **470**, 73; *(d)* A. T. Brunger, P. D. Adams, P. Fromme, R. Fromme, M. Levitt and G. F. Schroder, *Structure*, 2012, **20**, 957.

225 *(a)* K. Kawakami, Y. Umena, N. Kamiya and J. R. Shen, *Proc. Natl. Acad. Sci. U.S.A.*, 2009, **106**, 8567; *(b)* A. Guskov, J. Kern, A. Gabdulkhakov, M. Broser, A. Zouni and W. Saenger, *Nature Struct. Mol. Biol.*, 2009, **16**, 334; *(c)* Z. Chen, F. Medina, M. Y. Liu, C. Thomas, S. R. Sprang and P. C. Sternweis, *J. Biol. Chem.*, 2010, **285**, 21070; *(d)* M. Broser, C. Glockner, A. Gabdulkhakov, A. Guskov, J. Buchta, J. Kern, F. Muh, H. Dau, W. Saenger and A. Zouni, *J. Biol. Chem.*, 2011, **286**, 15964; *(e)* J. Kern, R. Alonso-Mori, J. Hellmich, R. Tran, J. Hattne, H. Laksmono, C. Glockner, N. Echols, R. G. Sierra, J. Sellberg, B. Lassalle-Kaiser, R. J. Gildea, P. Glatzel, R. W. Grosse-Kunstleve, M. J. Latimer, T. A. McQueen, D. DiFiore, A. R. Fry, M. Messerschmidt, A. Miahnahri, D. W. Schafer, M. M. Seibert, D. Sokaras, T. C. Weng, P. H. Zwart, W. E. White, P. D. Adams, M. J. Bogan, S. Boutet, G. J. Williams, J. Messinger, N. K. Sauter, A. Zouni, U. Bergmann, J. Yano and V. K. Yachandra, *Proc. Natl. Acad. Sci. U.S.A.*, 2012, **109**, 9721; *(f)* J. Kern, R. Alonso-Mori, R. Tran, J. Hattne, R. J. Gildea, N. Echols, C. Glockner, J. Hellmich, H. Laksmono, R. G. Sierra, B. Lassalle-Kaiser, S. Koroidov, A. Lampe, G. Han, S. Gul, D. Difiore, D. Milathianaki, A. R. Fry, A. Miahnahri, D. W. Schafer, M. Messerschmidt, M. M. Seibert, J. E. Koglin, D. Sokaras, T. C. Weng, J. Sellberg, M. J. Latimer, R. W. Grosse-Kunstleve, P. H. Zwart, W. E. White, P. Glatzel, P. D. Adams, M. J. Bogan, G. J. Williams, S. Boutet, J. Messinger, A. Zouni, N. K. Sauter, V. K. Yachandra, U. Bergmann and J. Yano, *Science*, 2013, **340**, 491.

226 Y. Umena, K. Kawakami, J. R. Shen and N. Kamiya, *Nature*, 2011, **473**, 55.

227 F. H. Koua, Y. Umena, K. Kawakami and J. R. Shen, *Proc. Natl. Acad. Sci. U.S.A.*, 2013, **110**, 3889.

228 S. A. MacGowan, PhD Thesis, Trinity College Dublin, The University of Dublin, 2014.

229 M. Guergova-Kuras, B. Boudreaux, A. Joliot, P. Joliot and K. Redding, *Proc. Natl. Acad. Sci. U.S.A.*, 2001, **98**, 4437.

230 A. R. Holzwarth, M. G. Muller, J. Niklas and W. Lubitz, *Biophys. J.*, 2006, **90**, 552.

231 K. Saito, Y. Umena, K. Kawakami, J. R. Shen, N. Kamiya and H. Ishikita, *Biochemistry*, 2012, **51**, 4290.

232 K. Saito, T. Ishida, M. Sugiura, K. Kawakami, Y. Umena, N. Kamiya, J. R. Shen and H. Ishikita, *J. Am. Chem. Soc.*, 2011, **133**, 14379.

233 J. Deisenhofer, O. Epp, I. Sinning and H. Michel, *J. Mol. Biol.*, 1995, **246**, 429.

234 *(a)* S. M. Dracheva, L. A. Drachev, A. A. Konstantinov, A. Y. Semenov, V. P. Skulachev, A. M. Arutjunjan, V. A. Shuvalov and S. M. Zaberezhnaya, *Eur. J. Biochem.*, 1988, **171**, 253; *(b)* G. Fritzsch, S. Buchanan and H. Michel, *Biochim. Biophys. Acta*, 1989, **977**, 157.

235 S. A. MacGowan and M. O. Senge, *Inorg. Chem.*, 2013, **52**, 1228.

236 B. W. Matthews, R. E. Fenna, M. C. Bolognesi, M. F. Schmid and J. M. Olson, *J. Mol. Biol.*, 1979, **131**, 259.

237 J. M. Olson, *Adv. Photosynth. Resp.*, 2005, **20**, 421.

238 D. E. Tronrud and B. W. Matthews, in *The Photosynthetic Reaction Center*, eds. J. Deisenhofer and J. R. Norris, Academic Press, San Diego, **vol. 1**, p. 13.

239 The site-energy of a chromophore in a multi-chromophore protein is its uncoupled excitation energy and arises due to its interactions with the protein matrix. The *intrinsic* site-energy refers to the site-energy of an individual chromophore in the absence of the protein environment and thus represents the contribution of differences in pigment conformation alone (or if relevant, chemical structure). In multichromophore proteins, the individual pigment site-energies give rise to a spatial distribution throughout the protein.

240 S. A. MacGowan and M. O. Senge, unpublished work.

241 In detail, by assigning the BChl atoms to meaningful atom groups and performing series of calculations containing all possible permutations of partial optimizations (*i.e.* a full-factorial design), with individual groups either frozen in the crystal geometry or optimized to *in vacuo* minima, and subsequent excited state calculations (PM6//ZINDO) on each of the various pigments, it is possible to delineate the specific effects of the conformations of each BChl component as well as mutual interactions between two or more such molecular fragments on the site-energy.

242 *(a)* G. Zucchelli, D. Brogioli, A. P. Casazza, F. M. Garlaschi and R. C. Jennings, *Biophys. J.*, 2007, **93**, 2240; *(b)* G. Zucchelli, S. Santabarbara and R. C. Jennings, *Biochemistry*, 2012, **51**, 2717.

243 L. Plate and M. A. Marletta, *Trends Biochem. Sci*, 2013, **38**, 566.

244 M. B. Winter, E. J. McLaurin, S. Y. Reece, C. Olea, Jr., D. G. Nocera and M. A. Marletta, *J. Am. Chem. Soc.*, 2010, **132**, 5582.

245 M. B. Winter, P. J. Klemm, C. M. Phillips-Piro, K. N. Raymond and M. A. Marletta, *Inorg. Chem.*, 2013, **52**, 2277.

246 C. Olea, Jr., J. Kuriyan and M. A. Marletta, *J. Am. Chem. Soc.*, 2010, **132**, 12794.

247 P. Pellicena, D. S. Karow, E. M. Boon, M. A. Marletta and J. Kuriyan, *Proc. Natl. Acad. Sci. U.S.A.*, 2004, **101**, 12854.

248 C. Olea, E. M. Boon, P. Pellicena, J. Kuriyan and M. A. Marletta, *ACS Chem. Biol.*, 2008, **3**, 703.

249 R. Tran, E. M. Boon, M. A. Marletta and R. A. Mathies, *Biochemistry*, 2009, **48**, 8568.

250 E. M. Boon and M. A. Marletta, *J. Am. Chem. Soc.*, 2006, **128**, 10022.

251 Z. Dai and E. M. Boon, *J. Am. Chem. Soc.*, 2010, **132**, 11496; *J. Inorg. Biochem.*, 2011, **105**, 784.

252 S. Muralidharan and E. M. Boon, *J. Am. Chem. Soc.*, 2012, **134**, 2044.

253 O. V. Evgenov, P. Pacher, P. M. Schmidt, G. Haskó, H. H. H. W. Schmidt and J.-P. Stasch, *Nat. Rev. Drug Discov.*, **2006**, *5*, 755.

254 Similarly, reconstitution of photosynthetic pigment-protein complexes with altered (bacterio)chlorophylls has been used widely to probe pigment-protein interactions and has also been used to modify the absorption and energy transfer properties of such systems. For typical examples see: *(a)* C. M. Davis, P. S. Parkes-Loach, C. K. Cook, K. A. Meadows, M. Bandilla, H. Scheer and P. A. Loach,

 

*Biochemistry*, 1996, **35**, 3072; *(b)* N. J. Fraser, P. J. Dominy, B. Ucker, I. Simonin, H. Scheer and R. J. Cogdell, *Biochemistry*, 1999, **38**, 9684.
255 J. J Woodward, N. I. Martin and M. A Marletta, *Nature Meth.*, 2007, **4**, 43.
256 *(a)* M. Germano, A. Y. Shkuropatov, H. Permentier, R.-de Wijn, A. J. Hoff, V. A. Shuvalov and H. J.-van Gorkom, *Biochemistry*, 2001, **40**, 11472; *(b)* A. Zehetner, H. Scheer, P. Siffel and F. Vacha, *Biochim. Biophys. Acta, Bioenerg.*, 2002, **1556**, 21.
257 V. S. Lelyveld, E. Brustad, F. H. Arnold and A. Jasanoff, *J. Am. Chem. Soc.*, **2011**, *133*, 649.
258 *(a)* S. E. Bowman and K. L. Bren, *Inorg. Chem.*, 2010, **49**, 7890; *(b)* M. D. Liptak, R. D. Fagerlund, E. C. Ledgerwood, S. M. Wilbanks and K. L. Bren, *J. Am. Chem. Soc.*, 2011, **133**, 1153.
259 M. D. Liptak, X. Wen and K. L. Bren, *J. Am. Chem. Soc.*, 2010, **132**, 9753.
260 M. Can, G. Zoppellaro, K. K. Andersson and K. L. Bren, *Inorg. Chem.*, 2011, **50**, 12018.
261 The particular A7F point-mutation was expected to alter the heme conformation through interaction with the Cys-X-X-Cys-His motif.
262 M. L. Reniere, G. N. Ukpabi, S. R. Harry, D. F. Stec, R. Krull, D. W. Wright, B. O. Bachmann, M. E. Murphy and E. P. Skaar, *Mol. Microbiol.*, 2010, **75**, 1529.
263 S. J. Takayama, G. Ukpabi, M. E. Murphy and A. G. Mauk, *Proc. Natl. Acad. Sci. U.S.A.*, 2011, **108**, 13071.
264 G. Ukpabi, S. J. Takayama, A. G. Mauk and M. E. Murphy, *J. Biol. Chem.*, 2012, **287**, 34179.
265 D. E. Bikiel, F. Forti, L. Boechi, M. Nardini, F. J. Luque, M. A. Marti and D. A. Estrin, *J. Phys. Chem. B*, 2010, **114**, 8536.
266 Q. M. Tran, C. Fong, R. A. Rothery, E. Maklashina, G. Cecchini and J. H. Weiner, *PloS One*, 2012, **7**, e32641.
267 E. S. Burgie, A. N. Bussell, J. M. Walker, K. Dubiel and R. D. Vierstra, *Proc. Natl. Acad. Sci. U.S.A.*, 2014, **111**, 10179.
268 Y. Hirose, N. C. Rockwell, K. Nishiyama, R. Narikawa, Y. Ukaji, K. Inomata, J. C. Lagarias and M. Ikeuchi, *Proc. Natl. Acad. Sci. U.S.A.*, 2013, **110**, 4974.
269 *(a)* W. Rüdiger, F. Thümmler, E. Cmiel and S. Schneider, *Proc. Natl. Acad. Sci. U.S.A.*, 1983, **80**, 6244; *(b)* C. Song, G. Psakis, C. Lang, J. Mailliet, W. Gärtner, J. Hughes and J. Matysik, *Proc. Natl. Acad. Sci. U.S.A.*, 2011, **108**, 3842.
270 For recent discussions about structural changes involving ring A see: *(a)* A. T. Ulijasz, G. Cornilescu, C. C. Cornilescu, J. Zhang, M. Rivera, J. L. Markey and R. D. Vierstra, *Nature*, 2010, **463**, 250; *(b)* C. Song, G. Psakis, J. Kopycki, C. Lang, J. Matysik and J. Hughes, *J. Biol. Chem.*, 2014, **289**, 2552.
271 *(a)* S.-L. Tu and J. C. Lagarias in *Handbook of Photosensory Receptors*, eds. W. R. Briggs and J. L. Spudich, Wiley, Weinheim, 2005, p. 121; *(b)* M. E. Auldridge and K. T. Forest, *Crit. Rev. Biochem. Mol. Biol.*, 2011, **46**, 67.
272 For a detailed discussion of the subtle interplay between chromophore chemistry, protein interactions and photophysics and the development of new photoresponsive materials see Scheer *et al.*[17]
273 P. P. Peng, L. L. Dong, Y. F. Sun, X. L. Zeng, W. L. Ding, H. Scheer, X. Yang and K. H. Zhao, *Acta Cryst.*, 2014, **D70**, 2558.
274 J. R. Wagner, J. Shang, D. von Stetten, M. Günther, D. H. Murgida, M. A. Mroginski, J. M. Walker K. T. Forest, P. Hildebrandt and R. D. Vierstra, *J. Biol. Chem.*, 2008, **283**, 12212.
275 Y. Shichida and T. Matsuyama, *Philos. Trans. R. Soc. London B Biol. Sci.*, 2009, **364**, 2881.
276 O. Weingart, *J. Am. Chem. Soc.*, 2007, **129**, 10618.
277 *(a)* E. W. Hernández-Rodriguez, E. Sánchez-Garcia, R. Crespo-Otero, A. L. Montero-Alejo, L. A. Montero and W. Thiel, *J. Phys. Chem. B*, 2012, **116**, 1060; *(b)* E. W. Hernández-Rodriguez, A. L. Montero-Alejo, R. López, E. Sánchez-Garcia, L. A. Montero-Cabrera and J. M. de la Vega, *J. Comput. Chem.*, 2013, **34**, 2460.
278 *(a)* A. T. Taguchi, P. J. O'Malley, C. A. Wraight and S. A. Dikanov, *Biochemistry*, 2013, **52**, 4648; *(b)* W. B. de Almeida, A. T. Taguchi, S. A. Dikanov, C. A. Wraight and P. J. O'Malley, *J. Phys. Chem. Lett.*, 2014, **5**, 2506.
279 B. Meunier, *Chem. Rev.*, 1992, **92**, 1411.
280 T. Fekner, J. Galluci and M. K. Chan, *J. Am. Chem. Soc.*, 2004, **126**, 223.
281 *(a)* N. Chaudhri and M. Sankar, *RSC Adv.*, 2015, **5**, 3269; *(b)* M. O. Senge, *ECS Trans.*, 2015, in press.
282 T. V. Esipova and S. A. Vinogradov, *J. Org. Chem.*, 2014, **79**, 8812.
283 J. A. Shelnutt, Y. M. Tian, K. E. Martin and C. J. Medforth, in *Handbook of Porphyrin Science*, eds. G. C. Ferreira, K. M. Kadish, K. M. Smith and R. Guilard, Worldscientific, Singapore, 2014, **vol 28**, p. 227.
284 H. Shahroosvand, S. Zakavi and M. Eskandari, *Phys. Chem. Chem. Phys.*, 2015, **17**, 6347.

***Biographical Sketch M. O. Senge***

*Mathias O. Senge, born in Silbach, Germany, studied chemistry and biochemistry in Freiburg, Amherst, Marburg, and Lincoln and graduated as Diplom-Chemiker from the Philipps Universität Marburg in 1986. After a Ph.D. thesis in plant biochemistry with Prof. Horst Senger in Marburg (1989) and a postdoctoral fellowship with Prof. Kevin M. Smith at UC Davis, he received his habilitation in Organic Chemistry in 1996 at the Freie Universität Berlin. Next he was a Heisenberg fellow at the Freie Universität Berlin and UC Davis and held visiting professorships at Greifswald and Potsdam. In 2002 he was appointed Professor of Organic Chemistry at the Universität Potsdam and since 2005 holds the Chair of Organic Chemistry at Trinity College Dublin. He was the recipient of fellowships from the Studienstiftung des Deutschen Volkes and the Deutsche Forschungsgemeinschaft; from 2005-2009 he was a Science Foundation Ireland Research Professor. His main interests are synthetic organic chemistry, the (bio)chemistry of tetrapyrroles, photochemistry, -biology and -medicine, structural chemistry, and history of science.*

***Biographical Sketch S. A. MacGowan***

*Stuart MacGowan studied Chemistry and Mathematics at the University of the West of Scotland before moving to Trinity College Dublin and completing a PhD in Chemistry in 2014. His research involved predicting the biophysical effects of chlorophyll and heme distortion in proteins using theoretical and structure analysis methods. He is now a post-doctoral researcher at the University of Dundee developing approaches for analyzing human DNA sequences for the diagnosis of ultra-rare genetic diseases and rationalizing the phenotypic activity of protein altering variants in the context of 3D structures in an attempt to link protein structure to function.*

***Biographical Sketch J. M. O'Brien***

*Jessica M. O'Brien is in her final year studying Medicinal Chemistry in Trinity College Dublin. She is currently completing her research project in the Senge group in the area of molecular scaffolds and C-H activation reactions. Her research interests include synthetic porphyrin chemistry and molecular motors.*

Table of Contents – Graphic

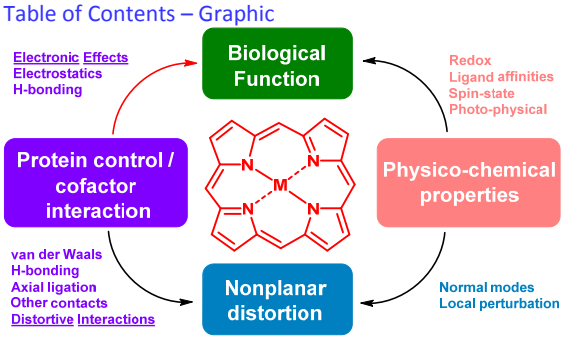


Table of Contents – Text

The biological function of tetrapyrroles and their use in designer proteins is critically dependent on their conformational flexibility.